



REPORT

SP8 – Soil Parameters in Geotechnical Design (GEODIP)

GEODIP'S HIGH-QUALITY DATABASE: CLAY

DOC.NO. 20150030-02-R
REV.NO. 2 / 2018-01-17

Neither the confidentiality nor the integrity of this document can be guaranteed following electronic transmission. The addressee should consider this risk and take full responsibility for use of this document.

This document shall not be used in parts, or for other purposes than the document was prepared for. The document shall not be copied, in parts or in whole, or be given to a third party without the owner's consent. No changes to the document shall be made without consent from NGI.

Ved elektronisk overføring kan ikke konfidensialiteten eller autentisiteten av dette dokumentet garanteres. Adressaten bør vurdere denne risikoen og ta fullt ansvar for bruk av dette dokumentet.

Dokumentet skal ikke benyttes i utdrag eller til andre formål enn det dokumentet omhandler. Dokumentet må ikke reproduseres eller leveres til tredjemand uten eiers samtykke. Dokumentet må ikke endres uten samtykke fra NGI.



Project

Project title: SP8 – Soil Parameters in Geotechnical Design (GEODIP)
Document title: GEODIP's high-quality database: Clay
Document no.: 20150030-02-R
Date: 2015-12-18
Revision no. /rev. date: 2 / 2018-01-17

Client

Client: Norwegian Research Council (NFR)
Client contact person: Anders Solheim
Contract reference: Strategic Project (SP8)

for NGI

Project manager: Jean-Sebastien L'Heureux
Prepared by: Priscilla Paniagua (rev. 0), Priscilla Paniagua & Jean-Sebastien L'Heureux (rev. 1), Aleksander Sæthereng Gundersen & Priscilla Paniagua (rev. 2)
Reviewed by: Tom Lunne & Jean-Sebastien L'Heureux (rev. 0), Tom Lunne (rev.1), & Jean-Sebastien L'Heureux (rev. 2)

Summary

The purpose of this report is to present GEODIP's high quality database for clay materials. The database integrates existing high quality data from block sampling in clay as well as supplementary data from research and development (R&D) assignments, both offshore and onshore. The data is presented in the form of plots for possible correlations between strength and deformation parameters against index properties. The data is also compared to correlations found in the literature. Suggestions are given for field and laboratory work to supplement the data already included in the database.

The report has been revised and updated in 2016-2017 (revision 1 and revision 2) to include the following: a) notes from a quality control of the data included in the database (section 5), b) notes about the scatter of the data in the database (section 6), and c) mineralogical data obtained from the literature and laboratory work performed in selected sites in the database (section 8).

Contents

1	Introduction	5
1.1	Background	5
1.2	Review of the project SP8	6
1.3	Objectives and results of the work	6
2	GEODIP's high quality database	8
2.1	General	8
2.2	Quality of data	8
2.3	Test sites available in GEODIP's high-quality database	11
2.4	Soil properties included in GEODIP's high-quality database	16
2.5	Classification of cone penetration test results	19
3	Correlations from GEODIP's high-quality database	20
3.1	Correlations between index properties	20
3.2	Correlations with undrained shear strength	24
3.3	Correlations with 1D compression parameters	29
4	Suggested supplementary work performed in 2016	40
5	Quality control of the data included in the database	41
6	Observations about scatter of the data in the database	42
7	Advanced lab and field work in 2016 from selected sites	43
8	Conclusions	43
9	Acknowledgements	44
10	References	44

Appendix

Appendix A	Notes regarding the quality control of included data in the database
Appendix B	MASW data from Koa and Skatval
Appendix C	Laboratory test results for block samples from Koa
Appendix D	Laboratory test results for block samples from Skatval

Review and reference page

1 Introduction

1.1 Background

All building and construction work onshore and offshore requires the reliable choice of geotechnical design parameters, which enable construction work to be assessed and planned. If the geotechnical side of a project is neglected, this can result in over-designed and unnecessarily expensive foundations, damage to infrastructure, risk of landslides and in a worst case scenario, the loss of human life. The geotechnical community in Norway and abroad agrees that we need a better understanding of the behaviour of silt and clay in order to improve geotechnical design, make it more innovative, and to reduce risks related to landslides. It is essential that we improve, update and develop field and laboratory methods, databases and the basis for correlating data to be used in the choice of design parameters in clay and silty soil types.

In the case of clays, data from block sampling collected over the period 1982-2010 was compiled by NGI (2012). The data involves 22 different locations in Norway and one location in the UK. At each site 2 to 5 block samples were recovered for undertaking odometer tests, undrained triaxial tests and direct simple shear (DSS) laboratory tests. The main results of individual tests were summarized and compared against index data for the different clays. This resulted in a series of different proposed correlation diagrams that are found useful for future engineering use, see NGI (2012).

The GEODIP SP8 project combines NGI's key skills in field-testing, laboratory testing and the interpretation of the results of site investigations in order to evaluate and develop our understanding of soil behaviour and expand the basic information used to choose geotechnical design parameters for applications onshore and offshore. The project aims to increase collaboration and make a significant contribution towards the creation of a common basis, understanding and method of onshore and offshore foundation design, and achieve a more consistent interpretation of laboratory and *in situ* results. In particular, the project focuses on increasing the understanding of the behaviour of silt and clay, and on interpretation methods and procedures used to choose the strength, dynamic and settlement parameters in clay, soft clay, silt and layered soil.

More and more of NGI's clients are asking for a quantification of sample disturbance and its effects on the choice of design parameters. However, clients also want to see cheaper and more efficient laboratory and site investigation methods. This means that developing a high-quality database that can be used in geotechnical design, and improving the way geophysical and geotechnical results can be integrated in order to interpret soil parameters are key themes for the GEODIP project.

1.2 Review of the project SP8

The main objective of the GEODIP project is to improve our understanding of the behaviour of silt and clay, and to test and verify new and innovative site investigation methods and test procedures, in order to improve our understanding and interpretation of soil parameters.

Improving our understanding of the behaviour of silt and clay, and developing site investigation methods will result in more cost-effective and sustainable solutions in the building and construction, transport and energy sectors, and help reduce the risks associated with climate change, flooding and landslides. It will also result in higher-quality samples and better methods of interpreting the parameters of these soil types. All told, GEODIP will greatly help to increase internal and external collaboration, and will make a significant contribution towards the creation of a common basis for a more consistent interpretation of laboratory and *in situ* results, and will improve our understanding of soil behaviour, enabling us to achieve better and more innovative geotechnical design onshore and offshore. The project will also reinforce NGI's position as a leader within geoscience, both nationally and internationally.

The present report belongs to the GEODIP's subsidiary objective #2: "To develop high-quality databases (supplements to the block sample database) for a range of parameters (strength, dynamic and settlement parameters) and correlations against index properties, mineralogy and pore water chemistry" (NGI, 2015a). This report focuses on the development of the high-quality database for clay materials.

1.3 Objectives and results of the work

The objectives of the present work (in 2015) are:

- a) To integrate existing high quality data from block sampling in clay as well as supplementary data from research and development (R&D) assignments, both offshore and onshore.
- b) To establish a basis for the improvement and development of correlations between strength and deformation parameters against index properties and CPTU (i.e. cone penetration tests with pore pressure measurements) data for clay materials.
- c) To give an overview of the available data for planning supplementary field and laboratory work.

The results from the work are (in 2015):

- A database in Excel that compiles CPTU data, high quality data of index, strength and deformation clay parameters from existing block samples and supplementary data from offshore and onshore R&D and consulting projects.
- Plots between strength and deformation parameters against index properties and CPTU data (this last one will be included in another report for 2016) for evaluation

of the high quality data included in the database. The correlations apply to clay materials.

- A work plan of the field and laboratory work in other research fields that will supplement the existing high-quality data. The test were carried out during 2016.

After the workshop held in December 2015, it was concluded that before going into developing new correlations between laboratory and CPTU data, we should look at the reasons of scatter in the data and a deep quality control of the data.

In 2016, the objectives of the present work focus on:

- a) To control the quality of the data included in the database regarding the assumptions performed in the laboratory tests (i.e. consolidation stress, *in situ* effective stress)
- b) To study the scatter of the data after the quality control and identify the sites that contribute most to the scatter.
- c) To perform advanced laboratory and field work according to the conclusions from last year.
- d) To analyse the mineralogy of selected sites as a reason that could explain the scatter of the data.

The results from the work are (in 2016):

- A revised database in Excel that compiles CPTU data, high quality data of index, strength and deformation clay parameters from existing block samples and supplementary data from offshore and onshore R&D and consulting projects.
- Updated plots of strength and deformation parameters against index properties for evaluation of the high quality data included in the database.
- A compilation of the mineralogical data obtained from literature and laboratory tests for selected sites.

During 2017, the database has been used for developing correlations between soil parameters. These correlations are presented in separate reports.

2 GEODIP's high quality database

2.1 General

GEODIP's high quality database is a compilation of index properties, triaxial anisotropic consolidation undrained compression (CAUC) test results, triaxial anisotropic consolidation undrained extension (CAUE) test results, triaxial isotropic consolidation undrained compression (CIUE) test results, direct shear test (DSS) results, odometer test results and CPTU results; obtained from high quality offshore and onshore samples.

The database is organized in six different sheets as follows:

- a) CAUC & CPTU, containing data from CAUC, CPTU tests and index properties
- b) CAUE & CPTU, containing data from CAUE, CPTU tests and index properties
- c) CIUC & CPTU, containing data from CIUC, CPTU tests and index properties
- d) DSS & CPTU, containing data from DSS, CPTU tests and index properties
- e) OEDO & CPTU, containing data from odometer, CPTU tests and index properties
- f) Readme, containing a description of each column in the different sheets

2.2 Quality of data

The quality of the sample tested is evaluated based on the initial void ratio and the axial strain at the *in situ* stress according to the classification included in the Norwegian Geotechnical Society (NGF, 2013). This classification is included in the ISO Standard 19901-8 (2014) and based on Lunne et al. (1998). The quality criteria is presented in Table 1.

Table 1. Evaluation of sample quality (NGF, 2013)

OCR	$\Delta e/e_0$			
1 to 2	< 0,04	0,04 to 0,070	0,070 to 0,14	> 0,14
2 to 4	< 0,03	0,03 to 0,050	0,050 to 0,10	> 0,10
4 to 6	< 0,02	0,02 to 0,035	0,035 to 0,07	> 0,07
Quality	1: very good to excellent	2: good to fair	3: poor	4: very poor

The data compiled in GEODIP's database is categorized as high quality (i.e. class 1 and class 2) which varies from good to fair and very good to excellent. Figure 1, Figure 2 and Figure 3 show as an example the variation of sample quality with depth for part of the data included in the database.

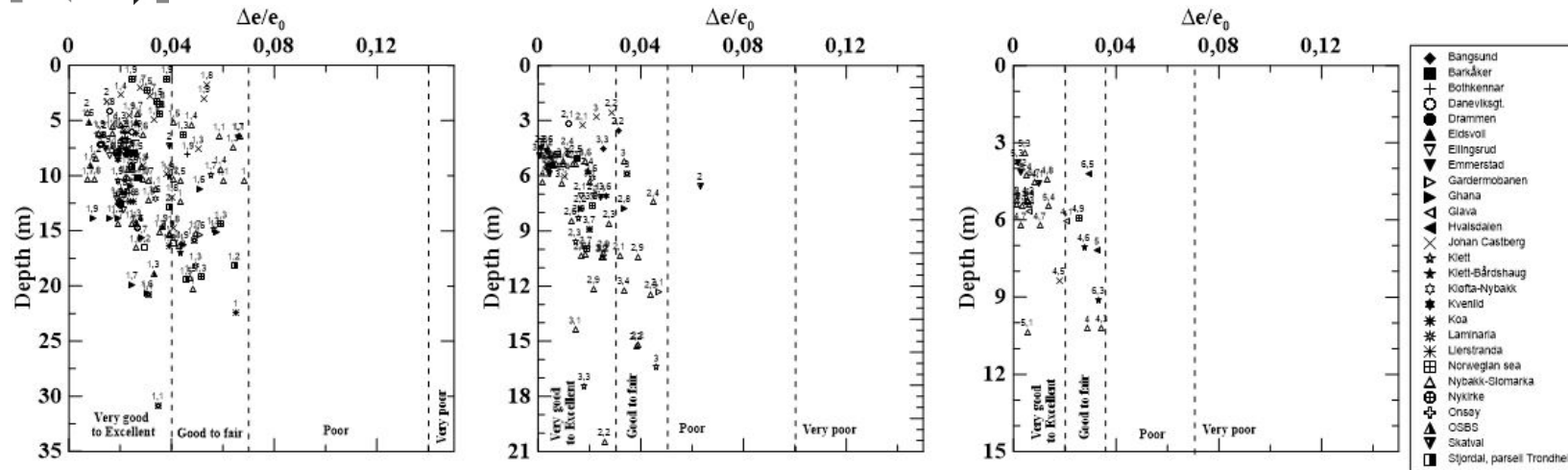


Figure 1: Sample quality for CAUC tests, for OCR between a) 1 and 2, b) 2 and 4 and c) 4 and 6. The OCR is shown above the symbols.

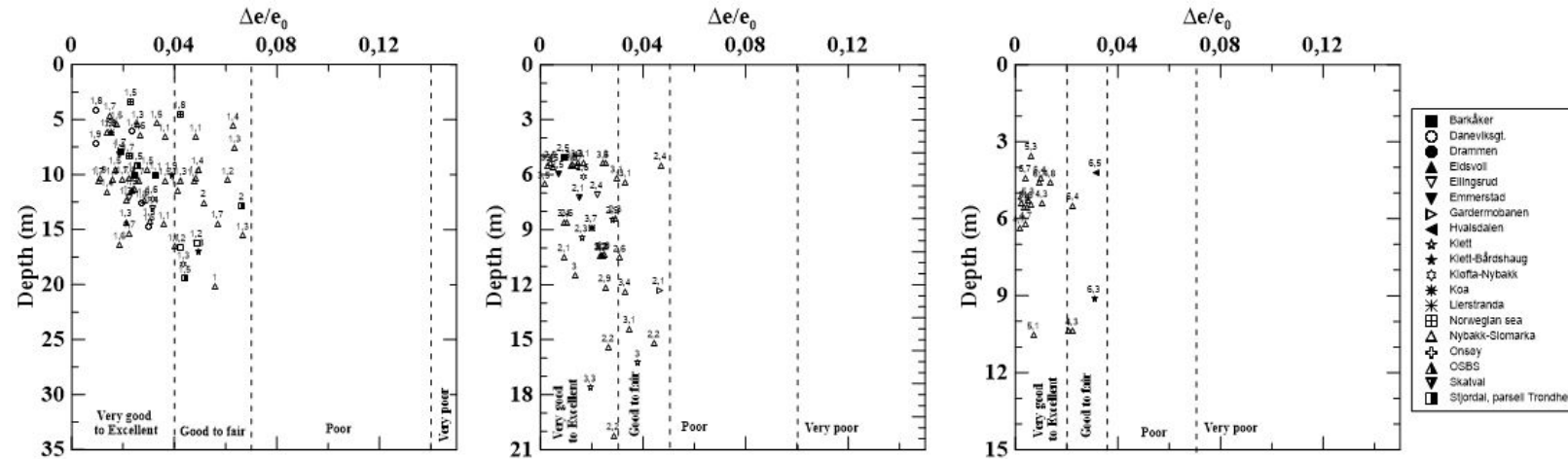


Figure 2: Sample quality for CAUE tests, for OCR between a) 1 and 2, b) 2 and 4 and c) 4 and 6. The OCR is shown above the symbols.

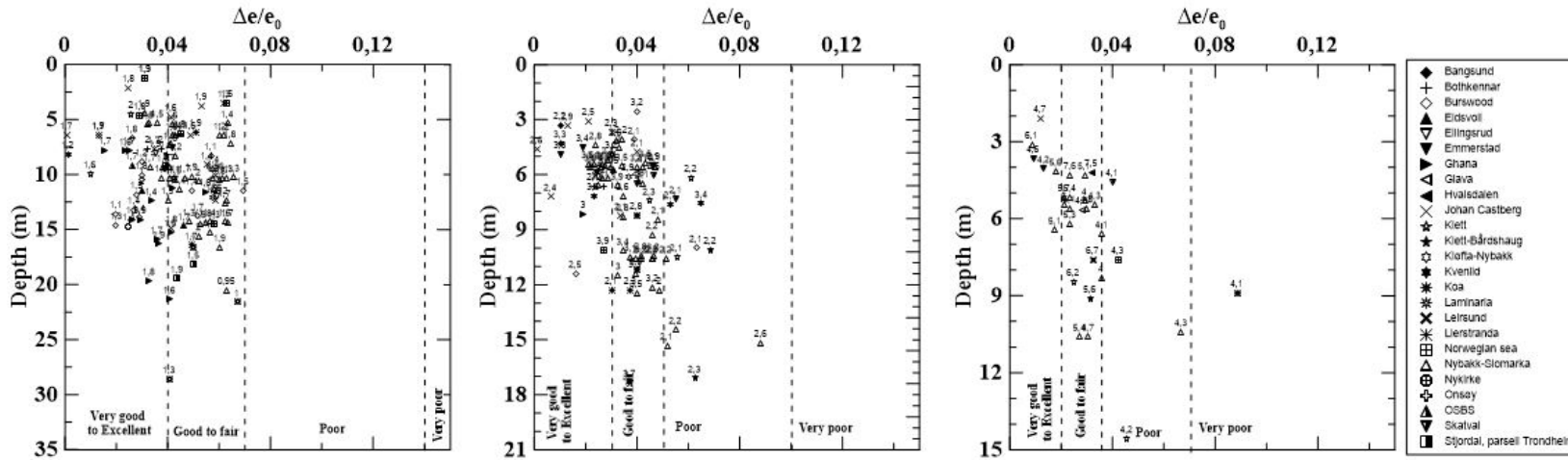


Figure 3: Sample quality for oedometer tests, for OCR between a) 1 and 2, b) 2 and 4 and c) 4 and 6. The OCR is shown above the symbols.

2.3 Test sites available in GEODIP's high-quality database

High quality data has been obtained from sampling carried out at Norwegian clay sites and at other international onshore and offshore locations, as part of consulting projects and research purposes.

Sources of existing data include e.g. work by NGI (2006, 2012, 2013, 2014a, 2014b, 2015b). In this report we assembled previously published information with new field data in GEODIP's clay database.

The data originates from a total of 39 sites as summarized in Table 2. Out of these sites, 14 are located in south-eastern Norway while 18 are in mid Norway (Figure 4). The other sites included in the database are 5 offshore sites and 3 international onshore sites (Figure 5).

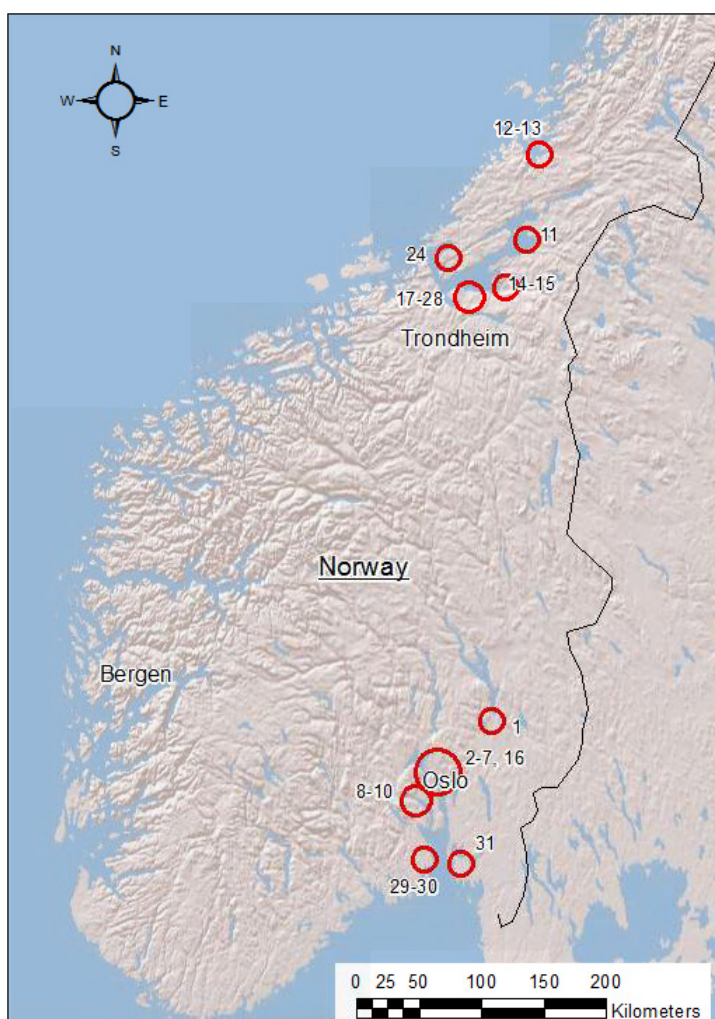


Figure 4: Overview map showing location of onshore Norwegian study sites included in database. The numbers indicate the site name according to Table 2.



Figure 5: Overview map showing location of international onshore and offshore study sites included in database. The numbers indicate the site name according to Table 2.

Figure 6 shows an overview of the distribution of the data in GEODIP's high-quality database where 86% of the data comes from onshore sites and 14% from offshore sites. 40% of the offshore data belongs to the Johan Castberg site and about 54% of the onshore data comes from the Nybakk-Slomarka site. The reader is referred to the respective references of the sites (see Table 1) for detailed map locations and through description of each site.

The compiled database contains index and engineering properties obtained from classification tests, strength tests and consolidation tests. The database includes index properties such as total unit weight, water content, clay content, remoulded shear strength, sensitivity and Atterberg limits. Also, engineering properties such as undrained shear strength derived from CAUC, CAUE and DSS, net cone resistance, *in situ* effective vertical stress and 1D compression parameters based on the classical Janbu theory (Janbu, 1963, 1989); Karlsrud method (Karlsrud & Hernandez-Martinez, 2013); and Casagrande method (Casagrande, 1936). A summary of index properties at the different study sites is given in Table 3.

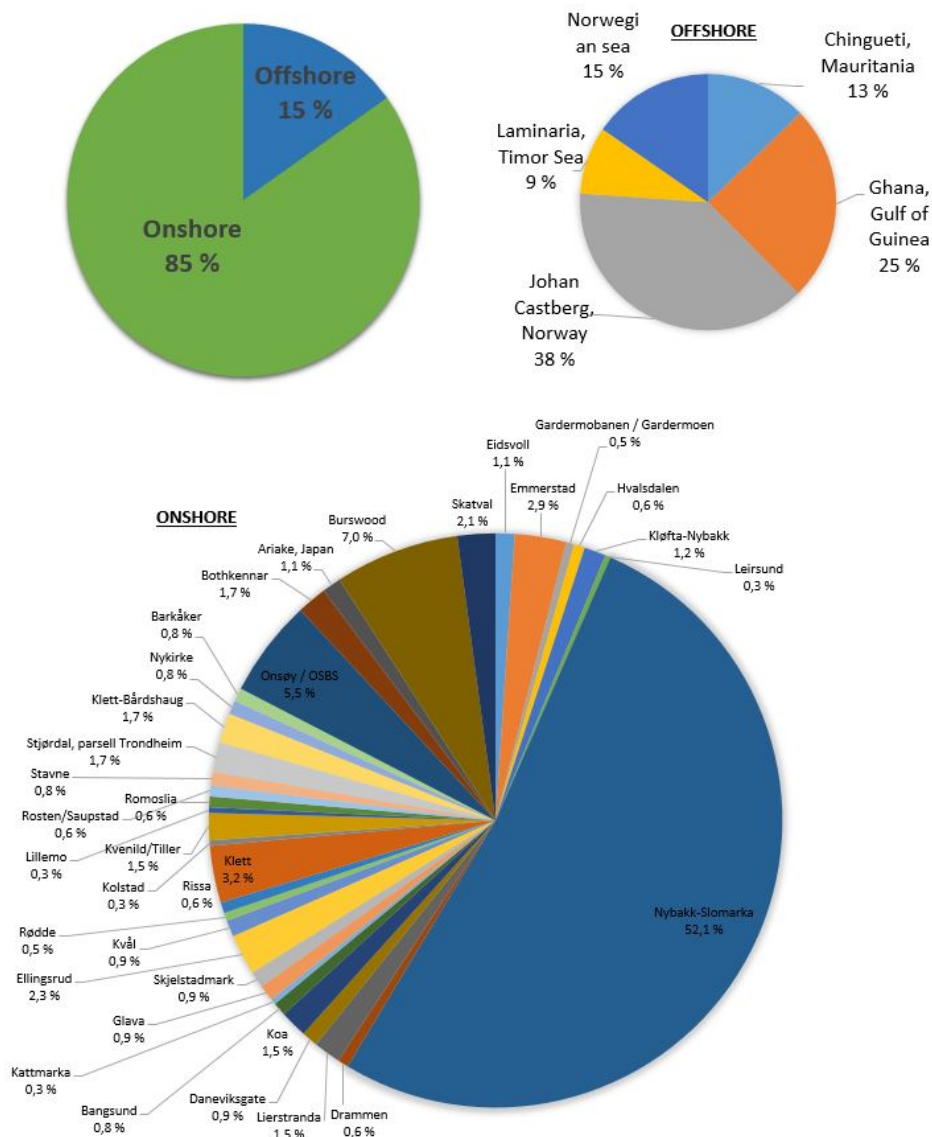


Figure 6: Overview of the distribution of the data in GEODIP's high-quality database.

Table 2. Summary of sites from where high quality data has been collected.

No.	Location	Site	Soil type	Sampling method	Tests						References for sites
					CAUC	CAUE	CIUC	DSS	OEDO	CPTU	
1	Akershus	Eidsvoll	Firm to stiff clay (silty)	Block	x	x			x	x	(NGI, 2012)
2	Akershus	Emmerstad	Quick clay	Block	x	x		x	x	x	(NGI, 2012)
3	Akershus	Gardermobanen / Gardermoen	Clay / Quick clay	Block	x	x				x	(NGI, 2012)
4	Akershus	Hvalsdaalen	Firm to stiff clay	Block	x	x			x	x	(NGI, 2012)
5	Akershus	Kløfta-Nybakk	Clay – Quick clay	Block	x	x			x	x	(NGI, 2012)
6	Akershus	Leirsund	Clay	Block			x		x	x	(NGI, 2012)
7	Akershus	Nybakk-Slomarka	Silty clay, clay and quick clay	72 mm Block	x	x			x	x	(NGI, 2014a) (NGI, 2016b)
8	Burskerud	Drammen	Soft clay with thin silt / sand layers	Block	x	x					(NGI, 2012)
9	Burskerud	Lierstranda	Soft clay	Block	x	x			x	x	(NGI, 2012)
10	Burskerud	Daneviksgate	Soft clay	Block	x	x				x	(NGI, 2012)
11	Nord-Trøndelag	Koa	Quick clay	72 mm Block	x				x	x	NGI Trondheim database & This report
12	Nord-Trøndelag	Bangsund	Clay & quick clay	54 mm	x				x	x	NGI Trondheim database
13	Nord-Trøndelag	Kattmarka	Layered soft clay	-	x					x	(NGI, 2015b)
14	Nord-Trøndelag	Glava	Medium stiff to stiff clay	Block	x		x		x	x	(NGI, 2012)
15	Nord-Trøndelag	Skjelstadmark	Clay	54 mm	x				x	x	NGI Trondheim database
16	Oslo	Ellingsrud	Quick clay, silty	Block	x	x		x	x		(NGI, 2012)
17	Sør-Trøndelag	Kvål	Quick silty clay	72 mm	x			x	x	x	NGI Trondheim database
18	Sør-Trøndelag	Rødde	Quick clay	72 mm	x			x	x	x	NGI Trondheim database
19	Sør-Trøndelag	Rissa	Soft & quick clay	72 mm	x				x	x	NGI Trondheim database
20	Sør-Trøndelag	Klett	Soft silty quick clay	72 mm & miniblock	x	x			x	x	NGI Trondheim database
21	Sør-Trøndelag	Kolstad	Quick clay	75 mm	x				x	x	NGI Trondheim database
22	Sør-Trøndelag	Kvenild-Tiller	Soft to medium quick clay	Block	x		x		x	x	(NGI, 2012)
23	Sør-Trøndelag	Lillemo	Quick clay	72 mm	x				x	x	NGI Trondheim database
24	Sør-Trøndelag	Romoslia	Clay	72 mm	x				x	x	NGI Trondheim database
25	Sør-Trøndelag	Rosten/Saupstad	Soft clay & firm to quick clay	-		x			x		NGI Trondheim database
26	Sør-Trøndelag	Stavne	Quick clay & clay	72 mm	x			x	x	x	NGI Trondheim database
27	Sør-Trøndelag	Stjørdal, parsell Trondheim	Silty clay - clay	Block	x	x		x	x		NGI Trondheim database
28	Sør-Trøndelag	Klett-Bårdshaug	Quick clay	Block	x	x			x	x	(NGI, 2012)
29	Vestfold	Nykirke	Quick clay	54 mm	x	x			x	x	(NGI, 2012)
30	Vestfold	Barkåker	Clay	Block	x	x				x	(NGI, 2012)
31	Østfold	Onsøy / OSBS	Soft to medium clay	Block	x	x		x	x	x	(NGI, 2012)

No.	Location	Site	Soil type	Sampling method	Tests						References for sites
					CAUC	CAUE	CIUC	DSS	OEDO	CPTU	
32	Japan	Ariake	Soft silt & clay	Japanese sampler 75 mm				x		x	(NGI, 2012)
33	Western Australia	Burswood	Soft plastic silty clay	Piston & block	x	x		x	x	x	(NGI, 2006)
34	Offshore	Chingueti, Mauritania	Homogenous, calcareous clayey silt and silty clay	72 mm	x	x		x		x	(NGI, 2006)
35	Offshore	Ghana, Gulf of Guinea	Soft and very plastic clay	72 mm	x				x	x	(NGI, 2014b)
36	Offshore	Johan Castberg, Norway	Clay	72 mm	x				x	x	(NGI, 2013)
37	Offshore	Laminaria, Timor Sea	Homogenous, calcareous silty clay and clayey silt	72 mm	x	x			x	x	(NGI, 2006)
38	Offshore	Norwegian Sea	Very soft clay	72 mm	x	x			x	x	(NGI, 2006)
39	Scotland	Bothkennar	Soft clay / silt	Block	x				x	x	(NGI, 2006)
40	Nord-Trøndelag	Skatval	Quick clay	72 mm Block	x	x		x	x	x	NGI (2016a) This report

Table 3. Summary of soil properties at study sites.

No.	Site	Water content %w	Total unit weight γ_r (kN/m ³)	Clay content (%)	Plasticity index Ip (%)	St	OCR
1	Eidsvoll	25-35	19-20	37-48	13-19	2-5	2-6
2	Emmerstad	40-48	17,6-18,1	27-40	3-12	77-225	3,65-5,26
3	Gardermobanen / Gardermoen	31-40	18,2	44-50	9-19	5-240	2,6-2,1
4	Hvalsdalen	31-39	18,6-19,5	40-49	9-18	5-20	2-6
5	Kløfta-Nybakk	32-46	18,4-19	33,2-45,9	8-19	7-135	1,3-2,6
6	Leirsund	30-39	19,2	36-49	9-18	5-20	6,25
7	Nybakk-Slomarka	30-45	17,5-19,5	13-67	7-28	1-170	1-9
8	Drammen	31,5-39,1	18,6	36	11,4-15,9	4-10	1,13
9	Lierstranda	32-42	18,3-19,5	31-36	13-19	7-15	1,4-2,0
10	Daneviksgate	50-55	17,2-17,8	48	30	7-8	1,5
11	Koa	29,3-30,7	19,7-19,8	-	7-10,9	12-60	2,37-2,82
12	Bangsund	24,7-38,9	18,5-20,3	26-42	9-19	7-167	2,2-3,3
13	Kattmarka	28-50	19,4-20	37-55	1,4-1,8	7-43	1,45-7
14	Glava	30-35	18-20	30-60	15-30	7-10	4-5
15	Skjelstadmark	26-35	19,3-19,9	-	13-17	4-6	1-1,2
16	Ellingsrud	34-40	18,3-19,1	37	5-8	15-61	1,4-2,1
17	Kvål	31-33	19,2	-	5,4-20,2	10-295	1,46-2,66
18	Rødde	32,5	19,1	33	8	90	1,21
19	Rissa	28-40	18,5-20	42-47	7-12	10-60	2-4
20	Klett	25-35	19,2-19,4	30-35	4-10	10-240	1,5-3
21	Kolstad	38	-	31	4	400	1,84
22	Kvenild-Tiller	30-46	17,5-19	31-47	10-14	22-63	1,6-3,1
23	Lillemo	31	19,9	-	3	240	1,2
24	Romoslia	28,9-36,4	18,7-19,9	30-55	8,5-20	5-18	1,6-8,6
25	Rosten/Saupstad	20-34	20-22,3	32-39	4-10	4-150	2,5-9
26	Stavne	26,5-44,3	17,7-19,8	31,9	8,2	18-95	2,1-2,6
27	Stjørdal, parsell Trondheim	33-43	17,8-19,6	37-38	7-8	200	1,2-2
28	Klett-Bårdshaug	26-35	19-19,7	30-33	6,3-13	10-160	1,8-6,2

No.	Site	Water content %w	Total unit weight γ_r (kN/m ³)	Clay content (%)	Plasticity index I_p (%)	St	OCR
29	Nykirke	25-35	19,5	20-55	4-9	65-80	3,6-4,9
30	Barkåker	32-40	18,4-18,9	31-34	11	85	-
31	Onsøy / OSBS	60-65	15,3-16,3	20-60	32-42	4,5-6	1,2-2,1
32	Ariake, Japan	90-150	-	-	40-100	1,7-5,5	1,2-1,7
33	Burswood	59-115	-	-	39-72	1,6-1,2	1,3-2,7
34	Chingueti, Mauritania	27-71	-	-	5-80	2-10	1,2-4
35	Ghana, Gulf of Guinea	90-145	13-15	45-65	70-95	2-6	1-3
36	Johan Castberg, Norway	22-38	18,1-20,3	30-45	20-42	1,1-2,8	1,2-4,5
37	Laminaria, Timor Sea	45-80	15-17,5	20-38	20-38	1,3-4,4	1-4
38	Norwegian Sea	90-16	-	-	15-66	1,3-7	1,2-2
39	Bothkennar	66-72	15,8-16,1	17-35	42-53	8-13	2
40	Skatval	32	19,4	35-43	11-17	5-50	2-4

2.4 Soil properties included in GEODIP's high-quality database

The clays in the database are mostly of marine or glaciomarine origin. Natural water content (w) data ranges between 20 and 150% with most of the data in the range between 30 to 50% (Figure 7a). The plasticity index (IP) defined as the difference between the liquid and plastic limits is presented in Figure 7b. Most of the plasticity index data vary between 5 and 30%. The clay content of the soil tested ranges from 5 to 80% with most of the data in the range between 30 to 60% (Figure 7c).

Due to the isostatic uplift and resulting emergence of the marine and glaciomarine deposits during the last c. 10,000 years, fluxes of fresh groundwater through the clay deposits have led to leaching of the salts within the grain structure of the material. According to Rosenqvist (1953), such process is the main factor affecting the sensitivity of the clays. Sensitivity is defined as the ratio of the undrained peak shear strength over the remolded shear strength. In the database, the sensitivity of the clays ranges between 1 and 400 with most of the data in the interval 1-20 (Figure 7d).

The histogram of sample depth for the clay samples in the database is presented in Figure 8a, and the corresponding vertical *in situ* effective vertical stress for these depths is shown in Figure 8b. The effective vertical stress in the database varies between 4 and 331 kPa with the highest number of observations between 40 and 80 kPa corresponding to a depth of approximately 4-8 m below ground surface.

Most of the clays have developed some apparent overconsolidation due to aging. The overconsolidation ratio (OCR) data range between 1 and 9 with most of the OCR data falling between 1,5 and 4,0; indicating that most of the soil samples in the database are normally consolidated to lightly overconsolidated (Figure 9a). Hence, the correlations to be developed after this may not be valid for heavily overconsolidated clays. The undrained shear strength data from CAUC triaxial tests concentrates in the range 20-60 kPa whereas results from CAUE and DSS tests are mostly below 40 kPa (Figure 9b).

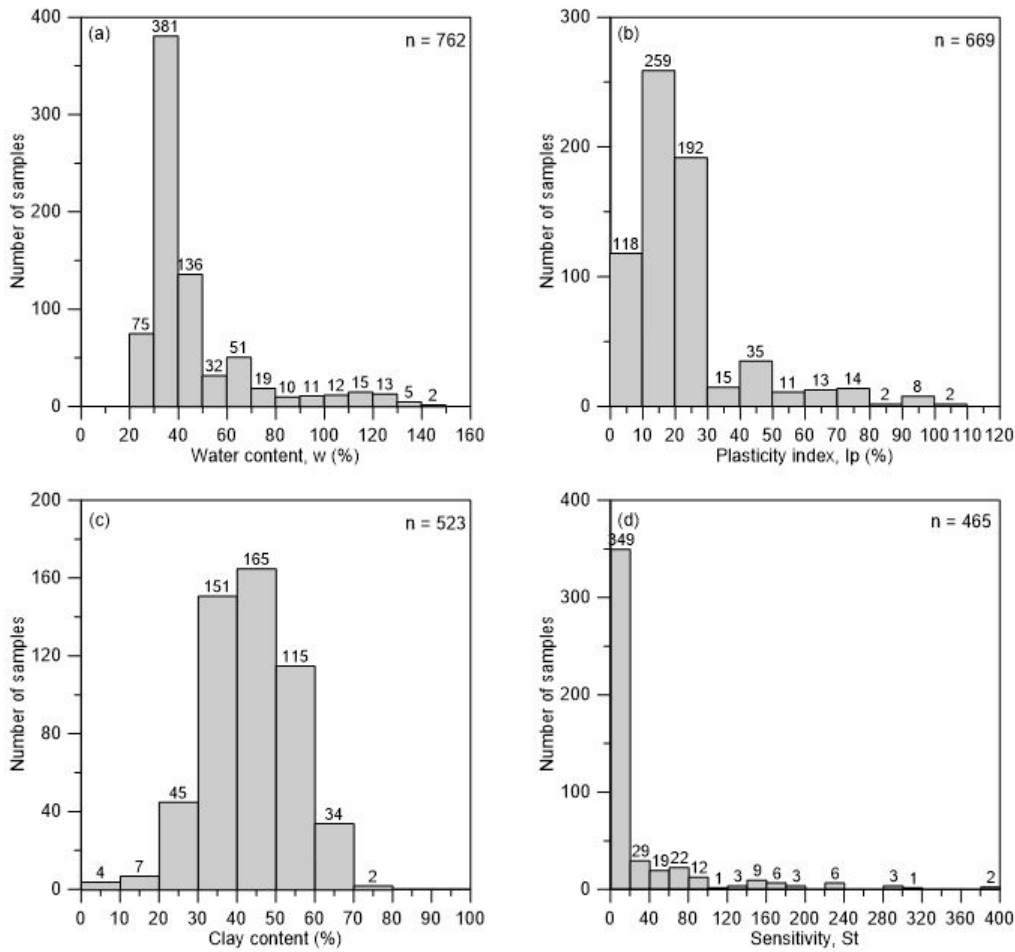


Figure 7: Histogram of a) water content, b) plasticity index, c) clay content and d) sensitivity showing content of GEODIP's clay database.

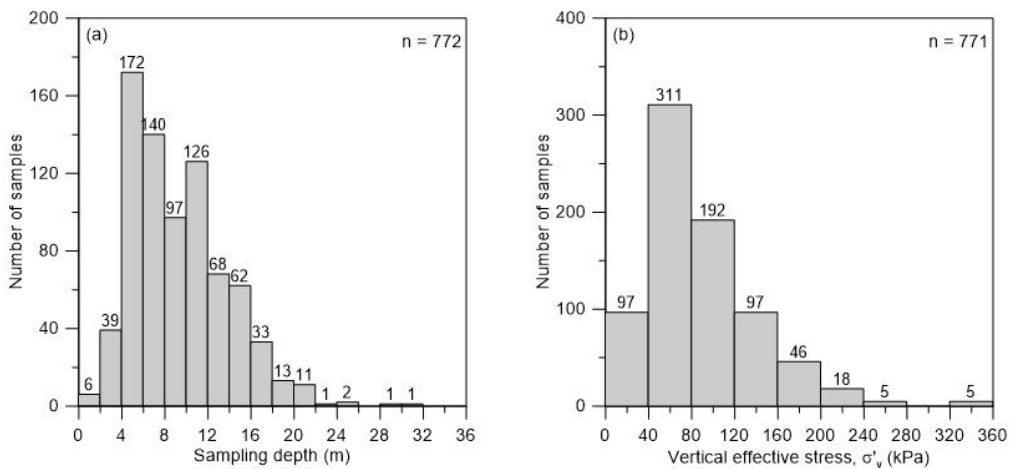


Figure 8: Histogram of a) sampling depth and b) vertical effective stress showing content of GEODIP's clay database.

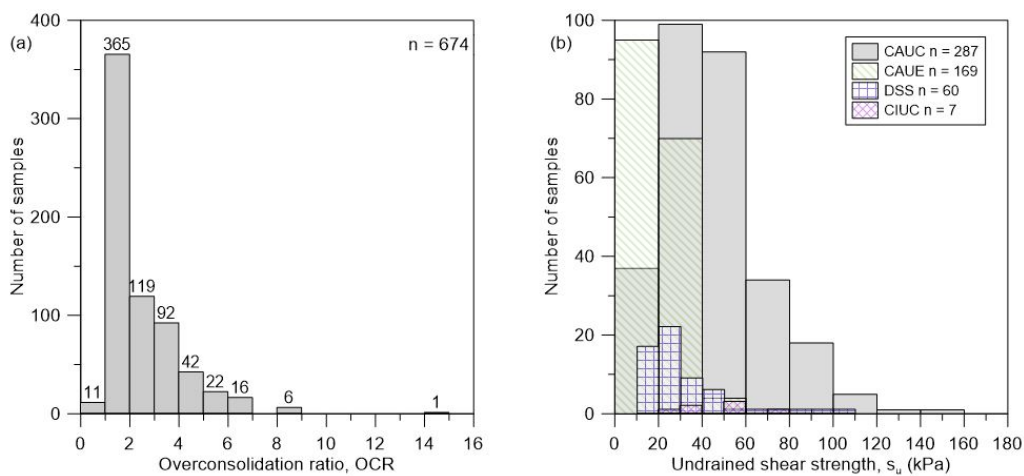


Figure 9: Histogram of a) overconsolidation ratio and b) undrained shear strength from CAUC, CAUE, DSS and CIUC tests showing content of GEODIP's clay database.

In addition to index properties and results from laboratory tests, the compiled database contains results from cone penetration tests (CPTU). Typically the selected CPTU data has been averaged over a 0,5 m thick zone, covering parts both above and below sampling depth. The net cone resistance (q_{net}) of the database falls within a wide range of 40 to 2000 kPa, with the highest number of observations between 400 and 800 kPa which corresponds to a shallow depth of about 4 to 8 m (Figure 10a). Values of normalized cone resistance Q_t are mostly lower than 9 as expected for clay materials (Figure 10b). Normalized pore pressure values B_q are mostly between 0,4 and 1,2 (Figure 10c) and the values of friction ratio are mostly lower than 3% (Figure 10d). It should be noted that the database includes less friction ratio data since sleeve friction was not directly reported in the sources where the data was collected from. This could be completed if required by looking at the raw files from CPTU measurements.

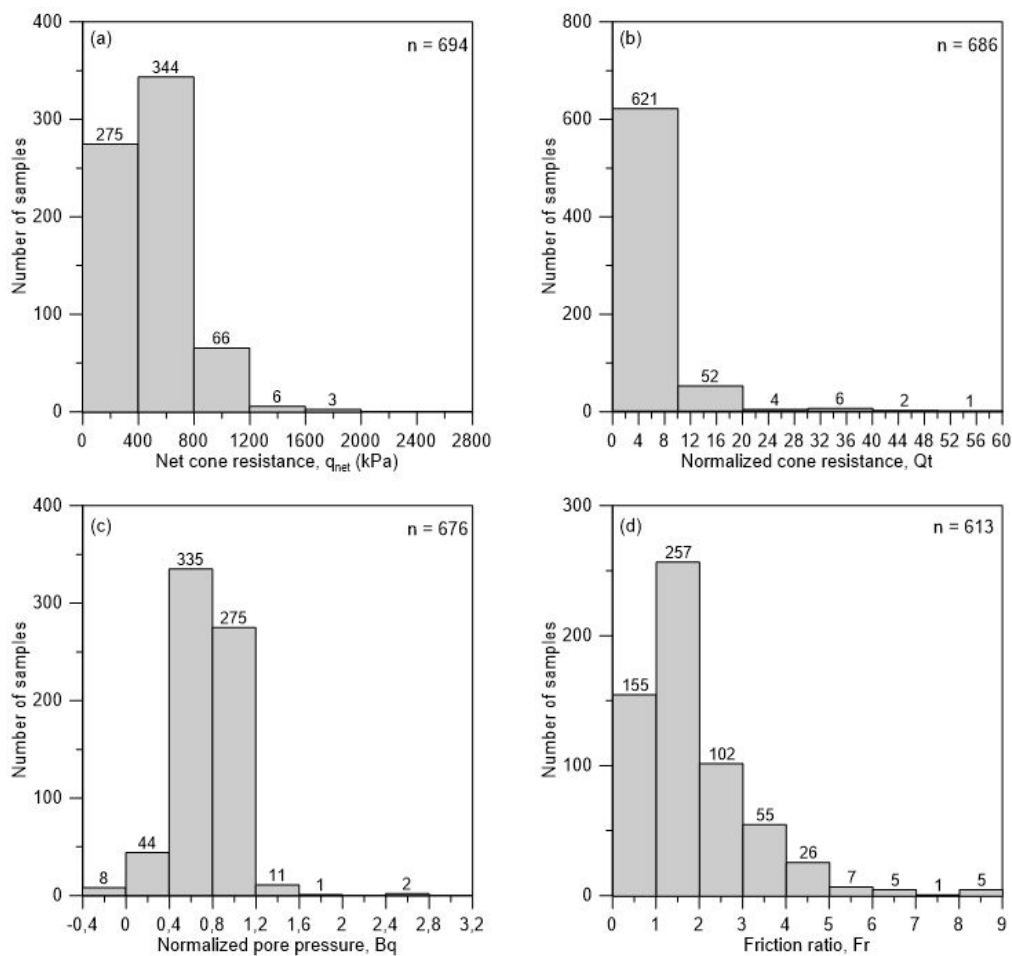


Figure 10: Histogram of a) net cone resistance from CPTU tests, b) normalized cone resistance, c) normalized pore pressure and d) friction ratio showing content of GEODIP's clay database.

2.5 Classification of cone penetration test results

The piezocone penetration test (CPTU) is a common tool used for characterization of soft and sensitive clay deposits. Various researchers have studied relationships between CPTU parameters and strength properties for clayey soils (Lunne et al. 2011; Karlsrud & Lunne, 2005; Lunne et al. 1997). These studies have explored relationships between undrained shear strength and various parameters such as CPTU tip resistance (q_c), corrected tip resistance (q_t), cone net resistance (q_{net}), sleeve friction (f_s), pore pressure parameter (B_q), normalized cone resistance (Q_t), effective stress (σ'_v) and void ratio (e).

This topic is also a separate activity in GEODIP's project and it is studied in a single report. In the present report, no further details are given regarding correlations; however, the data in GEODIP's database is described following Robertson (1990) soil classification charts (Figure 11).

Figure 11 shows that GEODIP's high-quality database classifies mostly as clay (silty clay-clay) region and some data fall into the sensitive/fine grained region. Some points fall into the silt-sands regions that might be due to the dilative behavior of silt content in the clay materials.

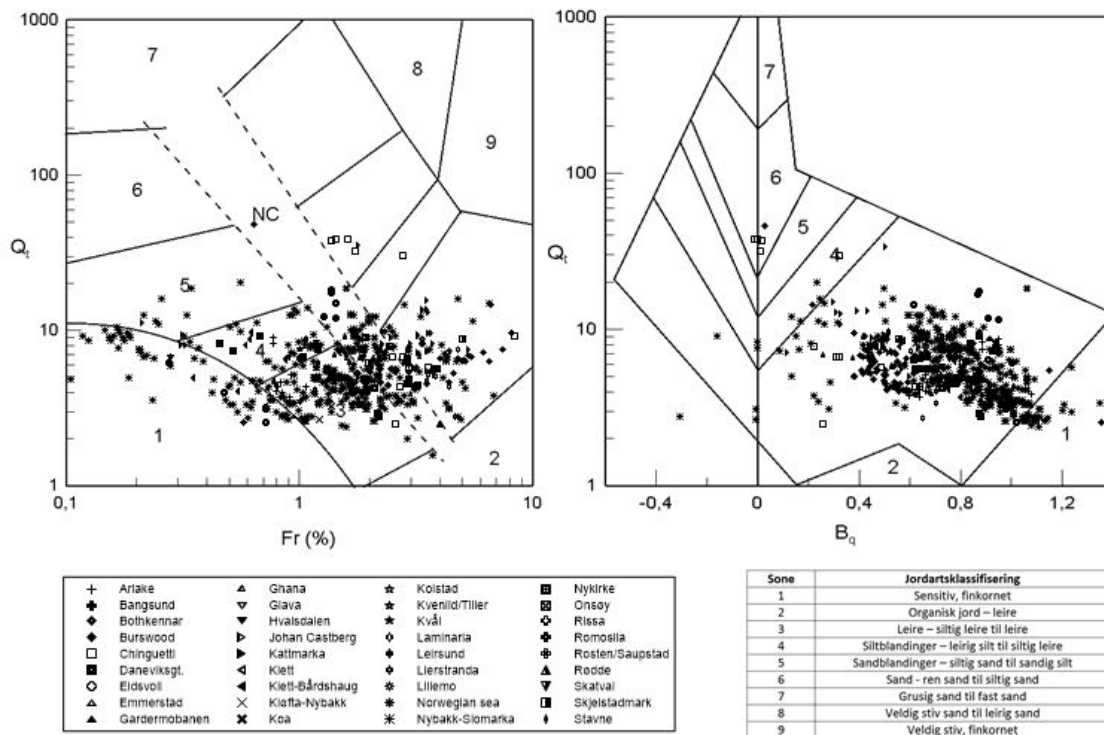


Figure 11: Soil classification from CPTU according to Robertson (1990).

3 Correlations from GEODIP's high-quality database

3.1 Correlations between index properties

Correlations between index parameters in the database can provide rapid estimates useful for preliminary design and for verifying *in situ* and laboratory tests. The following figures present the index data included in GEODIP's high-quality database to identify possible trends and relations between them. The data plotted in the figures is just block samples (i.e. Ø250 mm and Ø160 mm) data.

Figure 12 shows Atterberg limits data in the Casagrande plasticity chart. Most data plots above the A-line, confirming that the clays are generally inorganic. The clay from Ønsoy classify as high plasticity clays (i.e. CH zone). The rest of the sites are classified as low to medium plasticity clays; sandy clays and silty clays (i.e. CL zone).

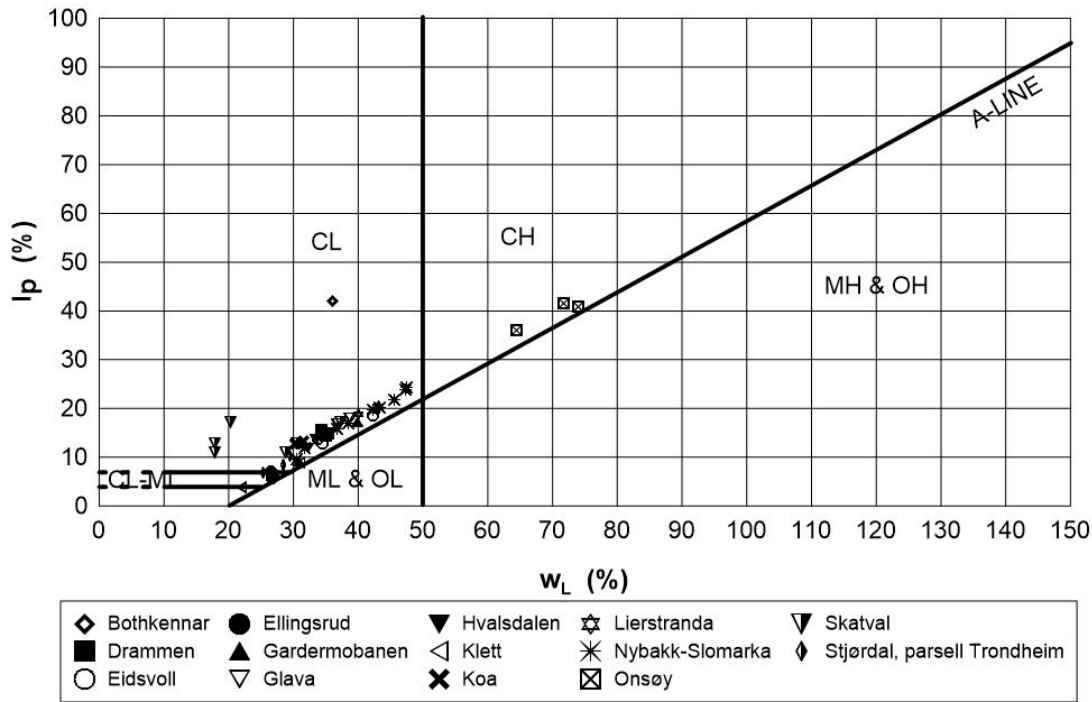


Figure 12: Summary of Atterberg limits of block samples in GEODIP's high quality database.

Figure 13 shows the relation between measured total unit weight and the *in situ* water content for all 40 sites in study that have block samples data. The data follows the trend expected according to equation 1 applicable for fully saturated soils.

$$\gamma_t = 9,81 \left[\left(\frac{1+w_i}{\rho_s + w_i} \right) \right] \quad (1)$$

where;

γ_t = total unit weight (kN/m³)

$9,81\rho_s = \gamma_s$ = unit weight of solids (kN/m³)

ρ_s = density of solids (specific gravity)

w_i = *in situ* water content (decimal)

The unit weight of solids required to match the data, lies for the most part in the range 26,5 to 28,5 kN/m³, which is quite typical for Norwegian clays.

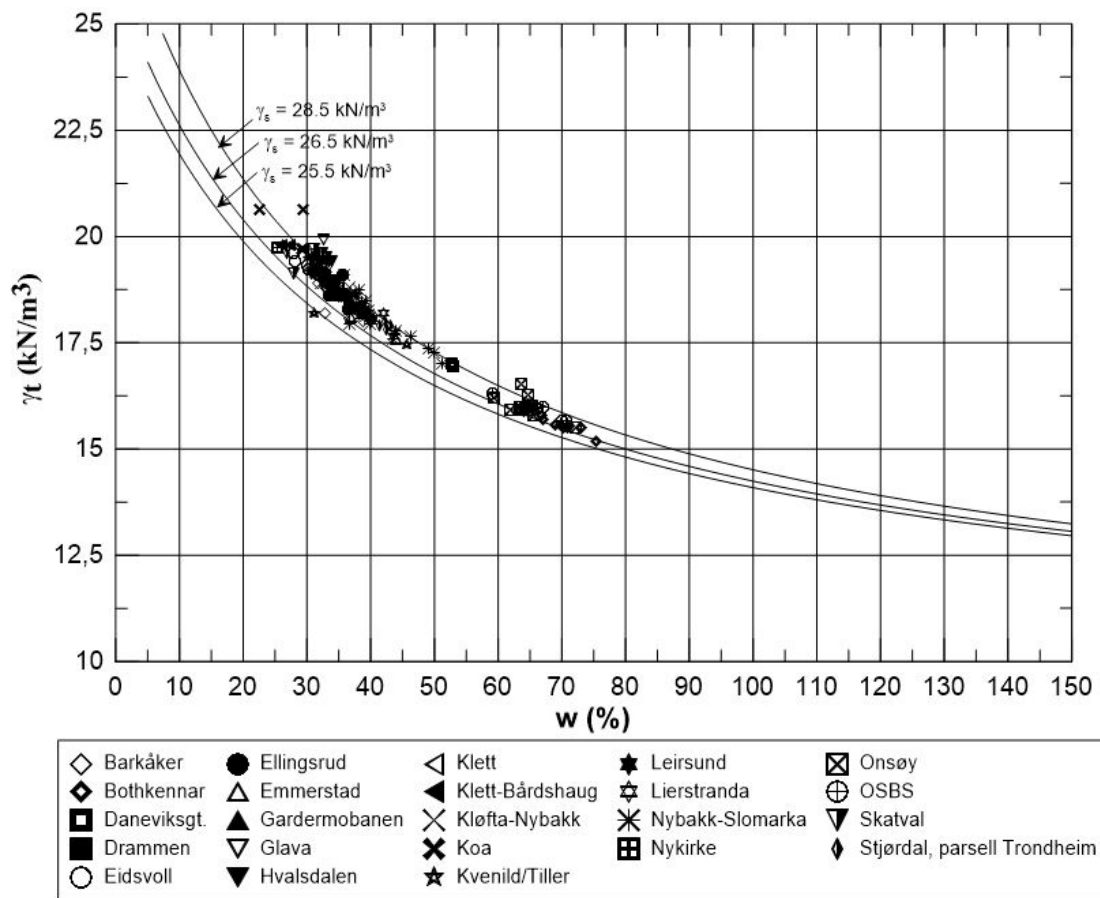


Figure 13: Summary of total unit weight of block samples in GEODIP's high quality database.

Figure 14 shows that the clay sensitivity is closely related to the liquidity index. According to Norwegian Geotechnical Society, a clay is defined as very or highly sensitive when $S_t > 30$, which from Figure 14 is the case when the liquidity index exceeds about $LI = 1,35$ as also presented by Karlsrud & Hernandez-Martinez (2013). To define a clay as quick, the remoulded shear strength must be less than 0,5 kPa. Some of the sites that show high sensitive clays are Skatval, Nybakk-Slomarka, Klett, Barkåker, Emmerstad, Stjørdal, Klett-Bårdshaug, Ellingsrud, among others.

It should be born in mind that remoulded shear strength, and hence sensitivity, depends on the way in which it is measured. In this project the remoulded shear strength has been measured by the fall cone test according to Norwegian Standard (ISO, 2014; De Groot et al., 2012; NGI, 2008).

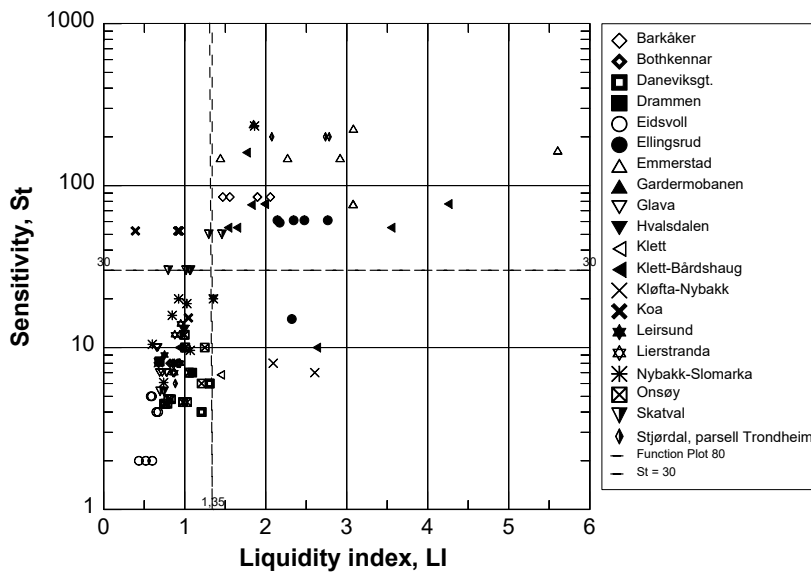


Figure 14: Relationship between sensitivity and liquidity index using block samples data.

Leroueil et al. (1983) propose the relationship in equation 2 between the liquidity index and the remoulded shear strength of clays. The data from GEODIP's high-quality database for block samples agrees well with the relation proposed (Figure 15). Some scatter is observed for remoulded shear strength values < 0,5 kPa. The top values correspond to data from Klett in Trøndelag. The large scatter at low remoulded undrained shear strength values can be linked to the resolution of the measurements and to the limit of the Swedish fall cone ~ 0,2 kPa. The values close to 1 reflect that the soil is at its liquid limit.

$$s_{ur} = \frac{1}{(LI - 0,21)^2} \quad (2)$$

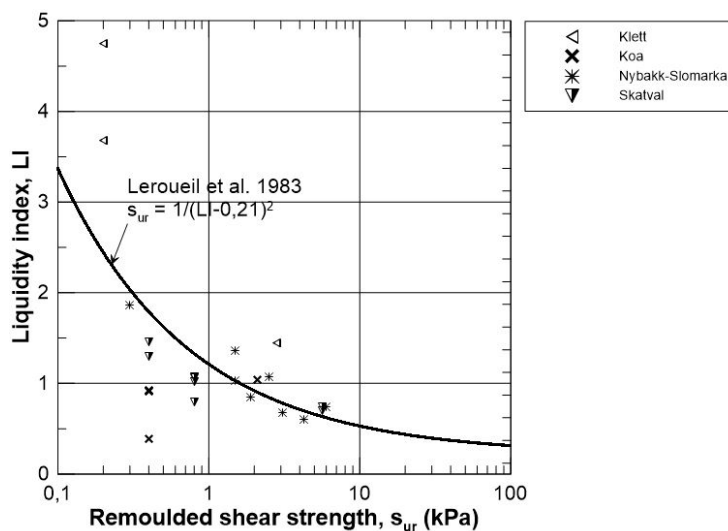


Figure 15: Relationship between remoulded shear strength and liquidity index using block samples data.

Figure 16 shows that the clay content, defined as particle size less than 0,002 mm, varies from 20% to 65% for the block samples in the database. There is a slight tendency of water content increasing with clay content if the data from Onsøy and Bothkennar is removed.

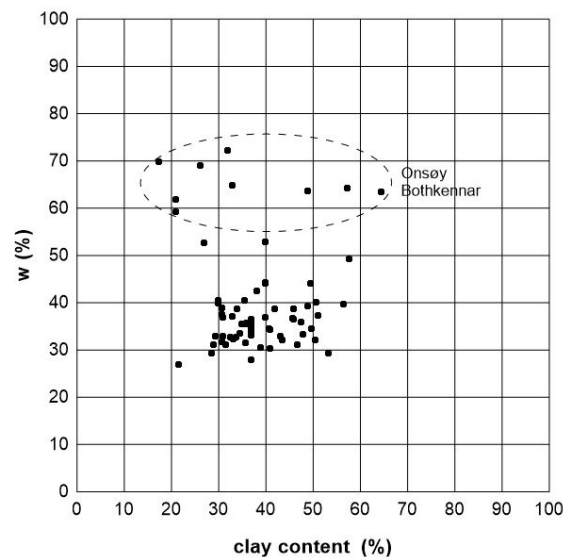


Figure 16: Relationship between clay content and water content using block samples data.

3.2 Correlations with undrained shear strength

It is convenient to express the undrained shear strength as a normalized value defined as s_u/σ'_{ac} . Ladd (1974) proposed a relationship between the overconsolidation ratio OCR and the normalized strength as shown in equation (3) that they called SHANSEP (i.e. Stress History And Normalized Soil Engineering Properties).

$$\frac{s_u}{\sigma'_{ac}} = \alpha OCR^m \quad (3)$$

The SHANSEP framework has been applied previously by Karlsrud & Hernandez-Martinez (2013) for comparing undrained strengths derived from undisturbed high-quality block samples, even though it was originally developed to study the undrained strength of artificially overconsolidated clays. Figure 17 presents the normalized strength versus OCR for the CAUC triaxial compression tests. The OCR is based on interpretation of mostly CRSC tests (see Section 3.3). One should keep in mind that CRSC tests gives the so-called rapid preconsolidation stress; whereas the SHANSEP approach really uses 24 h IL tests.

Figure 17 shows the range of values of the constant α and power m , proposed by Karlsrud & Hernandez-Martinez (2013). These correlations are included just as a comparison, since those are part of the general practice for soil material interpretation at

NGI (onshore department). The average line (i.e. $\alpha = 0,30$ and $m = 0,70$) agrees well with the data shown; however, the upper bound (i.e. $\alpha = 0,35$ and $m = 0,75$) and lower bound (i.e. $\alpha = 0,25$ and $m = 0,65$) can be adjusted in order to capture more data. Data over the upper bound are mainly from Emmerstad and Nybakk-Slomarka. Data under the lower bound are mostly from Kløfta-Nybakk, Klett, Tiller and Stjørdal sites

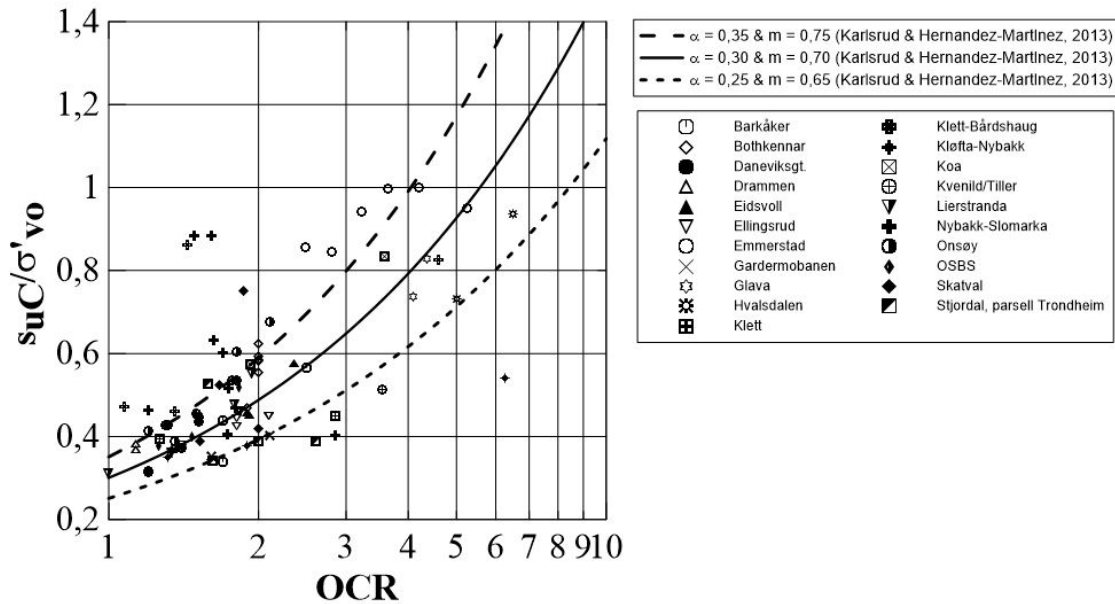


Figure 17: Normalized strength versus OCR from CAUC tests using block samples data.

Figure 18 shows normalized strength data for the CAUE triaxial extension tests. As observed by Karlsrud & Hernandez-Martinez (2013), the results also show significant scatter for a given OCR. Data over the upper bound correspond to Nybakk-Slomarka, Emmerstad and Onsøy sites. Data below the lower bound come from Nybakk-Slomarka.

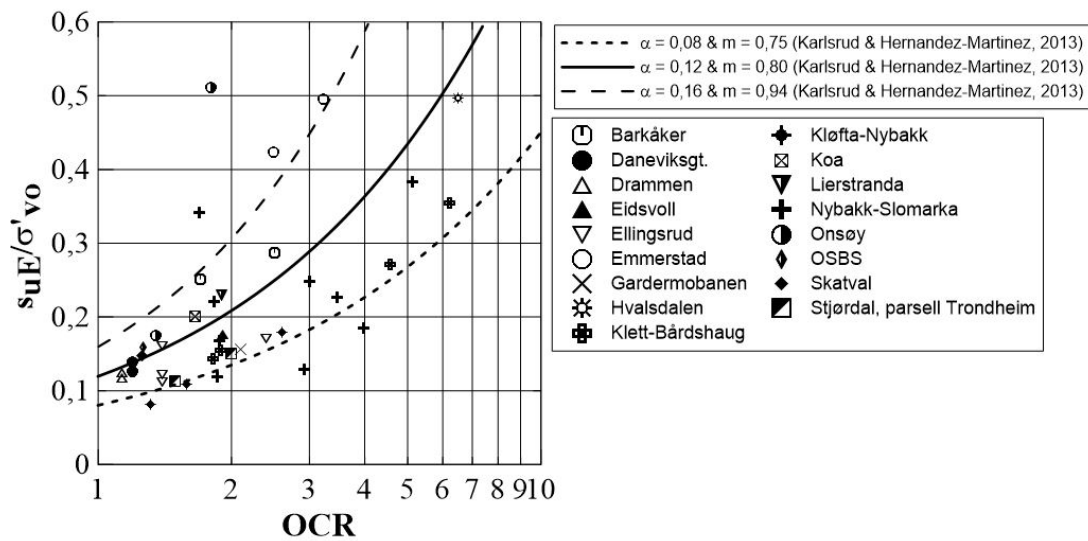


Figure 18: Normalized strength versus OCR from CAUE tests using block samples data.

Figure 19 presents the normalized strength diagram for the DSS tests against OCR. Fewer data points are plotted and some of the data is between the expected upper and lower ranges proposed by Karlsrud & Hernandez-Martinez (2013). Data over the upper bound correspond to Nybakk-Slomarka, Skatval and Onsøy sites. Data below the lower bound come from Nybakk-Slomarka.

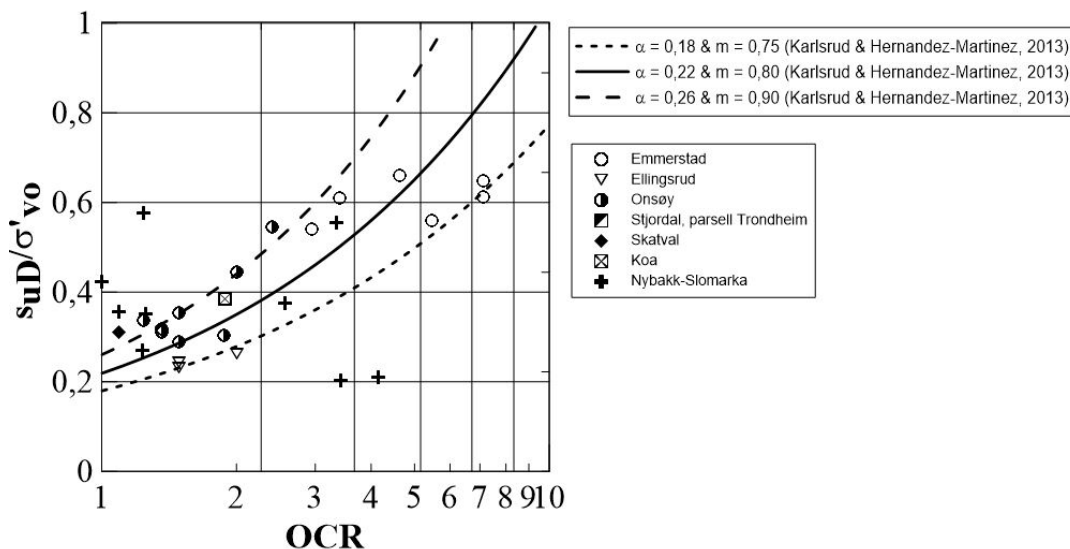


Figure 19: Normalized strength versus OCR from DSS tests using block samples data.

It was mentioned by Karlsrud & Hernandez-Martinez (2013) that some dependency on water content was observed in the relation between OCR and undrained shear strength. However, by looking closer at the values of water content in Figure 17, Figure 18 and

Figure 19; there is relatively high spreading for the clays with similar values of water content.

Figure 20 shows the anisotropic strength ratios of s_{uE}/s_{uC} and s_{uD}/s_{uC} seen in relation to the OCR and plasticity index IP. The scatter in the data is fairly large as also pointed out by Karlsrud & Hernandez-Martinez (2013). No difference is made regarding sensitivity values, this may be taken into a next evaluation stage. The CAUE tests suggest values of $s_{uE}/s_{uC} = 0,25$ to $0,45$ for clays with $OCR \leq 3$, increasing to a range between $0,45$ to $0,60$ at higher OCR values. The DSS tests included suggest $s_{uD}/s_{uC} = 0,55$ to $0,85$ for clays with $OCR < 2$ and $s_{uD}/s_{uC} = 0,50$ to $0,70$ for clays with $OCR > 2$. However, there is no clear dependence of the s_{uE}/s_{uC} and s_{uD}/s_{uC} ratios upon the OCR-value. There is a tendency of an increase in anisotropy ratio with IP, which agrees with the correlations proposed by NIFS (2014). Table 4 presents a summary of anisotropy factors.

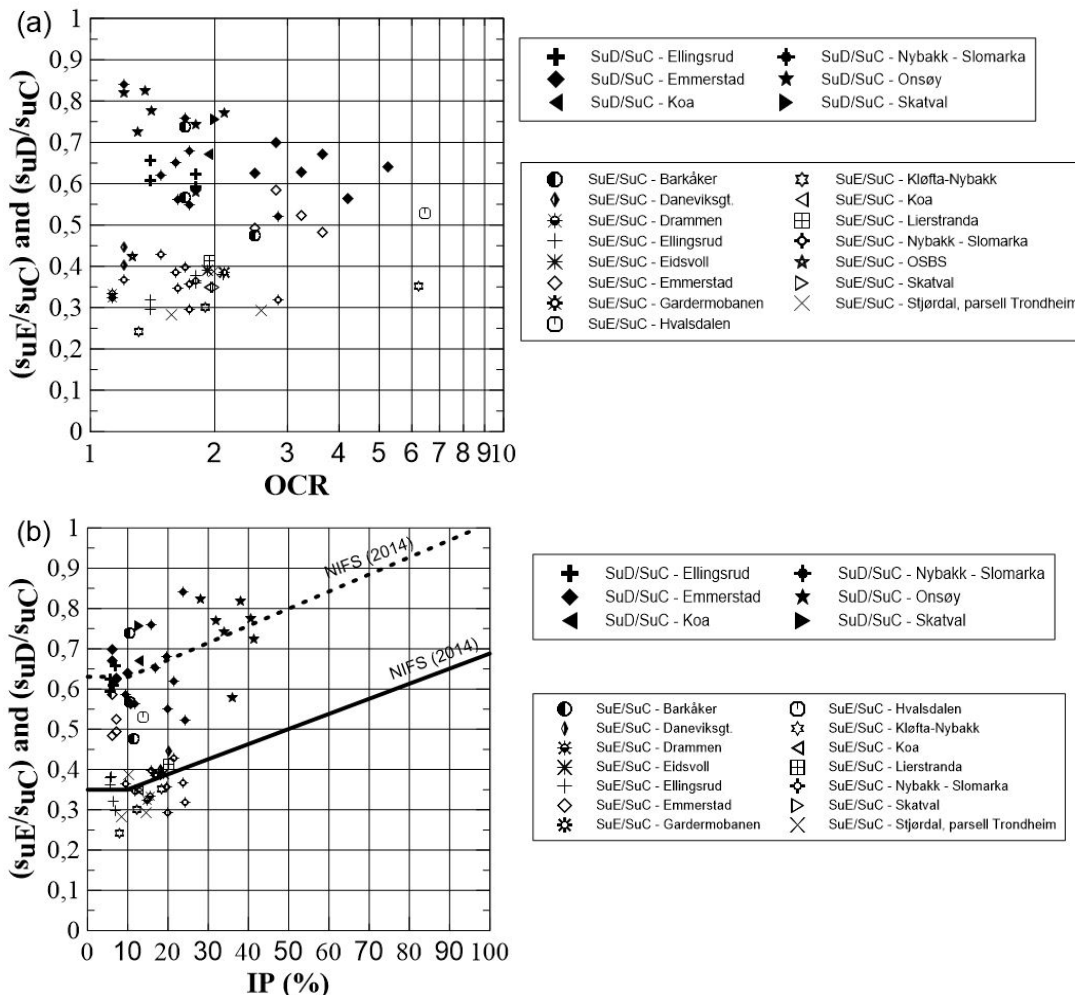


Figure 20: Anisotropic strength ratios versus: (a) OCR and (b) IP using block samples data.

Table 4. Summary of anisotropy factors.

Reference	s_{uE}/s_{uC}	s_{uD}/s_{uC}	Comments
This study	0,25-0,55	0,55-0,85	Range
(C.C. Ladd, 1974)	0,35-0,63	0,63-0,83	Range
(K. Karlsrud, 2005)	0,30-0,55 0,30	0,60-0,80 0,60	Range Recommend to use when IP <10%
(NIFS, 2014)*	0,35 0,35+0,00375*(IP-10)	0,63 0,63+0,00425*(IP-10)	Recommend to use when IP ≤10% Recommend to use when IP >10%

* The values proposed are average values from a large dataset where the range is different. This should be observed carefully in order to compare similar results.

Figure 21 shows that the anisotropic strength ratios s_{uE}/s_{uC} and s_{uD}/s_{uC} tend to increase with the water content of the clays as observed by Karlsrud & Hernandez-Martinez (2013), see Figure 21. Data over the s_{uD}/s_{uC} line correspond to Onsøy, Ellingsrud and Emmerstad. From these sites, Onsøy shows higher plasticity and water content than Ellingsrud and Emmerstad. Data under the s_{uE}/s_{uC} line are mainly from the Nybakk-Slomarka site (that shows water contents lower than 50%) with some single points corresponding to Onsøy (OSBS), Kløfta-Nybakk and Stjordal.

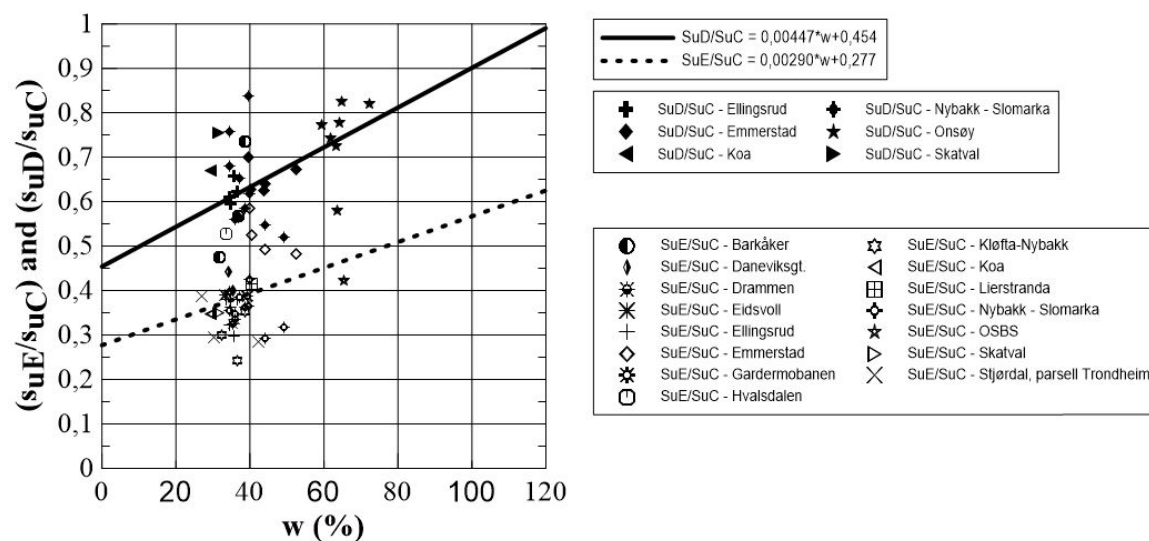


Figure 21: Anisotropic strength ratio versus water content using block samples data.

Figure 22 shows a correlation between the plasticity index (IP) and the peak friction angle summarized in Abramson et al. (2002). The data superposed correspond to block samples from GEODIP's high-quality database. Emmerstad data comes over the trends for low plasticity clays (IP < 10). Bothkennar data is plotted over the trends for medium plasticity clays (IP = 40-50). The rest of the data appear on and under the trend presented in the figure.

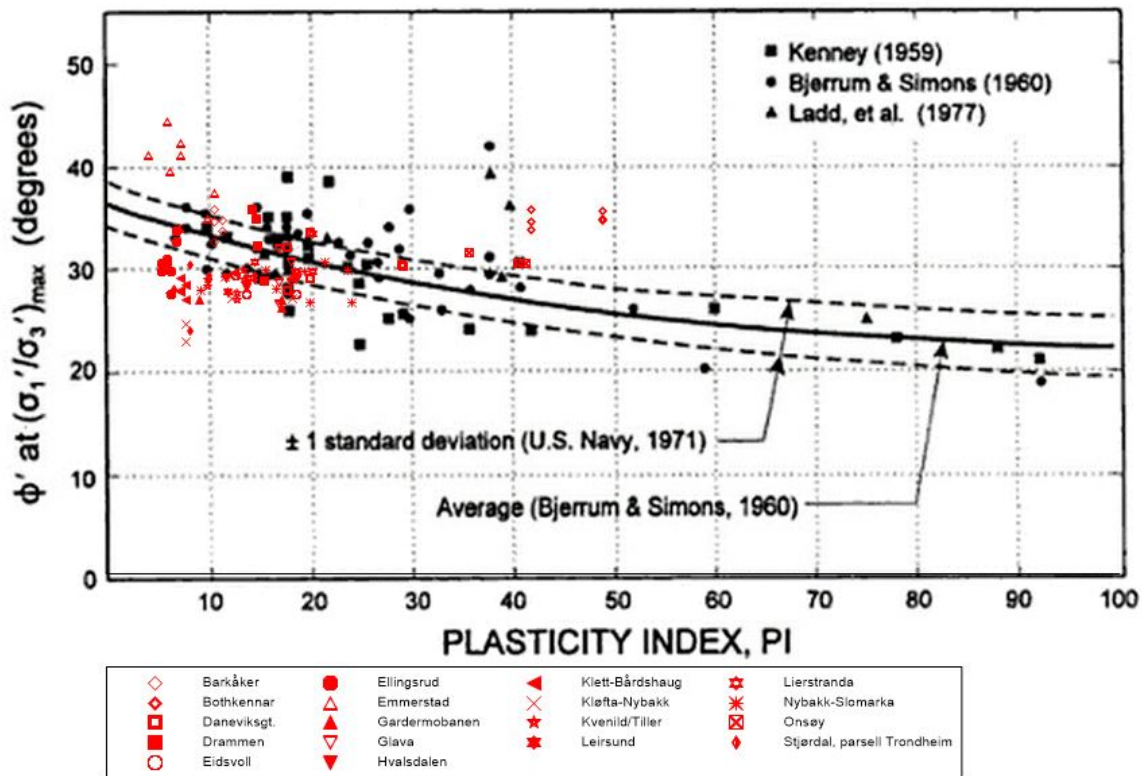


Figure 22: Correlation between plasticity index and peak friction angle ϕ' (Abramson et al. 2002) using block samples data.

3.3 Correlations with 1D compression parameters

Oedometer tests are the base for finding correlations between 1D compression parameters. Interpretation of such tests can be done by different approaches and currently the practice at NGI varies between Janbu (1963) and Casagrande (1936) methods (currently used by the Offshore Geotechnics Department), and Karlsrud (Karlsrud, 1991; Karlsrud & Hernandez-Martinez 2013) currently used by the Onshore Foundations Department.

Janbu's approach

Classical 1D compression parameters published by Janbu (1963) and Janbu (1989) suggested to base the determination of p_c' on plots of tangent constrained modulus values versus σ_v' . However, Janbu did not specify in detail how to do the p_c' -determination. The procedure used here is explained in the sketch shown in in Figure 23.

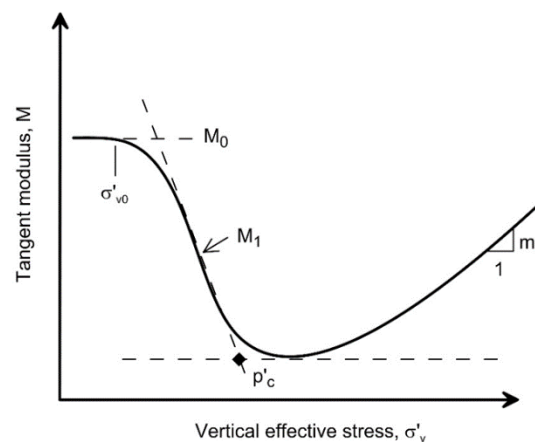


Figure 23: Classical Janbu tangent modulus versus stress model

Janbu (1963) used the resistance concept to interpret one dimensional consolidation in an oedometer test. He defined the tangent modulus (or the constrained modulus), M , as the ratio of the change in stress ($\delta\sigma'$) to the change in strain ($\delta\varepsilon$) for a particular load increment (i.e. $M = \delta\sigma'/\delta\varepsilon$). For a low stress level, around the *in situ* vertical effective stress (σ'_{v0}), the resistance against deformation (M_0) is large. When the stress increases this high resistance decreases appreciably owing to partial collapse of the grain skeleton. Resistance reaches a minimum (M_n) around the preconsolidation stress (p_c'). Subsequently when the effective stress is increased beyond p_c' the resistance increases linearly with increasing effective stress. In the overconsolidated range M_1 (the average between M_0 and M_n) is often used in design.

Behaviour in the normal consolidation stress range can be approximated by a linear oedometer modulus M . Hence, for $\sigma' > p_c'$, $M = m (\sigma' - \sigma_r')$ where m is the modulus number and σ_r' is the intercept on the σ' axis and it called the reference stress.

Casagrande's approach

Casagrande (1936) proposes a classical method to determine the preconsolidation stress using one of the primary results of a laboratory consolidation test: an empirical construction from the void ratio, e , and the logarithm of vertical effective stress, σ'_v , curve.

To determine the preconsolidation stress, p_c' , a geometrical approach is followed based on Figure 24: (i) draw a straight-line continuing back the BC part of the curve, (ii) determine point D where the maximum curvature on the recompression part AB of the curve is located, and (iii) draw the tangent to the curve at D and bisect the angle between the tangent and the horizontal through D. The vertical through the point of intersection of the bisector and CB gives the approximate value of the preconsolidation stress. The Casagrande construction is easy to use and gives good results, provided there is a well-defined break in the $e - \log p'$ plot or the $\varepsilon_v - \log p'$ plot (used by NGI), where ε_v is the vertical strain (Grozic, 2003).

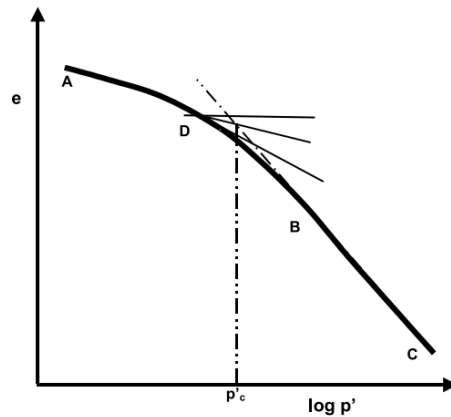


Figure 24: Determination of preconsolidation stress using the Casagrande construction.

Karlsrud's approach

Karlsrud (1991) and Karlsrud & Hernandez-Martinez (2013) use a similar construction as Janbu (1963) adding some other parameters and a different determination of the preconsolidation pressure. As detailed by Karlsrud & Hernandez-Martinez (2013), the modulus behaves as follows (see Figure 25):

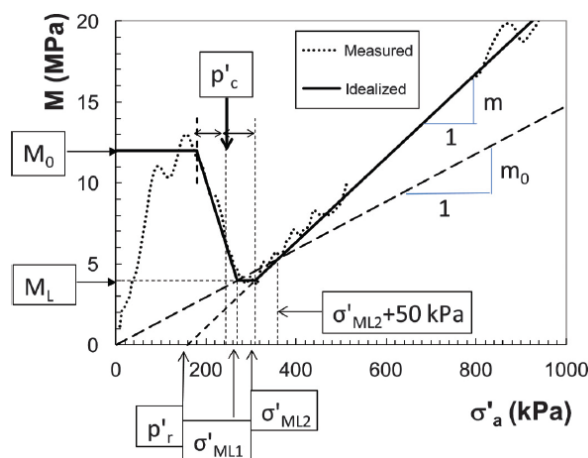


Figure 25: Definition of modulus relationships from oedometer tests according to Karlsrud & Hernandez-Martinez (2013).

- a) During loading from zero to the *in situ* vertical effective stress, the modulus generally increase gradually and then tends to reach a plateau defined as the maximum re-loading modulus, M_0 . The modulus then drops off more or less linearly to a minimum level defined as M_L (i.e. M_n), with corresponding stress defined as σ'_{ML1} . After this stress is reached the modulus increases linearly, but for some clays the modulus is constant up to a stress level defined as σ'_{ML2} before it starts to increase linearly. Janbu's modulus number, m , defines the rate of increase beyond this point. This line defines an $M = 0$ intercept on the stress axis defined as p'_r , which is the

same definition as used by Janbu (1963). Note that for very stiff as well as disturbed clays, p_r' may be negative.

- b) The procedure used for defining the apparent pre-consolidation pressure, p_c' , was first proposed by Karlsrud (1991). This method simply takes the preconsolidation pressure as the average stress at which the tangent modulus starts to drop off, until it starts to climb up again along the virgin modulus line.

In GEODIP's high-quality database, preconsolidation stress and OCR have been determined with the three different approaches detailed above. The rest of the 1D compression parameters are defined following the Karlsrud approach when this was possible.

Effect of the interpretation approach in preconsolidation stress and OCR

As a comparative study, the preconsolidation stress and OCR have been evaluated by the Janbu, Casagrande and Karlsrud methods. A total of 169 oedometer test results have been evaluated.

Figure 26 and Figure 27 show the values the values of p_c' and OCR obtained with the Casagrande, Janbu and Karlsrud approaches. The three methods give very similar values. Janbu values tend to be slightly higher than Casagrande (as observed by Grozic et al. 2003) and Karlsrud values. Karlsrud and Casagrande values tend to show similar values.

The values show more scatter for high p_c' and higher OCR that adds uncertainties to the data deviation. It seems that the data with quality 2 tend to add more deviation to the expected trend. Some exceptions are observed for data with quality 1 that come specifically from Johan Castberg and Kvenild sites. Data from Johan Castberg site was difficult to interpret regarding the definition of the tangents in the graphical methods. Kvenild data is reported as quality 1 data, however this couldn't be confirmed by $\Delta e/e_0$ values. The p_c' and OCR values vary between 4-12%. These differences are more visible for high values of p_c' (i.e. $p_c' > 400-500$ kPa) and OCR (i.e. $OCR > 4$).

In particular, the differences up to 12% are between the Janbu and Casagrande methods and the Janbu and Karlsrud methods. This result is somehow surprising considering that Janbu and Karlsrud are based on the same assumptions. However, the Karlsrud p_c' is calculated as an average from two single values and Janbu defines p_c' as a single point. In addition, it was experienced during the application of the methods a strong dependency of the values on the accuracy of the data plots used for interpretation.

Since all of them are graphical methods, the interpreter must have good plot resolution (large enough scale in the range of analysis) in order to clearly define tangents and pick the values with high accuracy.

Karlsrud & Hernandez-Martinez (2013) comment that a comparative study of different other methods for defining p_c' from oedometer tests was applied to 15 of the oedometer tests in the database used by them. The Karlsrud method comes out just about equal to the average of the other methods (0,8% on the high side).

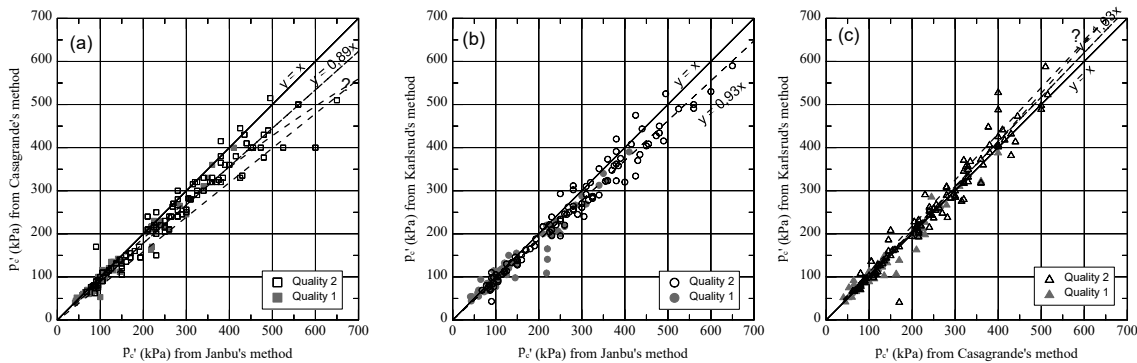


Figure 26: Comparison of preconsolidation stress obtained by: a) Janbu and Casagrande methods, b) Janbu and Karlsrud methods and c) Casagrande and Karlsrud methods.

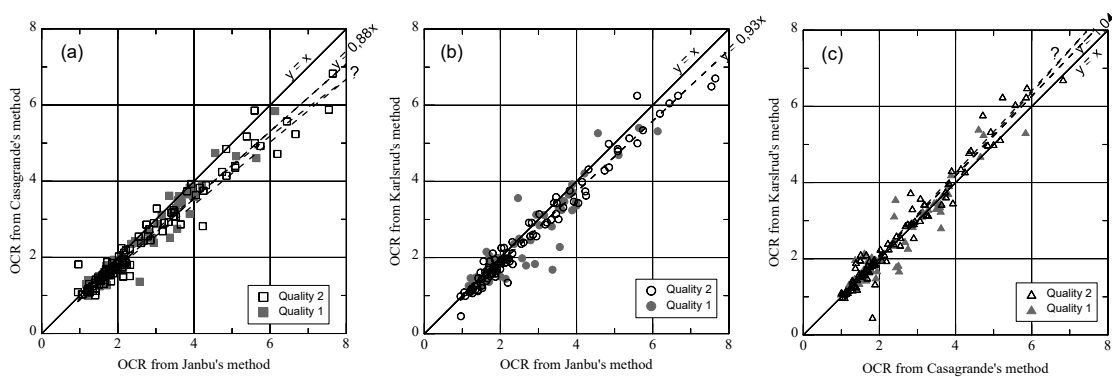


Figure 27: Comparison of OCR obtained by: a) Janbu method and Casagrande methods, b) Janbu and Karlsrud methods and c) Casagrande and Karlsrud methods.

Twelve tests results of the ones studied with Casagrande (1936), Janbu (1969) and Karlsrud (1991) methods (i.e. tests with quality 1 and quality 2, six of each one) were chosen to apply Pacheco Silva (1970) and Becker et al. (1987) methods. In addition, six tests results with quality 3 were included to study the effect of bad quality in the application and determination of p_c' .

Figure 28 and Figure 29 show the values of p_c' and OCR obtained with these approaches for the different specimens evaluated. As observed before, Janbu tends to have higher values of p_c' than the other methods. Janbu values can reach up to 14% difference in OCR and 10% in p_c' with Pacheco Silva method.

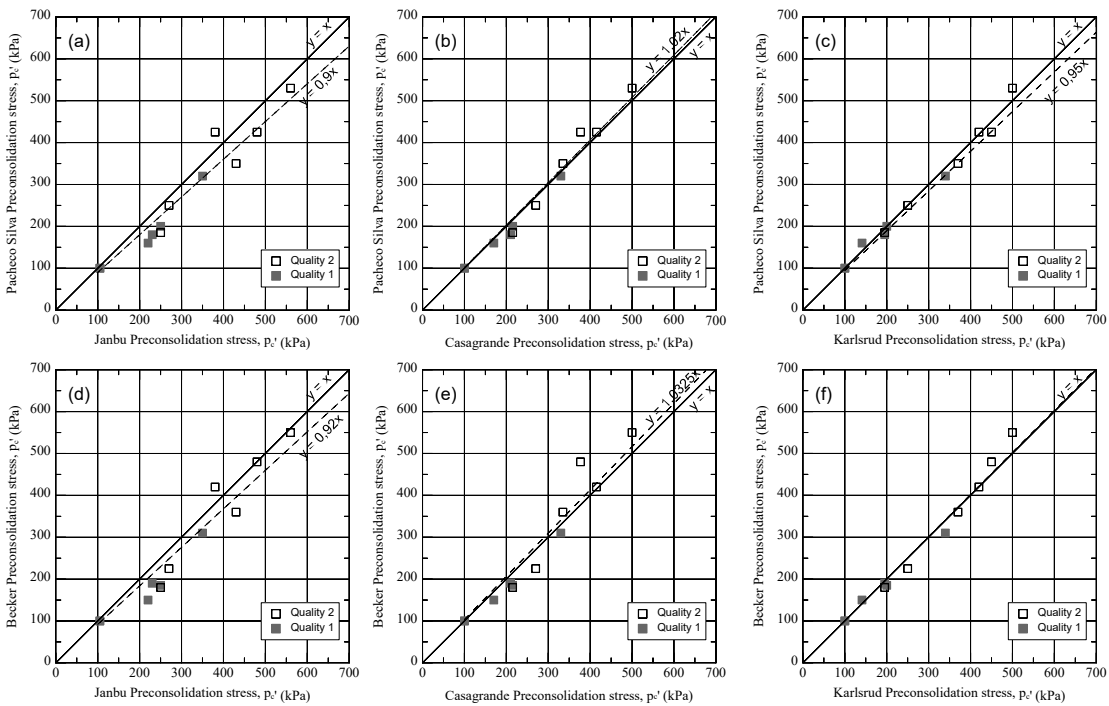


Figure 28: Comparison of p_c' obtained by: a) Pacheco Silva and Janbu methods, b) Pacheco Silva and Casagrande methods, c) Pacheco Silva and Karlsrud methods, d) Becker and Janbu methods, e) Becker and Casagrande and f) Becker and Karlsrud methods.

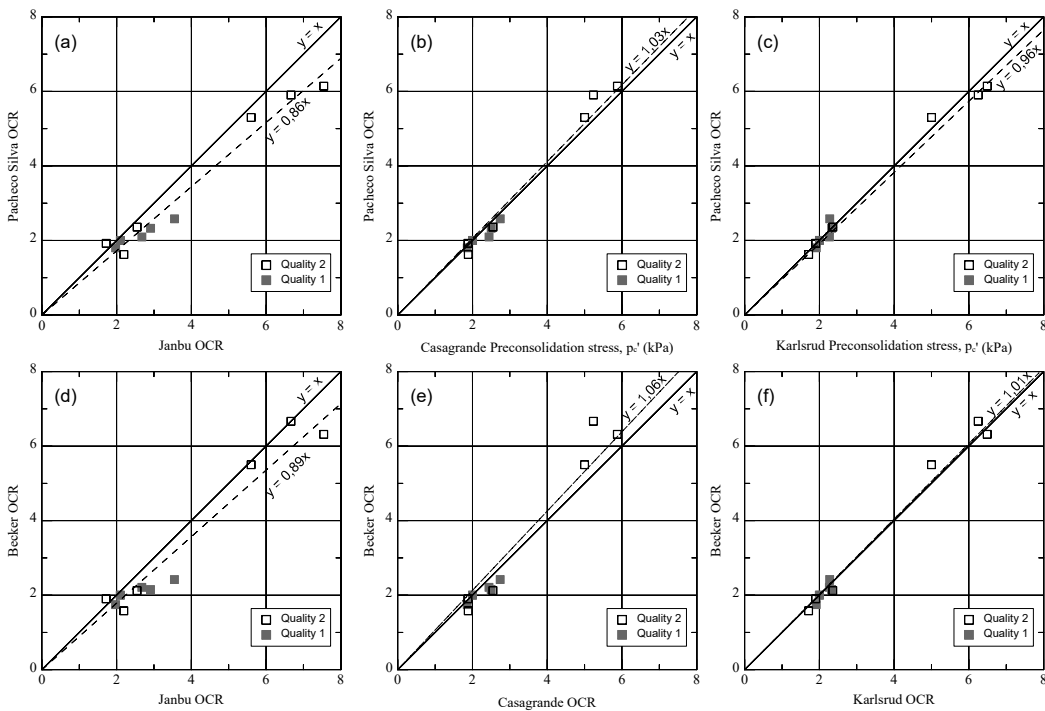


Figure 29: Comparison of OCR obtained by: a) Pacheco Silva and Janbu methods, b) Pacheco Silva and Casagrande methods, c) Pacheco Silva and Karlsrud methods, d) Becker and Janbu methods, e) Becker and Casagrande and f) Becker and Karlsrud methods.

Pacheco Silva and Becker fit pretty well with the Casagrande and Karlsrud methods. Some differences up to 5% are observed between the estimated values of p_c' and OCR. More deviation from the expected trend is observed for high p_c' (i.e. $p_c' > 500$ kPa) and OCR (i.e. $OCR > 4-5$) values, and in particular for samples with quality 2 and 3. The difference between the Pacheco Silva and Becker methods reach 6% for p_c' and OCR.

After these results, no strong p_c' and OCR variations are observed for high quality samples interpreted using the Casagrande, Karlsrud, Pacheco-Silva and Becker methods. The Janbu method gives the highest deviations. One reason could be that the Janbu method does not clearly specify the steps to follow for a graphical interpretation, therefore, it depends on the user's own experience and judgement.

The observation that more scatter is observed for high p_c' and OCR values might be due to the fact that a soil specimen undergoes higher reloading behaviour after sampling and unloading, or recompression, up to the point at which it reaches first the *in situ* condition and then the maximum stress it has experienced in the past, and then the "virgin" compression beyond p_c' . This unloading-reloading process might cause more disturbance in the skeleton and therefore quality reduction.

When comparing all methods, a very significant difference is that Casagrande's method and Pacheco-Silva's method as well as most international methods use double logarithmic scales. Janbu's and Karlsrud methods suggest that a linear scale should be used to avoid misinterpretations since double logarithmic scales can hide large scatter in the data.

One of the main difficulties in applying the graphical methods is the definition of the tangents to the data. Usually a stress-deformation curve from a CRSC odometer test has more data points than traditional incremental loading methods and the "best-fit" lines require some judgement and subjectivity.

Correlations from GEODIP's high-quality database

Figure 30a shows the normalized reloading modulus (i.e. maximum initial tangent modulus), defined as $M_o/(m_o p_c')$, as a function of the water content, w . The range of variation of this normalized modulus is between 1,5 and 6 which is slightly narrower than the range proposed by Karlsrud & Hernandez-Martinez (2013) (i.e. 2-7). This normalized reloading modulus tends to increase with water content as Karlsrud & Hernandez-Martinez (2013) pointed out.

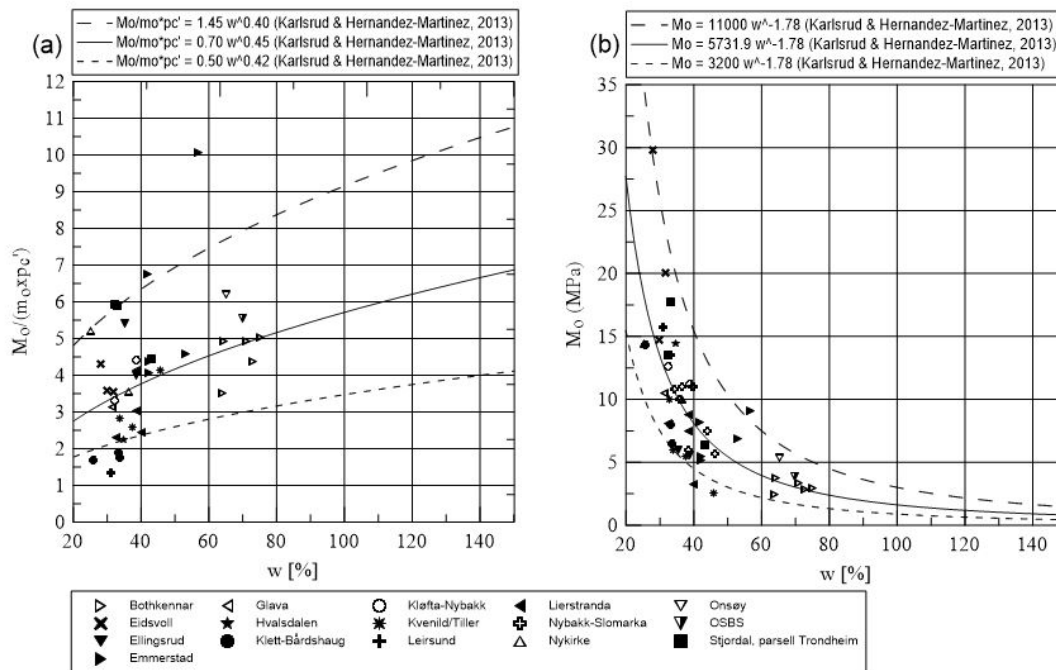


Figure 30: a) Normalized reloading modulus in relation to water content and b) Reloading modulus in relation to water content, both using block samples data.

Figure 30b shows the variation of the reloading modulus with the water content. The data ranges between 2,5 MPa and 20 MPa. The trend lines proposed by Karlsrud & Hernandez-Martinez (2013) are drawn and they seem to group most of the block samples data.

Figure 31 presents values for the modulus number, m , as a function of the water content. As expected, the modulus number decreases with an increase in the water content. A large scatter is observed for a given water content. The trend lines suggested by Karlsrud & Hernandez-Martinez (2013) and Janbu (1989) for Norwegian and Foreign clays are marked. These trends broadly cover GEODIP's high-quality block samples data. Some scatter is observed around 60-70% water content between GEODIP's block samples data and Janbu (1989) trend for Norwegian clays.

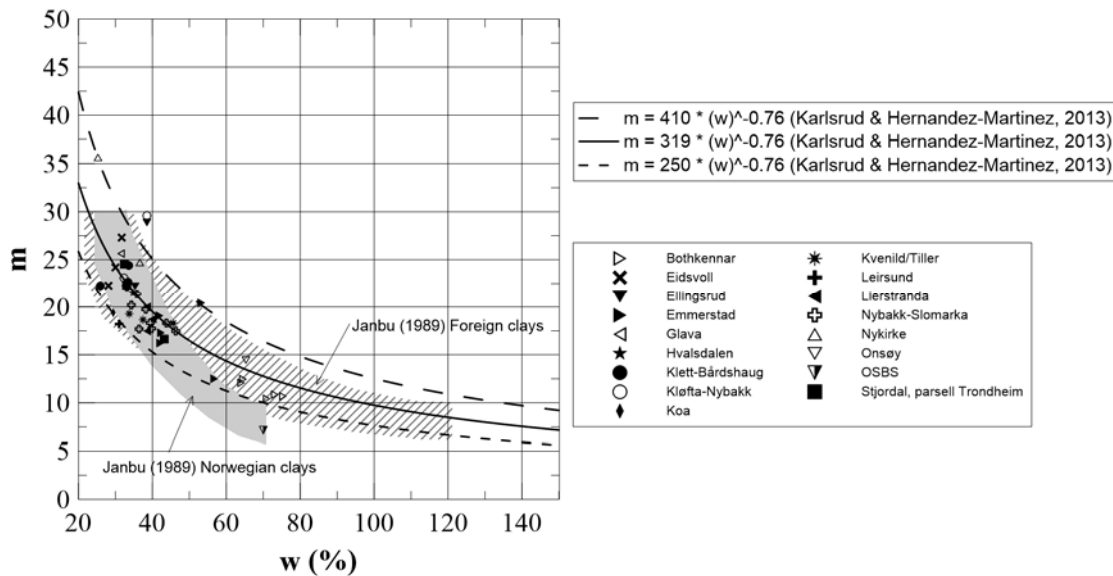


Figure 31: Modulus number, m , versus water content, using block samples data.

Figure 32 shows the correlation between the m_0 -values and water content. As observed by Karlsrud & Hernandez-Martinez (2013), the scatter is about the same as in Figure 31, but the m_0 -values are by definition lower. The correlations given by Karlsrud & Hernandez-Martinez (2013) agree well with GEODIP's block samples data.

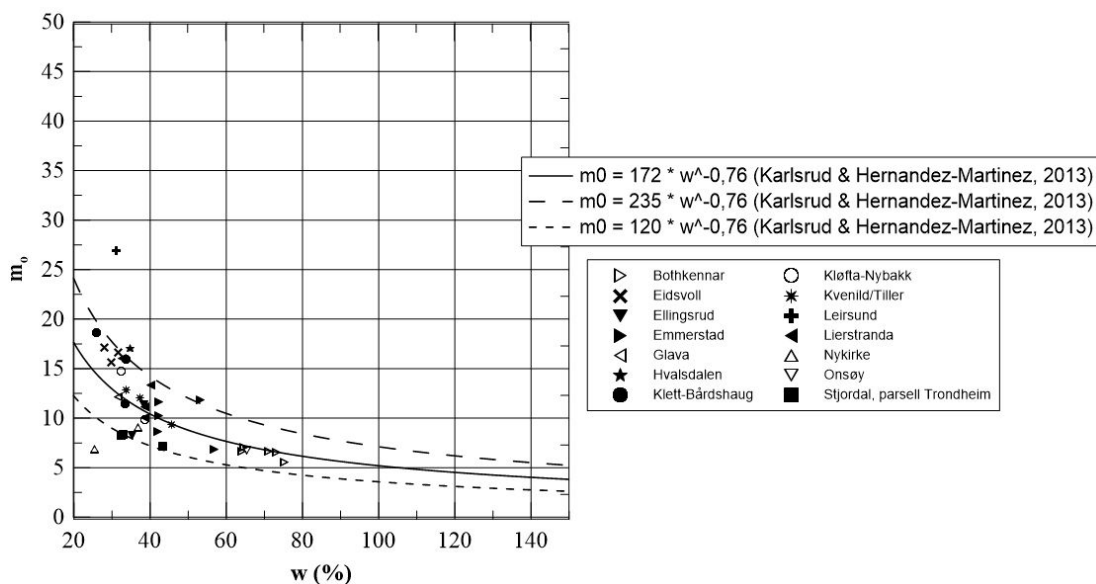


Figure 32: Variation of modulus number related to $p_r' = 0$, m_0 , with water content, using block samples data.

Figure 33 shows (with a high scatter) that measured normalized of p_r'/p_c' increase with water content and they tend to follow the average trend proposed by Karlsrud & Hernandez-Martinez (2013).

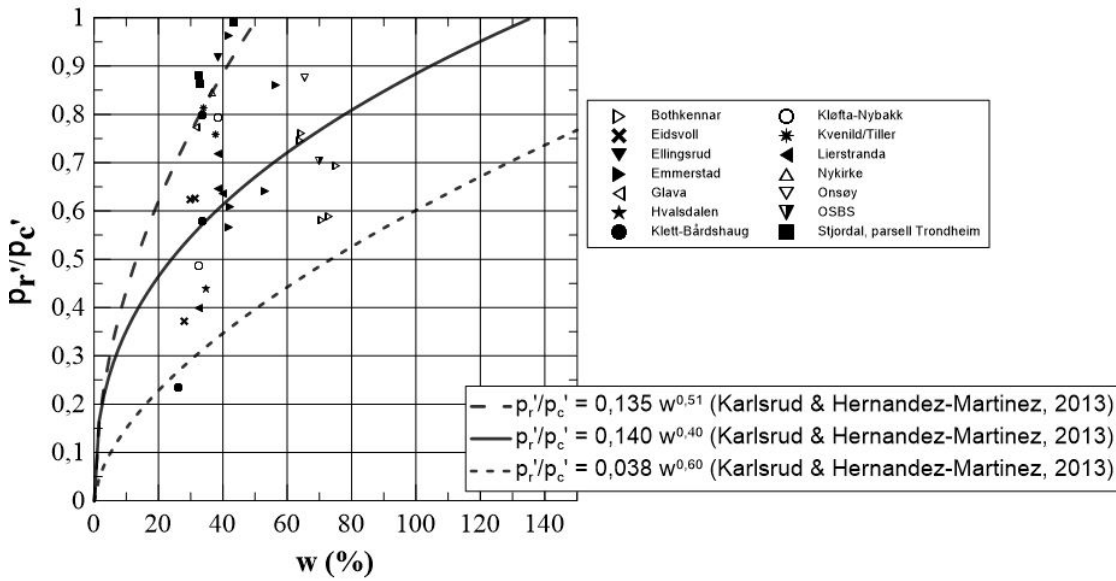


Figure 33: Normalized reference pressure p_r'/p_c' , vs water content, using block samples data.

Figure 34 shows that the reference pressure p_r' decreases with water content. Trend lines proposed by NGI (2012) are plotted and agree with the block samples data in GEODIP's high-quality database.

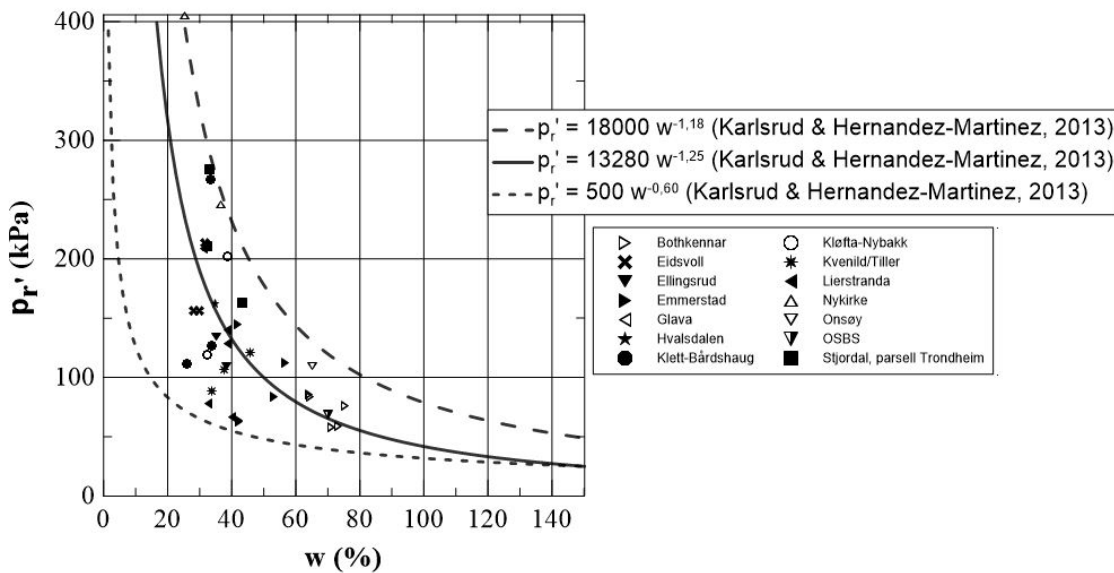


Figure 34: Variation of reference pressure, p_r' , with water content, using block samples data.

Figure 35 shows that the reference pressure p_r' increase with modulus number m as previously pointed out by NGI (2012).

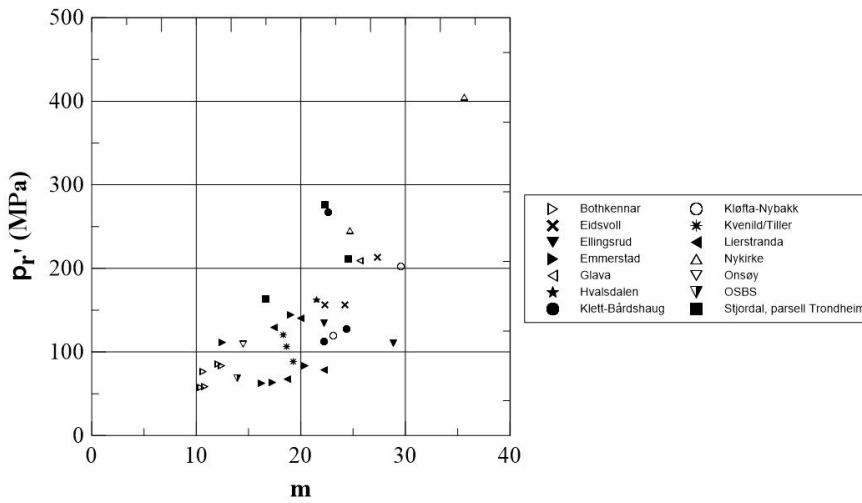


Figure 35: Variation of reference pressure, p_r' , with modulus number, m , using block samples data.

Figure 36 shows that the normalized value of σ'_{ML2}/p_c' decreases with increasing water content for water contents lower than 80%. What this ratio really shows is how fast the modulus drops from the peak M_0 -value to the minimum M_L -value, which is a reflection of the brittleness of the clay structure. The smaller the ratio σ'_{ML2}/p_c' , the more brittle the clay. In this context, for $w < 80\%$, the clay brittleness increases with water content.

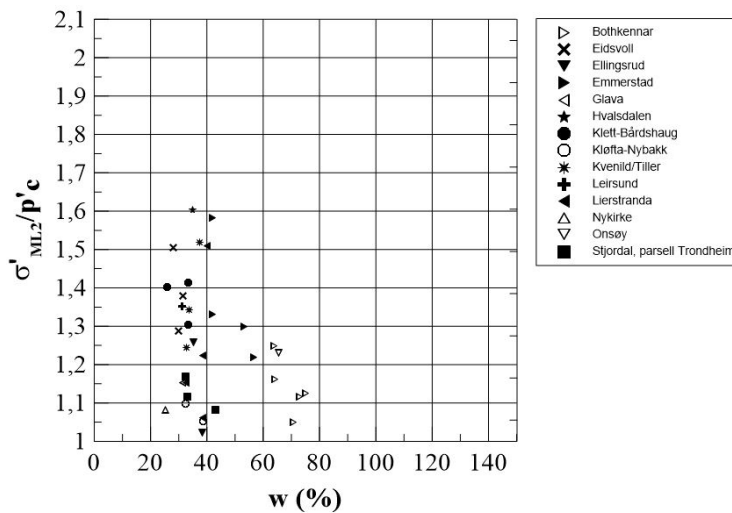


Figure 36: Measured normalized stress level, σ'_{ML2}/p_c' , in relation to water content, using block samples data.

Figure 37 shows that the normalized ratio $\sigma'_{ML2}/\sigma'_{ML1}$ tends to decrease with increasing water content when this value is lower than 80%.

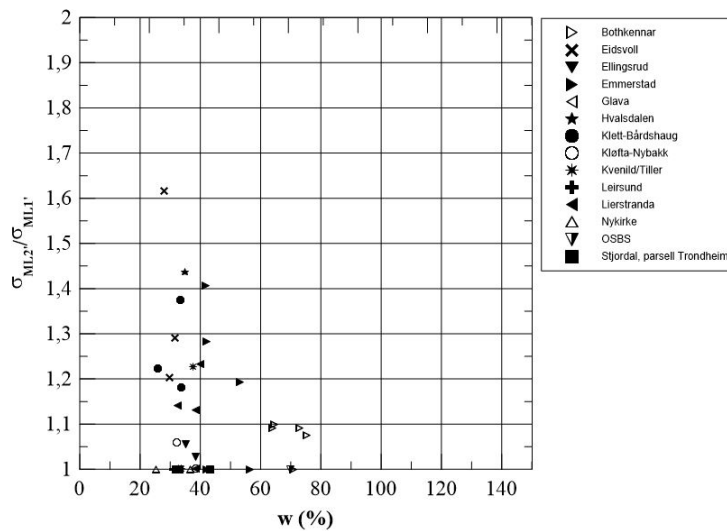


Figure 37. Normalized stress ratios, $\sigma'_{ML2}/\sigma'_{ML1}$, in relation to water content, using block samples data.

4 Suggested supplementary work performed in 2016

One of the objectives of GEODIP's high quality database development was to have an overview of the available data for planning supplementary field and laboratory work. Therefore, the correlations presented above have been compared to previous published correlations based on block samples (see NGI, 2012) and clear scatter is recognized. Particular scatter is observed for silty clays with medium plasticity and for high plasticity clays. The sites contributing more to the scatter (when all the data from the database was included) were Johan Castberg, Ghana and Nybakk-Slomarka (low to medium plasticity).

The sites mentioned have in common that the samples have been taken with 72 mm samplers. A parallel study was performed to quantify the effect of the sampling method in the soil strength and deformation properties. As a first to further investigate the outliers in the database, it was suggested to collect block samples to better study the effect of sample quality at sites where such data was unavailable. Additionally, special attention should be focused to the effect of mineralogy and pore water chemistry as a cause for some of the outliers in the database. Some exceptions could be made, for example, Yang et al. (2015) presented a study about Ghana clay and concluded that Ghana clay (high plasticity clay) is less susceptible to sample disturbance.

Johan Castberg and Ghana are offshore sites where additional sampling was not really possible. Comparing the main characteristics of the sites mentioned (Table 5), it is observed that Johan Castberg site could be compared to Nybakk-Slomarka site since the last one covers a wide range of clay characteristics, for example the low to medium plasticity and sensitivity. Therefore, supplementary block samples in Nybakk-Slomarka

site were recommended. In addition, the need of block samples in Nybakk-Slomarka is also due to its natural variability (observed in the wide range of sensitivity values and OCR, for example) of the data in the correlations presented before. Nybakk-Slomarka data show quite large deviations from the correlations presented above and new block samples at selected locations can shed light on the cause of the difference and to what extent it can be explained by the change in volume during the re-consolidation.

Table 5. Main soil properties of the sites giving scatter to the correlations

Site	Description	Sampler	%w	% clay	IP	St	OCR
Johan Castberg	Clay	72 mm	22-38	30-45	20-42	1,1-2,8	1,2-4,5
Nybakk-Slomarka	Silty clay, clay, quick clay	72 mm	30-45	17-67	7-28	1-170	1-9
Ghana	Clay	72 mm	90-145	45-65	70-95	2-6	1-3
Trøndelag	Silty clay and quick clay	72 mm	20-45	21-55	5-23	2-240	1-9

Some additional block samples from a region in Trøndelag (ie. Koa and Skatval) were also taken to recover low to medium plastic clays and high sensitive clays, with a high silt content. In addition, CPTU tests should be were carried out in these areas where more silt content was observed.

The supplementary field and laboratory testing covered CPTU, index testing, CAUC, CAUE and CRSC. DSS were included when possible to add more data for future correlations. Additional mineralogy tests and pore water chemistry were also included to try to explain the reasons for the high spreading in the database.

As a summary, the work plan carried out during 2016 collected block samples from particular locations at Nybakk-Slomarka, Skatval and Koa.

5 Quality control of the data included in the database

GEODIPS high quality database has been controlled in 2016 regarding assumptions made in laboratory tests (i.e. consolidation stress, *in situ* effective stress) and some other aspects that could add scatter to the data. A summary of the quality control performed for each site is presented in Appendix A.

6 Observations about scatter of the data in the database

After performing the quality control of GEODIPs of the data included in the database, additional observations are noted regarding the sites that contribute most to the scatter. As a starting point, the relations between OCR_{-SuC}/σ_{vo}' and OCR_{-SuE}/σ_{vo}' are used to look up at the scatter. The main objective is to identify the sites that contribute most to the scatter. Some observations have been pointed out and summarized below.

Figure 17 shows the relation between $Su_c-\sigma_{vo}'$ -OCR and the following remarks are observed regarding the scatter of data and the outliers to the main trend:

Test site	Observations
Norwegian sea	The highest point outside the trend has the lowest LI = 19% than the rest of the points. The rest of the points are also in the upper level and they LI > 100%. The point that fits the trend has a LI = 43%. OCR < 2.
Ghana	Very plastic clays (High IP > 70). OCR < 2-3.
Kvål Stavne Klett	The data is towards the lower bound of the general trend.
Koa Nybakk-Slomarka Skatval	The data is towards the lower bound of general trend. New laboratory data and mineralogy data has been collected (see Chapter 7).
Johan Castberg Emmerstad	The data is towards the upper bound of the general trend.
Laminaria	Data with LI > 100 % and OCR < 2 are towards the upper bound, and data that has LI = 97% and OCR = 3 is inside the trend.
Skjelstadmark Onsøy	Data is spread between upper and lower bounds.
Tiller	It has a point data outside the trend.

Figure 18 shows the relation between $Su_E-\sigma_{vo}'$ -OCR and the following remarks are observed regarding the scatter of data and the outliers to the main trend:

Test site	Observations
Rosten Kløfta-Nybakk	The data is towards the lower bound of the general trend.
Nybakk-Slomarka Skatval Koa	The data is towards the lower bound of the general trend. New lab data mineralogy data has been collected (see Chapter 7).
Norwegian sea Emmerstad	The data is towards the upper bound of the general trend.
Onsøy	It has a point data outside (in the top of) the trend.

7 Advanced lab and field work in 2016 from selected sites

During 2016, advanced laboratory and field work from three selected sites: Skatval, Koa and Nybakk-Slomarka was performed in order to study sample disturbance, mineralogy and the database scatter. In addition to the 72 mm samples, Sherbrooke Block samples (Ø250 mm) and miniblock samples (Ø160 mm) were collected at each site. At each of the sites the different samples were taken at similar depths.

Measurements of shear-wave velocity in the field (V_s - MASW) were obtained from multichannel analysis of surface waves (MASW) at Koa and Skatval (Appendix B). Unconfined measurements of shear-wave velocity (V_s -0) were collected on site and in the laboratory using the bender element device described by Landon et al. (2007). For this, samples were carefully trimmed from block sample size to a cube about 70x70x70 mm size due to restrictions in the equipment size.

The laboratory program included index testing, grain size distribution and more advanced tests such as triaxial tests (CAUC & CAUE), oedometer tests at constant rate of strain (CRS) and direct shear tests (DSS). Additional measurements of V_s were acquired after sample consolidation during CAUC, CAUE and DSS tests (V_s -lab).

The new collected lab data for Koa and Skatval are summarized in Appendix C and Appendix D. The new collected data for Nybakk-Slomarka is summarized in the report 20150030-08-R (NGI, 2016b). Part of the data has been presented in Paniagua et al. (2017).

Mineralogy has also been analysed for the sites Koa, Skatval and Nybakk-Slomarka. This data is summarized in rapport 20150030-12-R (NGI, 2017).

8 Conclusions

This study presents GEODIP's high quality database for clay materials. The database integrates existing high quality data from block sampling in clay as well as supplementary data from research and development (R&D) assignments, both offshore and onshore.

Relations between strength and deformation parameters against index properties obtained from block samples data in GEODIP's high quality database agree well with previously proposed correlations for clays found in the literature. However, high scatter in the data is observed. There is a need for understanding the outliers.

Updated and new correlations (presented in separate reports) take into account the inherent variability in index properties of the sites under study. Those results clearly show the importance of establishing site specific correlations when assessing geotechnical parameters in particular when CPTU tests are used. In soft and sensitive

clays, it is also particularly important that the correlations are established from large diameter samples of very high quality.

In general, it is recommended that engineers consider all available data including available relationships and site-specific geotechnical data. The use of correlations in geotechnical engineering should be limited to the conditions for which they were developed and calibrated. The recommendations presented in this report should be used in conjunction with the engineer's own experience and engineering judgment.

9 Acknowledgements

This work is funded through the NFR strategic research project SP8- GEODIP at NGI.

10 References

Abramson, L.W., Lee, T.S., Sharma, S. & Boyce, G.M. (2002). Slope stability and stabilization methods. John Wiley & Sons, Inc.

Becker, D.R., Crooks, J.H.A, Been, K. & Jefferies, M.G. (1987). Work as criterion for determining in-situ & yield stresses clays. *Can. Geotech. J.* 24: 549-564.

Casagrande A. (1936). The determination of the preconsolidation load and its practical significance. *Proc. First Intern. Conf. on Soil Mech. and Found. Eng., Cambridge, Mass USA*: 60-64.

Bryhn, O. R., Loken, T., and Reed, M. G. (1988). Stabilization of Sensitive Clays (Quick Clays) Using $Al(OH)_2.5Cl_{0.5}$. *Norges Geotekniske Institutt*, (170).

DeGroot, D.J., Lunne, T., Andersen, K.H., Boscardin, A.G. (2012). Laboratory measurement of the remoulded shear strength of clays with application to design of offshore infrastructure. *Offshore Site Investigation and Geotechnics, SUT Conference, London 12-14 September 2012, Proc. 7th International Conference*, pp. 355-364.

Grozic, J.L.H, Lunne, T. & Pande, S. (2003). An oedometer test study on the preconsolidation stress of glaciomarine clays. *Canadian Geotechnical Journal* 40: 857-872.

Grozic, J.L.H., Lunne, T. & Pande, S. (2003). An oedometer test study on the preconsolidation stress of glaciomarine clays. *Can. Geotech. J* 40, 857-872.

Grozic, J.L.H., Lunne, T. & Pande, S. (2005). Reply to the discussion by Clementino on: "An oedometer test study on the preconsolidation stress.

Gylland A., Long M., Emdal, A. & Sandven, R. (2013). Characterisation and engineering properties of Tiller clay. *Engineering Geology* 164: 86-100.

Hilmo, B.O. (1989). The Mineral Composition, Chemistry of Colloids and Mechanical Properties of Marine Sensitive Clays. (In Norwegian), PhD Thesis Norwegian University of Science and Technology (NTNU), Trondheim.

ISO (2014). ISO Standard 19901-8:2014. Part 8. Marine Soil Investigations.

Janbu, N. (1963). Soil compressibility as determined by oedometer and triaxial tests. *Proc. Euro. Conf. on Soil Mech. and Found. Eng.* 1: 19-25.

Janbu, N. (1989). *Grunnlag i Geoteknikk*. Trondheim: Tapir.

Karlsrud, K. & Hernandez-Martinez, F.G. (2013). Strength and deformation properties of Norwegian clays from laboratory tests on high-quality block samples. *Canadian Geotechnical Journal*: 1273-1293.

Karlsrud, K. & Lunne, T. (2005). CPTU correlations for clays. *Proc. of 16th ICSMGE*, 693-702.

Karlsrud, K. (1991). Sammenstilling av noen erfaringer med prøvetaking og effekt av prøveforstyrrelse i norske marine leire. NGI report 521500-6.

Ladd C.C. & Foot, R. (1974). New design procedure for stability soft clays. *Journal of the Geotechnical Engineering Division* 100 (7): 763-786.

Ladd, C. (1991). Stability Evaluation during Staged Construction. 22nd Terzaghi Lecture. *Journal of Geotechnical Engineering*, 117(4): 540-615.

Landon M.M., De Groot D.J. and Sheahan T.C. (2007). Nondestructive sample quality assessment of a soft clay using shear-wave velocity. *J Geotech Geoenv Eng ASCE* 133, 424-432

Leroueil, S., Tavenas, F. & Le Bihan J.-P. (1983). Propriétés caractéristiques des argiles de l'est du Canada. *Canadian Geotechnical Journal* 20 (4), 681-705.

Lunne, T., Robertson, P.K., and Powell, J.J.M. (1997). *Cone penetration testing in geotechnical practice*. Blackie Academic, EF Spon/Routledge Publ., New York.

Lunne, T., Berre, T., & Strandvik, S. (1998). Sample disturbance effects in deepwater soil investigations. *SUT Conference on Soil Investigations and Foundation Behaviour*, London: 199-220.

Lunne, T. (2002). Engineering properties of lean Lierstranda clay. In: Coastal Geotechnical Engineering in Practice, Nakase & Tsuchida (eds).

Lunne, T., Long, M., and Forsberg, C.F. 2003. Characterisation and engineering properties of Onsøy clay. In Proceedings of the International Workshop on Characterisation and Engineering Properties of Natural Soils, Natural Soils 2002, Singapore, 2–4 December 2002. Edited by T.S. Tan, K.K. Phoon, D.W. Hight, and S. Cerark. A.A. Balkema, Lisse, the Netherlands. Vol. 1, pp. 395–428

Lunne, T., Andersen, K., Low, H.R., Randolph, M.F. & Sjursen, M. (2011). Guidelines for offshore in situ testing and interpretation in deepwater soft clays. Canadian Geotechnical Journal 48 (4): 543-556.

NGF. (2013). Melding Nr. 11, Veiledning for prøvetaking. Norwegian Geotechnical Society.

NGI (2017). SP8 – Soil Parameters in Geotechnical Design (GEODIP). Mineralogy data for Skatval, Koa and Rakkestad clay sites. Report nr. 20150030-12-R, rev. 0.

NGI. (2016a). Datarapport – grunnundersøkelser. Detaljprosjektering Stjørdal-Steinkjer. Doknr. 20160026-03-R datert 2016-07-04.

NGI (2016b). SP8 – Soil Parameters in Geotechnical Design (GEODIP). Rakkestad clay – block sampling and laboratory results. Report nr. 20150030-08-R, rev. 0. Date 24.11.2016.

NGI. (2006). Shear Strength Parameters Determined by In Situ Tests for Deep Water Soft Soils. Report 20041618-1. 22.02.2006.

NGI. (2008). Measurement of Remoulded Shear Strength, Summary Report, Manual. Report 20061023-5, 02.09.2008.

NGI (2011). Time effects on pile capacity. Factual report, test site Onsøy. Report nr. 20061251-00-248-R, 23 September 2011

NGI. (2012). Summary of compressibility, strength and deformation parameters in relation to index properties. Report 20051014-00-1-R, 22.02.2012.

NGI. (2013). Johan Castberg – 2013 Soil Investigation. Report 20130280-02-R. 01.11.2013.

NGI. (2014a). E16 Nybakk-Slomarka. Detalj- og reguleringsplan - Tolking av jordartparametere. Oslo: NGI. Report 20120491-6-R, 18.12.2014.

NGI. (2014b). Ghana laboratory testing, 9756 Geotechnical re-port Part B. Report 20140080-01-R. 23.10.2014

NGI. (2015a). SP8 – Soil Parameters in Geotechnical Design (GEODIP). Report 20150030-01-R. 26.11.2015.

NGI. (2015b). Correlations between shear wave velocity and geotechnical parameters in Norwegian clays. Report 20150030-04-R. 02.11.2015.

NIFS (2014). En omforent anbefaling for bruk av anisotropifaktorer i prosjektering i norske leirer. Naturfareprosjektet DP. 6 Kvikkleire.

Paniagua, P., L'Heureux, J.-S., Carroll, R., Kåsin, K., Sjørusen, M. & Amundsen, H. (2017). Evaluation of sample disturbance of three Norwegian clays. Proceedings of the 19th International Conference on Soil Mechanics and Geotechnical Engineering, Seoul.

Pacheco Silva, F. (1970). A new graphical construction for determination of the pre-consolidation stress of a soil sample. Proceedings 4th Brazilian Conference Soil Mechanics and Foundation Engineering, Rio de Janeiro, 225-232.

Rosenqvist, I. T. (1953). Considerations on the Sensitivity of Norwegian Quick-Clays. Geotechnique 3: 195-20

Appendix A

NOTES REGARDING THE QUALITY CONTROL OF INCLUDED DATA IN THE DATABASE

Contents

A1	Leirsund	2
A2	Gardemoenbanen	2
A3	Hvalsdalen	2
A4	Eidsvoll B110	2
A5	Eidsvoll B116	2
A6	Glava	2
A7	Barkåker	2
A8	Lierstranda	3
A9	Bothkennar	3
A10	Drammen	3
A11	Emmerstad	3
A12	Ellingsrud	3
A13	Onsøy 1	3
A14	Onsøy 2	3
A15	Stjørdal parsell Trondheim	4
A16	Nykirke	4
A17	Danneviksgata	4
A18	Kvenhild	4
A19	Klett-Barshaug	4
A20	Kløfta	4
A21	Onsøy OSBS (2004)	4
A22	Nybakk-Slomarka	5
A23	Offshore data	5

A1 Leirsund

- ↗ Only one triaxial test meets the desired quality criteria (1-2) in accordance with Lunne et al. (2004)
- ↗ All CRS tests within quality class 3 or 4 have been excluded from the database
- ↗ Results with significantly higher consolidation stress in the laboratory compared to in-situ should be discarded from the database
- ↗ Test B151 from 11.95 m depth is not present in the database

A2 Gardemoenbanen

- ↗ All CRS tests have quality index above 3 and is therefore excluded from the database
- ↗ Two triaxial compression tests are classified as high-quality tests as well as one triaxial extension test

A3 Hvalsdalen

- ↗ Results from 4.2 m depth is included, but it should be emphasized that these tests are classified as weathered clay
- ↗ Two CRS test results are discarded due to low quality

A4 Eidsvoll B110

- ↗ SP8 database contains all results from this test site

A5 Eidsvoll B116

- ↗ Two CRS results are omitted from the database due to low quality and difficulty in interpretation of oedometer results
- ↗ As result of this, the corresponding triaxial results are omitted

A6 Glava

- ↗ SP8 database contains all results from this test site

A7 Barkåker

- ↗ Overconsolidation ratio is specified for the triaxial tests, but no data exist. Neither does CPTU data.

A8 Lierstranda

- ↗ Incorrect in-situ effective stresses for tests from depth 12.3 m, 16.4 m and 22.4 m – both for CRS and CAUC tests. Correct effective stresses are presented in Lunne (2000)
- ↗ Both IL and CRS oedometer tests have been carried out. SP8 database only contains CRS results due to consistency requirements

A9 Bothkennar

- ↗ This is a soft clay from Great Britain. These results are included in the SP8 database for comparison

A10 Drammen

- ↗ No available CRS test results on block samples
- ↗ No available CPTU test results

A11 Emmerstad

- ↗ Could be cemented clay. High values of undrained shear strength in comparison to typical Norwegian clays.
- ↗ These results are included in the database

A12 Ellingsrud

- ↗ SP8 database contains all results from this test site

A13 Onsøy 1

- ↗ SP8 database contains all results from this test site

A14 Onsøy 2

- ↗ SP8 database contains all results from this test site

A15 Stjørdal parsell Trondheim

- ↗ SP8 database contains all results from this test site which is more correctly referred to as "Møllenberg" test site.

A16 Nykirke

- ↗ SP8 database contains all results from this test site

A17 Danneviksgata

- ↗ IL 24h oedometer tests on 72-mm tests. CK0UC tests have also been carried out. See Lunne et al. (2006)

A18 Kvenhild

- ↗ Difficult to determine preconsolidation test from oedometer IL tests. Some corrections have been applied to obtain results presented in the database.
- ↗ Uncertainties in interpretation of in-situ pore pressure distribution and effective stresses leading to uncertainties in OCR. Should be checked.

A19 Klett-Barshaug

- ↗ Some issues related to estimation of p'_0 in the range of 4-30 kPa. It is assumed that p'_0 values are correct and the pore pressure, u_0 , is calculated from this assumption.

A20 Kløfta

- ↗ Some issues related to estimation of p'_0 in the range of 2-10 kPa. This is corrected for in the SP8 database.

A21 Onsøy OSBS (2004)

- ↗ Triaxial tests on samples from 9.18 m depth have been carried out with different strain rate (0.01-7%/hour).
- ↗ Sample quality data missing for 3 out of 4 CRS tests.
- ↗ Should be possible to compare CPTU results from this site

A22 Nybakk-Slomarka

- ↗ Consolidation stress in triaxial tests is different from the actual vertical effective stress in situ (p_o'), for some data points. The difference is due to the disagreement between the specifications made after "the best estimate" without in situ pore pressure data and the "final estimation" including pore pressure data and measured the water content (and unit weight).
- ↗ The data with a large difference between p_o' and the consolidation stress used in lab testing has been removed.

A23 Offshore data

- ↗ Data with significant difference between consolidation stress and in-situ stress are not included in the database

Appendix B

MASW DATA FROM KOA & SKATVAL



AGL16239B_01

**REPORT ON THE
GEOPHYSICAL SURVEYS
AT
SKATVAL & KOA, NORWAY
FOR THE
NORWEGIAN GEOTECHNICAL INSTITUTE**



APEX Geoservices Limited
Unit 6 Knockmullen Business Pk.,
Gorey,
Co. Wexford, Ireland

T: +353 402 21842
E: info@apexgeoservices.ie
W: www.apexgeoservices.com

10TH NOVEMBER 2016

PRIVATE AND CONFIDENTIAL

THE FINDINGS OF THIS REPORT ARE THE RESULT OF A GEOPHYSICAL SURVEY USING NON-INVASIVE SURVEY TECHNIQUES CARRIED OUT AT THE GROUND SURFACE. INTERPRETATIONS CONTAINED IN THIS REPORT ARE DERIVED FROM A KNOWLEDGE OF THE GROUND CONDITIONS, THE GEOPHYSICAL RESPONSES OF GROUND MATERIALS AND THE EXPERIENCE OF THE AUTHOR. APEX GEOSERVICES LTD. HAS PREPARED THIS REPORT IN LINE WITH BEST CURRENT PRACTICE AND WITH ALL REASONABLE SKILL, CARE AND DILIGENCE IN CONSIDERATION OF THE LIMITS IMPOSED BY THE SURVEY TECHNIQUES USED AND THE RESOURCES DEVOTED TO IT BY AGREEMENT WITH THE CLIENT. THE INTERPRETATIVE BASIS OF THE CONCLUSIONS CONTAINED IN THIS REPORT SHOULD BE TAKEN INTO ACCOUNT IN ANY FUTURE USE OF THIS REPORT.

PROJECT NUMBER	AGL16239B		
AUTHOR	CHECKED	REPORT STATUS	DATE
EURGEOL SHANE O'ROURKE P.GEO., M.Sc (GEOPHYSICS)	TONY LOMBARD M.Sc (GEOPHYSICS)	V.01	10 TH NOVEMBER 2016

CONTENTS

1.	EXECUTIVE SUMMARY.....	1
2.	INTRODUCTION	2
2.1	Survey Objectives.....	2
2.2	Site Background	2
2.2.1	Topography.....	3
2.2.2	Bedrock & Sediments	5
2.3	Survey Rationale	8
3.	SKATVAL RESULTS	9
3.1	MASW.....	9
3.2	Seismic Refraction Profiling.....	10
4.	KOA RESULTS	11
4.1	MASW.....	11
4.2	Seismic Refraction Profiling.....	12
5.	REFERENCES	13
6.	APPENDIX A: DETAILED METHODOLOGY	14
6.1	MASW.....	14
6.1.1	Principles	14
6.1.2	Data Collection	14
6.1.3	Data Processing	15
6.1.4	Relocation.....	15
6.2	Seismic Refraction Profiling.....	15
6.2.1	Principles	15
6.2.2	Data Collection	15
6.2.3	Data Processing	16
6.2.4	Relocation.....	16
7.	APPENDIX B: MASW RESULTS (S-WAVE)	17
8.	APPENDIX C: SEISMIC REFRACTION RESULTS (P-WAVE)	17
9.	APPENDIX D: DRAWINGS	20

1. EXECUTIVE SUMMARY

APEX Geoservices Limited was requested by the Norwegian Geotechnical Institute to acquire S-wave and P-wave velocities at the Skatval and Koa test sites, Norway. Both sites are covered in thick leached sensitive clay.

The objectives of the investigation were to provide S-wave (shear-wave) and P-wave velocities at the locations specified by the client.

The investigation consisted of MASW Profiling (Multichannel Analysis of Surface Waves) and Seismic Refraction Profiling.

Skatval

The shear wave velocities ranged from 142-195 m/s (average of 170 m/s) from 1.9-21.9m bgl.

The P-wave wave velocities ranged from 302-1736 m/s for overburden from 0-30.2m bgl. Bedrock has been interpreted as ranging from 26.4-30.2m bgl, with a velocity of 5665-5676 m/s.

Koa

The shear wave velocities ranged from 149-196 m/s (average of 179 m/s) from 2.9-19.5m bgl.

The P-wave wave velocities ranged from 330-1796 m/s for overburden from 0-25m bgl. Bedrock depth was not reached for the seismic refraction profiles at Koa.

2. INTRODUCTION

APEX Geoservices Limited was requested by the Norwegian Geotechnical Institute to acquire S-wave and P-wave velocities at the Skatval and Koa test sites, Norway.

2.1 Survey Objectives

The objectives of the survey were to:

1. To provide S-wave values at the locations specified by the client.
2. To provide P-wave values at the locations specified by the client.

2.2 Site Background

The Skatval and Koa test sites are areas of leached sensitive clay to the east of Trondheim.

The Skatval site is 10km north of Vaernes Airport, at the south-eastern side of Trondheimsfjorden, and approx. 100m west of the E6 motorway. The survey was carried out upon a crop field.

The Koa site is 60km north Vaernes Airport, at the north-eastern side of Trondheimsfjorden, and approx. 200m east of the E6 motorway. The survey was also carried out upon a crop field.

Apex Geoservices Ltd. carried out 1D MASW (Multichannel Analysis of Surface Waves) Profiling and Seismic Refraction Profiling in both areas to provide S-wave and P-wave values as part of the ongoing research.

The survey was carried out under the direction of the client, NGI.



Fig.2.1. Survey Locations (shown in red).

2.2.1 Topography

The topography for the Skatval survey area was generally flat to sloping, with elevation ranging from c.172-174 mOD (Fig.2.2). The topography for the Koa survey area was generally undulating, with elevation ranging from c.187-191 mOD (Fig.2.3).



Fig.2.2. Survey area for Skatval.



Fig.2.3. Survey area for Koa.

2.2.2 Bedrock & Sediments

Skatval

The 1:250000 Sediments map (<http://www.ngu.no/en/topic/datasets>) for the area (Fig.2.4) shows that outcrop is present approx. 300m to the north and south of the survey area (=5 in Fig.2.4). The Sediments map describes the survey area as being covered with “Ocean and inlet deposition, continuous cover, often with large thickness”.

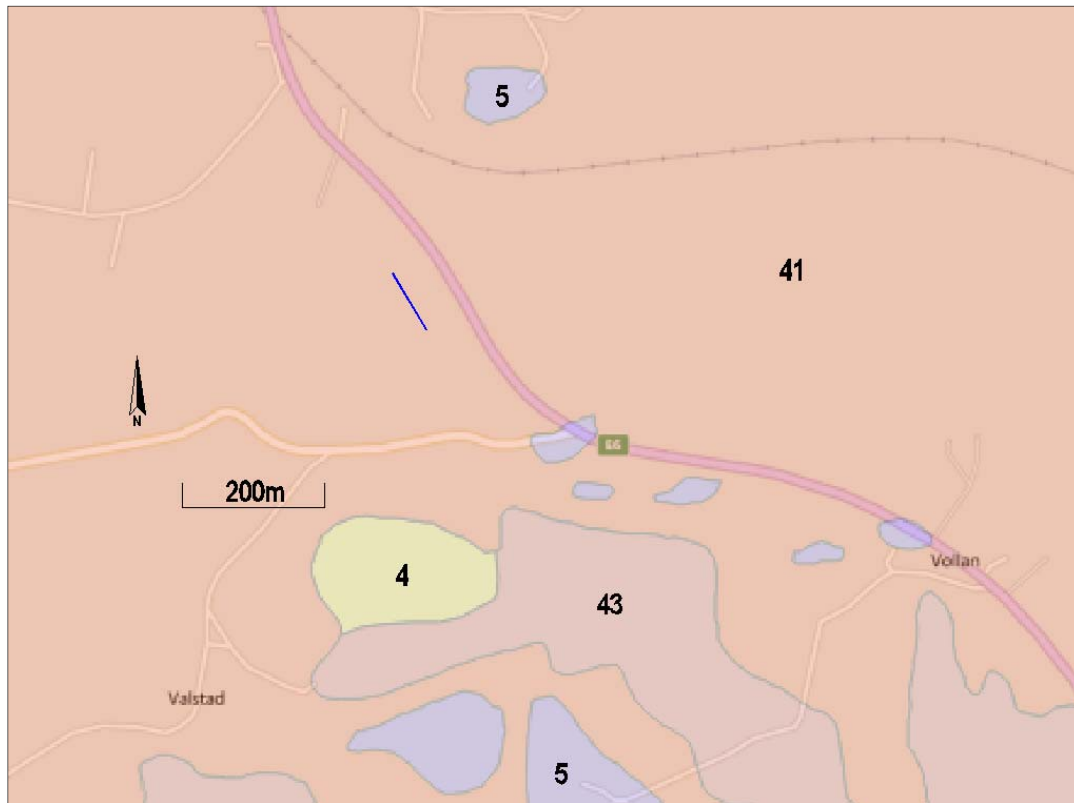


Fig.2.4. Sediments map for Skatval. Blue line indicates 92m P-wave profile.

4 = Humusdekke/tynt torvedke over berggrunn

41 = Hav-og fjordavsetning, sammenhengende dekke, ofte med stor mektighet.

43 = Hav- og fjordavsetnin og strandavsetning, usammenhengende eller tynt dekke over berggrunnen

5 = Bart fjell

Koa

The 1:250000 Sediments map (<http://www.ngu.no/en/topic/datasets>) for the area (Fig.2.5) shows that outcrop is present approx. 200m to the north and south-west of the survey area (=5 in Fig.2.5). The Sediments map describes the survey area as being covered with "Ocean and inlet deposition, continuous cover, often with large thickness".

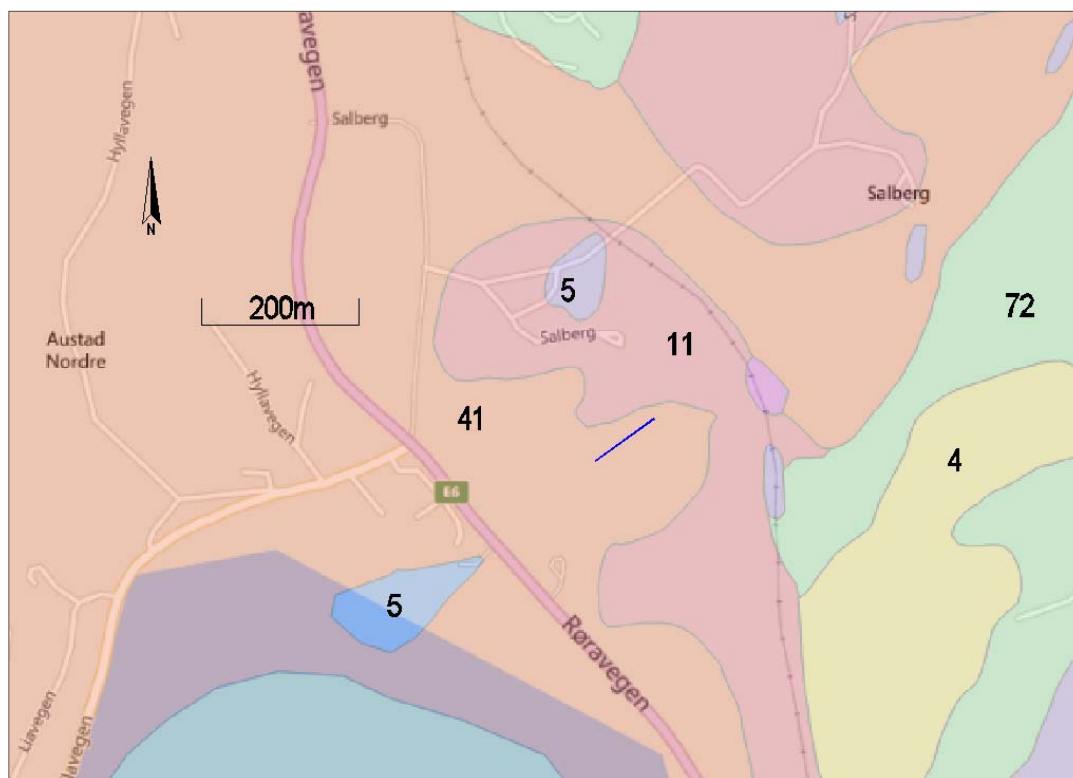


Fig.2.5. Sediments map for Koa. Blue line indicates 92m P-wave profile.

4 = Humusdekke/tynt torvdekke over berggrunn

41 = Hav-og fjordavsetning, sammenhengende dekke, ofte med stor mektighet.

72 = Forvittringsmateriale, usammenhengende eller tynt dekke over berggrunnen

5 = Bart fjell

2.3 Survey Rationale

The **MASW** method is used to estimate shear-wave (S-wave) velocities in the ground material to indicate possible soft zones. Overburden material with an S-wave velocity of <175 m/s is generally classified as soft. The depth of investigation for this method will depend on the source type and geophone spacing. In this survey an effective depth of investigation of 2-22m bgl was achieved.

Seismic Refraction Profiling measures the velocity of refracted seismic waves (P-waves) through the overburden and rock material and allows an assessment of the thickness and quality of the materials present to be made. Stiffer and stronger materials usually have higher seismic velocities while soft, loose or fractured materials have lower velocities. Readings are taken using geophones connected via multi-core cable to a seismograph.

3. SKATVAL RESULTS

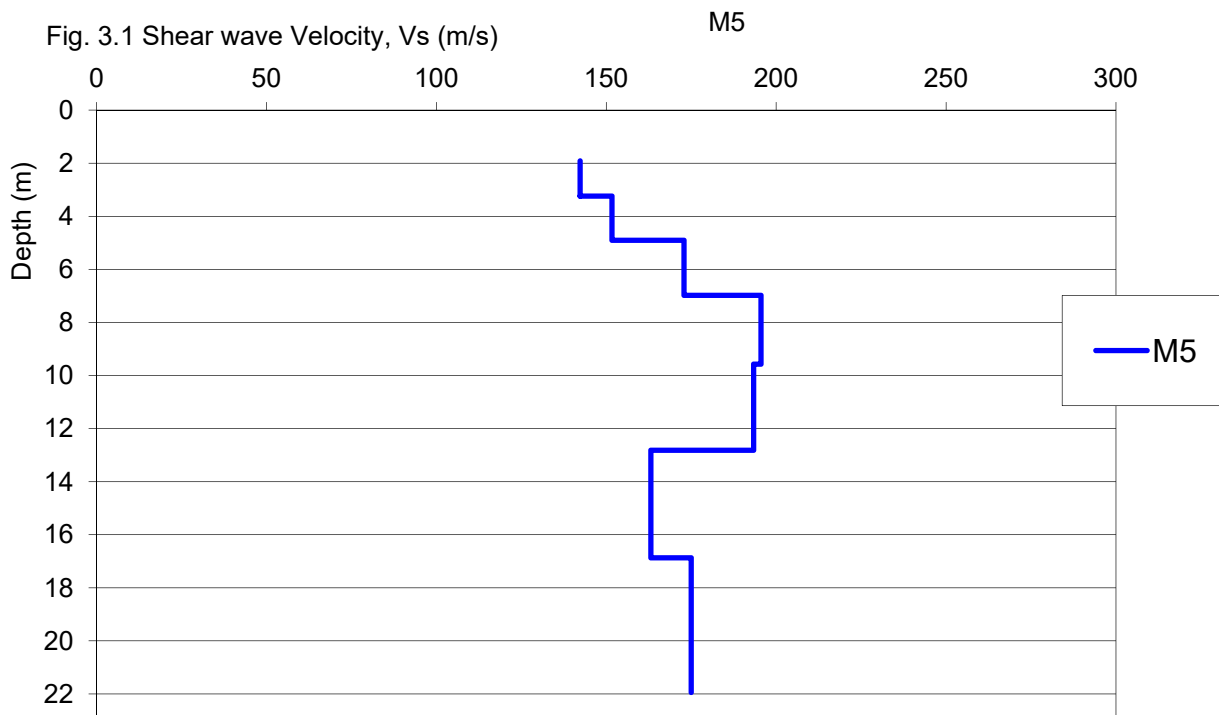
Two seismic spreads (Profiles S5-S6) were recorded at Skatval (Drawing AGL16239B_01). Profile S5 was 69m in length with a 3m geophone spacing and S6 was 92m in length with a 4m geophone spacing. Both profiles were centred at the borehole location.

3.1 MASW

MASW processing was carried out on each of the Profiles S5-S6, with the most coherent dispersion curves selected for inversion. The resulting shear-wave velocity profile (V_s) is denoted M5.

Fig. 3.1 depicts the V_s (shear-wave velocity) results, with the results also presented in Appendix B.

Shear wave velocities ranged from 142-195 m/s (average of 170 m/s) from 1.9-21.9m bgl.



3.2 Seismic Refraction Profiling

Profile S6 was selected for P-wave processing with the following results (Appendix C).

The seismic data has outlined four velocity layers and has been generally interpreted on the following basis:

Layer	Seismic Velocity (m/s)	Average Seismic Velocity (m/s)	Thickness (m)	Interpretation	Stiffness/Rock Quality
1	302-460	370	1.2-2.6	Overburden	Soft/Loose
2	971-1096	1035	0.1-4.0	Overburden	Firm-Stiff/Medium Dense-Dense
3	1629-1736	1684	22.5-25.4	Overburden	Stiff-very Stiff/Dense-very Dense
4	5665-5676	5671		Slightly Weathered-Fresh Bedrock	Good

Layer 1 with a velocity of 302-460 m/s has been interpreted as soft/loose overburden which is 1.2-2.6m thick.

Layer 2 with a velocity of 971-1096 m/s has been interpreted as firm-stiff/medium dense-dense overburden which is 0.1-4.0m thick.

Layer 3 with a velocity of 1629-1736 m/s has been interpreted as stiff-very stiff/dense-very dense overburden which is 22.5-25.4m thick.

The overall thickness of the overburden has been interpreted as 26.4-30.2m.

Layer 4 with a velocity of 5665-5676 m/s has been interpreted as slightly weathered-fresh bedrock.

4. KOA RESULTS

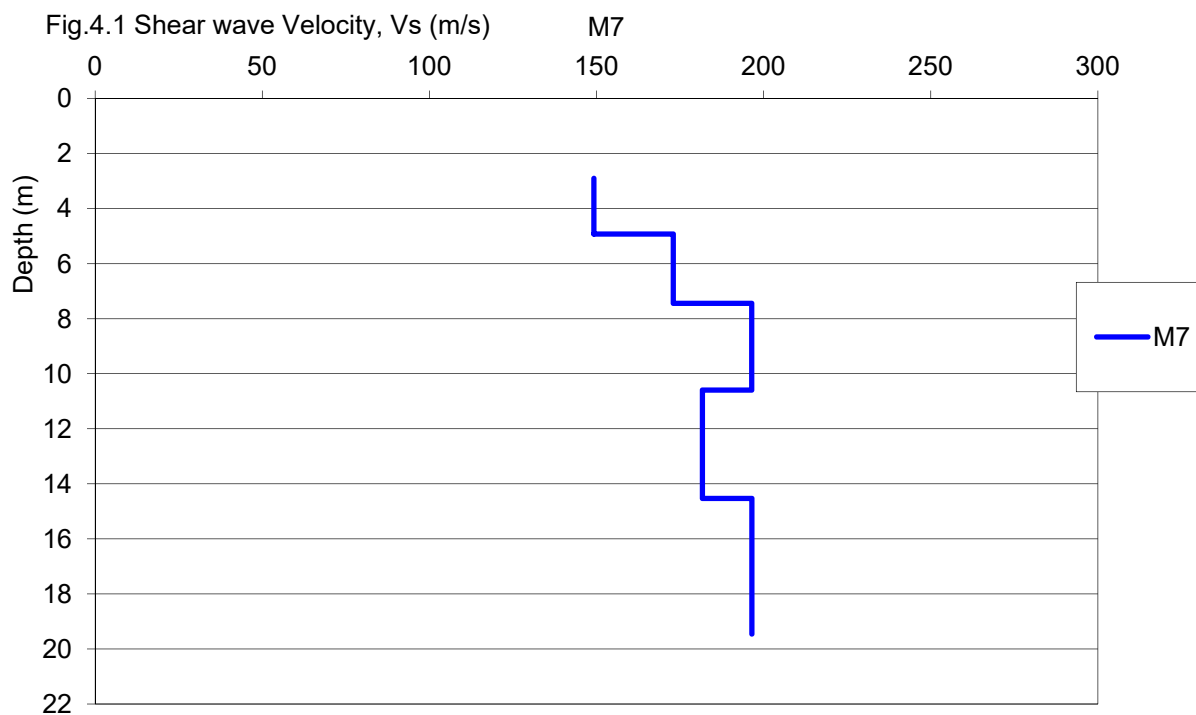
Two seismic spreads (Profiles S7-S8) were recorded at Koa (Drawing AGL16239B_03). Profile S7 was 69m in length with a 3m geophone spacing and S8 was 92m in length with a 4m geophone spacing. Both profiles were centred at the borehole location.

4.1 MASW

MASW processing was carried out on each of the Profiles S7-S8, with the most coherent dispersion curves selected for inversion. The resulting shear-wave velocity profile (V_s) is denoted M7.

Fig. 4.1 depicts the V_s (shear-wave velocity) results, with the results also presented in Appendix B.

Shear wave velocities ranged from 149-196 m/s (average of 179 m/s) from 2.9-19.5m bgl.



4.2 Seismic Refraction Profiling

Profile S8 was selected for P-wave processing with the following results (Appendix C).

The seismic data has outlined four velocity layers and has been generally interpreted on the following basis:

Layer	Seismic Velocity (m/s)	Average Seismic Velocity (m/s)	Thickness (m)	Interpretation	Stiffness/Rock Quality
1	320-444	359	0.8-1.3	Overburden	Soft/Loose
2	593-762	681	0.2-1.9	Overburden	Firm/Medium Dense
3	1143-1185	1167	0.1-3.3	Overburden	Stiff/Dense
4	1602-1796	1684		Overburden	Stiff-Very Stiff/Dense-Very Dense

Layer 1 with a velocity of 320-444 m/s has been interpreted as soft/loose overburden which is 0.8-1.3m thick.

Layer 2 with a velocity of 593-762 m/s has been interpreted as firm-stiff/medium dense-dense overburden which is 0.2-1.9m thick.

Layer 3 with a velocity of 1143-1185 m/s has been interpreted as stiff/ dense overburden which is 0.1-3.3m thick.

Layer 4 with a velocity of 1602-1796 m/s has been interpreted as stiff-very stiff/dense-very dense overburden.

The overall depth of investigation of Profile S8 is estimated at 25m bgl.

5. REFERENCES

Bell F.G., 1993;

'Engineering Geology', Blackwell Scientific Press.

Hagedoorn, J.G., 1959;

'The plus - minus method of interpreting seismic refraction sections', Geophysical Prospecting, 7, 158 - 182.

Palmer, D., 1980;

'The Generalized Reciprocal Method of seismic refraction interpretation', SEG.

Redpath, B.B., 1973;

'Seismic refraction exploration for engineering site investigations', NTIS, U.S. Dept. of Commerce

Soske, J.L., 1959;

'The blind zone problem in engineering geophysics', Geophysics, 24, pp 359-365.

KGS, 2015, Surfseis v5 Users Manual, Kansas Geological Survey.

Park, C.B., Miller, R.D., and Xia, J., 1998;

Ground roll as a tool to image near-surface anomaly:SEG Expanded Extracts, 68th Annual Meeting, New Orleans, Louisiana, 874-877.

Park, C.B., Miller, R.D., and Xia, J., 1999;

Multi-channel analysis of surface waves (MASW): Geophysics, May-June issue.

<http://www.ngu.no/en/topic/datasets>

6. APPENDIX A: DETAILED METHODOLOGY

6.1 MASW

6.1.1 Principles

The Multi-channel Analysis of Surface Waves (MASW) (Park et al., 1998, 1999) utilizes Surface waves (Rayleigh waves) to determine the elastic properties of the shallow subsurface. Surface waves carry up to two-thirds of the seismic energy but are usually considered as noise in conventional body wave reflection and refraction seismic surveys.

The penetration depth of surface waves changes with wavelength, i.e. longer wavelengths penetrate deeper. When the elastic properties of near surface materials vary with depth, surface waves then become dispersive, i.e. propagation velocity changes with frequency. The propagation (or phase) velocity is determined by the average elastic property of the medium within the penetration depth. Therefore the dispersive nature of surface waves may be used to investigate changes in elastic properties of the shallow subsurface.

The MASW method employs the multi-channel recording and processing techniques (Sheriff and Geldart, 1982) that have similarities to those used in a seismic reflection survey and which allow better waveform analysis and noise elimination. To produce a shear wave velocity (V_s) profile and a stiffness profile of the subsurface using Surface waves the following basic procedure is followed:

- (i) A point source (eg. a sledgehammer) is used to generate vertical ground motions,
- (ii) The ground motions are measured using low frequency geophones, which are disposed along a straight line directed toward the source,
- (iii) the ground motions are recorded using either a conventional seismograph, oscilloscope or spectrum analyzer,
- (iv) a dispersion curve is produced from a spectral analysis of the data showing the variation of surface wave velocity with wavelength,
- (v) the dispersion curve is inverted using a modeling and least squares minimization process to produce a subsurface profile of the variation of Surface wave and shear wave velocity with depth,
- (vi) a stiffness-depth profile (shear modulus, G) can be derived from elastic theory.

6.1.2 Data Collection

The recording equipment consisted of a Geode 24 channel digital seismograph, 24 no. 4.5hz vertical geophones and a 24 take-out cable, with a 3-4m geophone spacing. Fieldwork was carried out on the 21st October 2016. Weather conditions were generally good. Overall data quality was good.

1D MASW Profiles with a 3m and 4m geophone spacing were acquired at both sites. The data was acquired in both Active and Passive mode. In Active mode, the equipment comprised a 10kg hammer energy source with mounted trigger, with shots taken at various offsets at either end of each spread, with 2 sec. long records and a 0.25ms sample rate. A total of sixty active shots were taken at each site.

In Passive mode, twenty 16 sec. records were recorded with a 1 sec. sample rate.

6.1.3 Data Processing

MASW processing was carried out using the SURFSEIS processing package developed by Kansas Geological Survey (KGS, 2000). SURFSEIS is designed to generate a shear wave (Vs) velocity profile.

SURFSEIS data processing involves three steps:

(i) Preparation of the acquired multichannel record. This involves converting the data file into the processing format.

(ii) Production of a dispersion curve from a spectral analysis of the data showing the variation of Raleigh wave phase velocity with wavelength. Confidence in the dispersion curve can be estimated through a measure of signal to noise ratio (S/N) which is obtained from a coherency analysis. Noise includes both body waves and higher mode surface waves. To obtain an accurate dispersion curve the spectral content and phase velocity characteristics are examined through an overtone analysis of the data.

(iii) Inversion of the dispersion curve is then carried out to produce a subsurface profile of the variation of shear wave velocity with depth.

The most coherent dispersion curve for each site was chosen for the final 1D Vs data.

6.1.4 Relocation

All data was referenced by the client using a Garmin GPS system with c.2m accuracy.

6.2 Seismic Refraction Profiling

6.2.1 Principles

The seismic refraction profiling method measures the velocity of refracted seismic waves through the overburden and rock material and allows an assessment of the thickness and quality of the materials present to be made. Stiffer and stronger materials usually have higher seismic velocities while soft, loose or fractured materials have lower velocities. Readings are taken using geophones connected via multi-core cable to a seismograph.

6.2.2 Data Collection

Two P-wave seismic spreads was recorded at each site (with only profiles S6 and S8 processed) on the 21st October 2016 using a Geode high-resolution 24 channel digital seismograph with geophone spacings of 4m. The source of the seismic waves was a sledgehammer.

6.2.3 Data Processing

The recorded data was interpreted using the ray-tracing and intercept time methods, to acquire depths to layer boundaries and the P-wave velocities of these layers, using the FIRSTPIX and GREMIX programs.

GREMIX interprets seismic refraction data as a laterally varying layered earth structure. It incorporates the slope-intercept method, parts of the Plus-Minus Method of Hagedoorn (1959), Time-Delay Method, and features the Generalized Reciprocal Method (GRM) of Palmer (1980). Up to four layers can be mapped, one deduced from direct arrivals and three deduced from refractions. Phantomming of all possible travel time pairs can be carried out by adjusting reciprocal times of off shots.

6.2.4 Relocation

All data was referenced by the client using a Garmin GPS system with c.2m accuracy.

7. APPENDIX B: MASW RESULTS (S-WAVE)

Table 7.1 depicts the interpreted shear wave velocities, and table 7.2 lists their locations in UTM 32N.

Table 7.1

M5		M7	
Depth	Vs	Depth	Vs
m	m/s	m	m/s
1.9	142.3	2.9	149.2
3.2	142.3	4.9	149.2
3.2	151.7	4.9	173.0
4.9	151.7	7.4	173.0
4.9	172.9	7.4	196.5
7.0	172.9	10.6	196.5
7.0	195.5	10.6	181.7
9.6	195.5	14.5	181.7
9.6	193.4	14.5	196.5
12.8	193.4	19.5	196.5
12.8	163.1		
16.9	163.1		
16.9	175.0		
21.9	175.0		

Table
7.2

	Easting	Northing
M5	592693	7042715
M7	618367.5	7082438

8. APPENDIX C: SEISMIC REFRACTION RESULTS (P-WAVE)

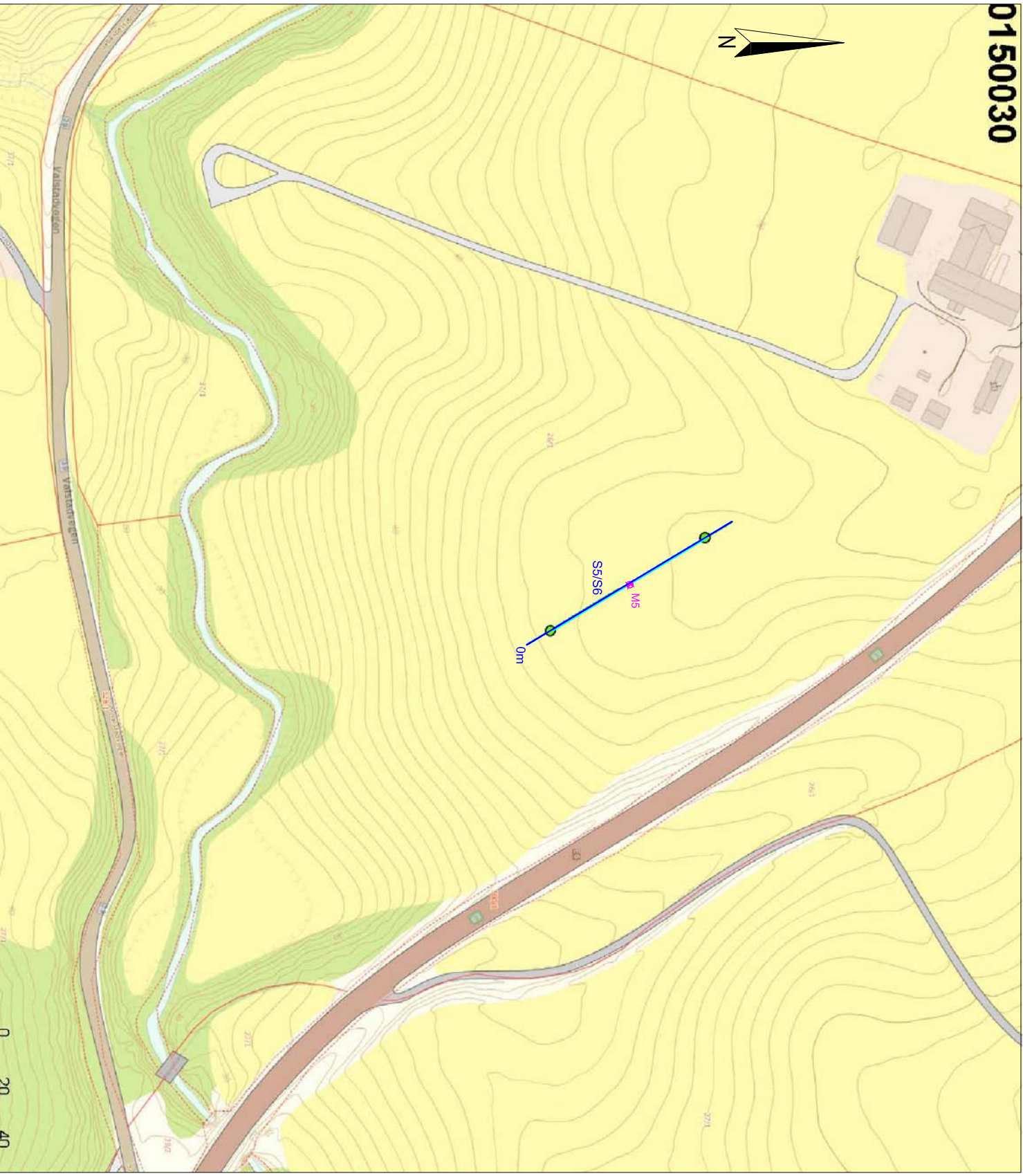
PROFILE	EAST	NORTH	STATION (m)	PWAVE VELOCITY LAYER (m/s)				LAYER DEPTH (m)			LAYER ELEVATION (mOD)			
				1	2	3	4	1	2	3	1	2	3	4
S6	592669	7042754	0	381.0	1066.7	1684.2	5665.0	1.24	4.44	27.03	173	171.8	168.6	146
Skatval	592671	7042750.5	4	378.7	1057.1	1684.2	5665.5	1.28	3.52	27.52	173.3	172	169.8	145.8
	592673	7042747	8	376.5	1047.5	1676.6	5666.0	1.32	3.91	27.13	173.6	172.3	169.7	146.5
	592675	7042743.5	12	374.3	1037.8	1668.9	5666.4	1.36	4.3	26.75	173.9	172.5	169.6	147.2
	592677	7042740.5	16	372.1	1028.2	1668.9	5666.9	1.4	3.79	27.01	173.9	172.5	170.1	146.9
	592679	7042737	20	372.1	1018.6	1668.9	5667.4	1.45	3.69	27.05	173.9	172.5	170.2	146.9
	592681	7042733.5	24	358.1	1009.0	1653.7	5667.9	1.44	3.26	26.99	173.9	172.5	170.7	146.9
	592683	7042730	28	344.1	999.4	1653.3	5668.4	1.43	3.14	26.94	173.9	172.5	170.8	147
	592686	7042726.5	32	330.0	989.8	1695.3	5668.8	1.41	3.72	27	173.9	172.5	170.2	146.9
	592688	7042723	36	316.0	980.2	1695.3	5669.3	1.39	3.87	26.75	173.9	172.5	170.1	147.2
	592690	7042719.5	40	302.0	970.6	1702.8	5669.8	1.37	3.78	26.76	173.9	172.6	170.2	147.2
	592692	7042716.5	44	302.0	970.6	1643.6	5670.3	1.37	3.34	26.41	173.9	172.6	170.6	147.5
	592694	7042713	48	333.6	985.5	1643.6	5670.7	1.38	4.22	26.68	173.9	172.6	169.7	147.3
	592696	7042709.5	52	365.1	1000.4	1629.1	5671.2	1.37	4.5	27.13	173.9	172.6	169.4	146.8
	592698	7042706	56	396.7	1015.4	1698.1	5671.7	1.34	4.44	28.96	174	172.6	169.5	145
	592700	7042702.5	60	428.2	1030.3	1698.1	5672.2	1.28	4.35	29.79	174	172.7	169.6	144.2
	592702	7042699	64	459.8	1045.2	1698.1	5672.7	1.19	4.98	30.14	174	172.8	169	143.8
	592704	7042695.5	68	459.8	1045.2	1698.1	5673.1	1.19	5.2	30.15	174	172.8	168.8	143.8
	592706	7042692.5	72	433.1	1068.7	1698.1	5673.6	1.64	4.9	29.29	174	172.3	169.1	144.7
	592708	7042689	76	406.5	1092.1	1735.6	5674.1	2.28	3.87	28.57	174	171.7	170.1	145.4
	592710	7042685.5	80	379.8	1092.1	1720.1	5674.6	2.57	2.86	27.54	174	171.4	171.1	146.4
	592712	7042682	84	353.2	1092.1	1704.6	5675.0	2.43	2.56	27.21	174	171.6	171.4	146.8
	592714	7042678.5	88	326.5	1092.1	1689.2	5675.5	2.22	2.55	26.96	174	171.8	171.4	147
	592716	7042675	92	326.5	1095.9	1700.0	5676.0	2.29	2.4	27.05	174	171.7	171.6	146.9

PROFILE	EAST	NORTH	STATION (m)	PWAVE VELOCITY LAYER (m/s)				LAYER DEPTH (m)			LAYER ELEVATION (mOD)			
				1	2	3	4	1	2	3	1	2	3	4
S8	618331	7082411	0	320.0	592.6	1142.9	1711.0	0.92	2.85	3.39	189.6	188.7	186.8	186.2
Koa	618334	7082413.5	4	320.7	600.3	1145.2	1739.3	0.95	2.8	4.25	190	189.1	187.2	185.8
	618337	7082415.5	8	321.3	608.0	1147.6	1767.5	0.99	2.76	5.1	190.5	189.5	187.7	185.4
	618341	7082418	12	322.0	615.7	1150.0	1795.7	1.02	2.71	5.96	190.4	189.4	187.7	184.4
	618344	7082420.5	16	322.7	623.4	1152.4	1795.7	1.06	2.67	5.92	190.1	189	187.4	184.2
	618347	7082423	20	323.3	631.1	1154.8	1738.6	1.09	2.62	4.97	189.8	188.7	187.2	184.8
	618350	7082425	24	324.0	638.8	1157.1	1738.6	1.13	2.56	3.5	189.4	188.3	186.9	185.9
	618353	7082427.5	28	324.7	646.5	1159.5	1795.7	1.17	2.01	2.2	189	187.9	187	186.8
	618357	7082430	32	325.3	654.2	1161.9	1795.7	1.2	1.93	2.23	188.5	187.3	186.6	186.3
	618360	7082432	36	326.0	661.9	1164.3	1602.2	1.24	2.39	3.51	187.9	186.7	185.5	184.4
	618363	7082434.5	40	326.7	669.6	1166.7	1602.2	1.27	2.32	3.09	187.5	186.2	185.2	184.4
	618366	7082437	44	326.7	677.3	1166.7	1602.2	1.31	2.25	2.37	187.1	185.8	184.8	184.7
	618370	7082439	48	337.4	684.9	1168.4	1602.2	1.28	2.17	2.35	186.9	185.6	184.8	184.6
	618373	7082441.5	52	348.1	692.6	1170.0	1602.2	1.26	1.87	2.02	187	185.7	185.1	185
	618376	7082444	56	358.8	700.3	1171.7	1684.4	1.23	1.63	1.75	187	185.8	185.4	185.3
	618379	7082446.5	60	369.5	708.0	1173.4	1602.2	1.19	1.39	1.53	187.2	186	185.8	185.6
	618383	7082448.5	64	380.2	715.7	1175.1	1602.2	1.15	1.56	1.73	187.3	186.1	185.7	185.6
	618386	7082451	68	390.9	723.4	1176.8	1636.6	1.11	1.88	2.08	187.5	186.3	185.6	185.4
	618389	7082453.5	72	401.6	731.1	1178.5	1636.6	1.06	2.26	2.37	187.6	186.6	185.4	185.2
	618392	7082455.5	76	412.3	738.8	1180.1	1636.6	1.01	2.25	2.77	187.8	186.8	185.6	185
	618396	7082458	80	423.0	746.5	1181.8	1671.0	0.96	2.23	2.58	188	187.1	185.8	185.5
	618399	7082460.5	84	433.7	754.2	1183.5	1671.0	0.9	2.21	2.45	188.3	187.4	186.1	185.8
	618402	7082462.5	88	444.4	761.9	1185.2	1671.0	0.83	2.18	3.06	188.5	187.7	186.3	185.5
	618405	7082465	92	444.4	761.9	1185.2	1711.0	0.83	2.18	3.14	188.8	188	186.6	185.7

9. APPENDIX D: DRAWINGS

The information derived from the geophysical investigation is presented in the following drawings:

AGL16239B_01	Skatval Profile Locations	1:2000 @ A4
AGL16239B_02	Skatval P-Wave Profiles S6	1:1000 @ A4
AGL16239B_03	Koa Profile Locations	1:2000 @ A4
AGL16239B_04	Koa P-Wave Profiles S8	1:1000 @ A4



LEGEND:

- SEISMIC REFRACTION PROFILE
(4m Geophone Spacing)
- SEISMIC REFRACTION PROFILE
(3m Geophone Spacing)
- ID MASW PROFILE



6 Krockmullen Business Park, Regus House, Herald Way
 Gorey, Co. Wexford
 Ireland.
 T +353 (0)402-21942
 F +353 (0)402-21843
 E info@apexgeoservices.ie
 www.apexgeoservices.ie

PROJECT: SKATVAL & KOA
 GEOPHYSICAL SURVEY
 DRAWING No.: AGL16239B_01 SKATVAL PROFILE LOCATIONS

DATE: 09.11.16

CLIENT: NGI

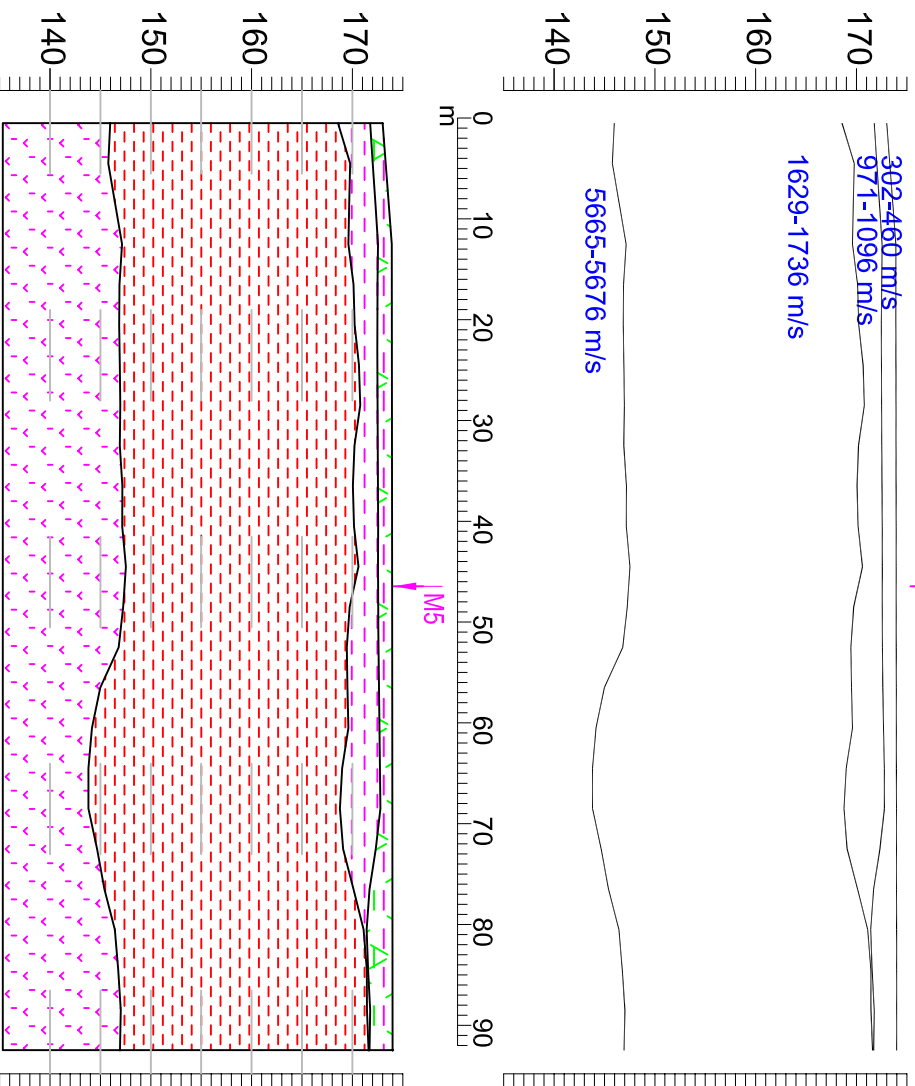
SCALE: 1:2000 @ A4

Version	Date	Drawn By	Checked
1	09.11.16	SOR	TL

SE

S6

NW



LEGEND:

429-576 m/s P-WAVE VELOCITY LAYER

SOFT/LOOSE OVERBURDEN

STIFF/DENSE OVERBURDEN

STIFF-VERY STIFF/DENSE-VERY DENSE OVERBURDEN

SLIGHTLY WEATHERED-FRESH BEDROCK



6 Knockmullen Business Park Regus House, Herald Way
 Gorey
 Co. Wexford
 Castle Donington
 Derby DE74 2TZ
 Ireland
 T +353 (0)402-21942
 F +353 (0)402-21843
 E info@apexgeoservices.ie
 www.apexgeoservices.ie

PROJECT: SKATVAL & KOA
 GEOPHYSICAL SURVEY

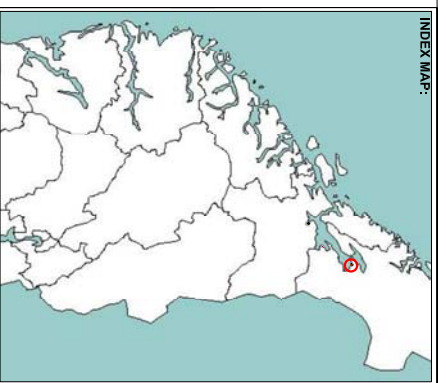
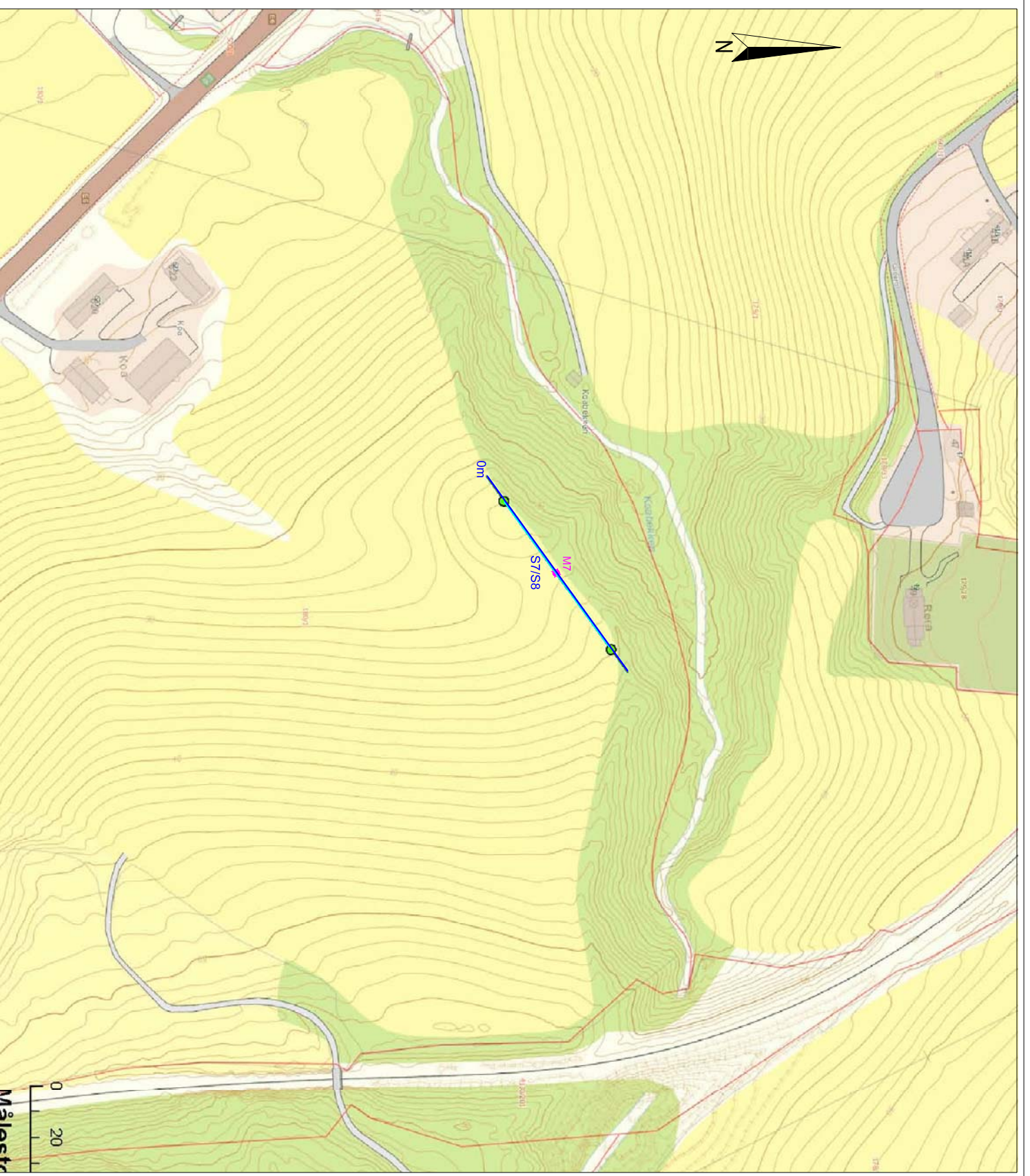
DRAWING No.: AGL162398_02 SKATVAL_P-WAVE PROFILE S6

DATE: 09.11.16

CLIENT: NCI

SCALE: 1:1000 @ A4

Version	Date	Drawn By	Checked
1	09.11.16	SOR	TL



LEGEND:

SEISMIC REFRACTION PROFILE
(4m Geophone Spacing)

SEISMIC REFRACTION PROFILE
(3m Geophone Spacing)

M7 1D MASW PROFILE



6 Knockmullen Business Park, Regus House, Herald Way
 Gorey, Co. Wexford
 Castle Donington
 Derby, DE74 2TZ
 Ireland.
 T +353 (0)402-21942
 F +353 (0)402-21843
 E info@apexgeoservices.ie
 www.apexgeoservices.ie

PROJECT: SKATVAL & KOA
 GEOPHYSICAL SURVEY

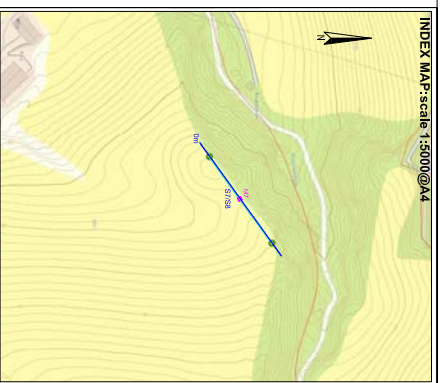
DRAWING No.: AGU162398_03 KOA PROFILE LOCATIONS

DATE: 09.11.16





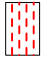
CLIENT: NGI

SCALE: 1:2000 @ A4

Version	Date	Drawn By	Checked
1	09.11.16	SOR	TL



LEGEND:

-  429-576 m/s P-WAVE VELOCITY LAYER
-  SOFT/LOOSE OVERBURDEN
-  FIRM/MEDIUM DENSE OVERBURDEN
-  STIFF/DENSE OVERBURDEN
-  STIFF-VERY STIFF/DENSE-DENSE OVERBURDEN



6 Knockmullen Business Park Regus House, Herald Way
 Gorey Co. Wexford Regus Business Park
 Castle Donington Derby DE74 2TZ
 Ireland. T +44 (0)844 8700 692
 F +353 (0)402-21843 E info@apexgeoservices.co.uk
 www.apexgeoservices.ie www.apexgeoservices.co.uk

PROJECT: SKATVAL & KOA
 GEOPHYSICAL SURVEY

DRAWING No.: AGL162398_04 KOA P-WAVE PROFILE S8

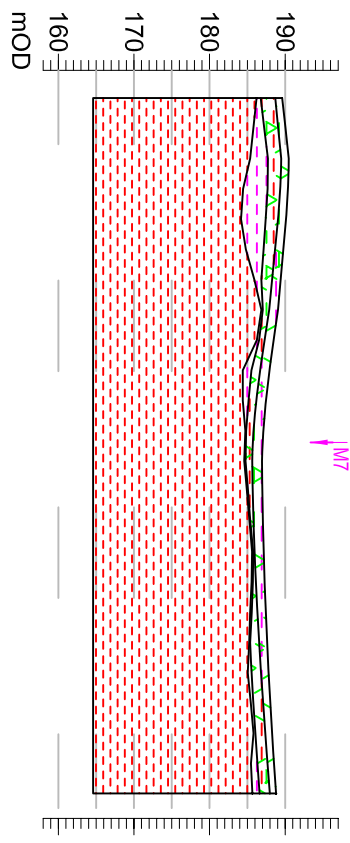
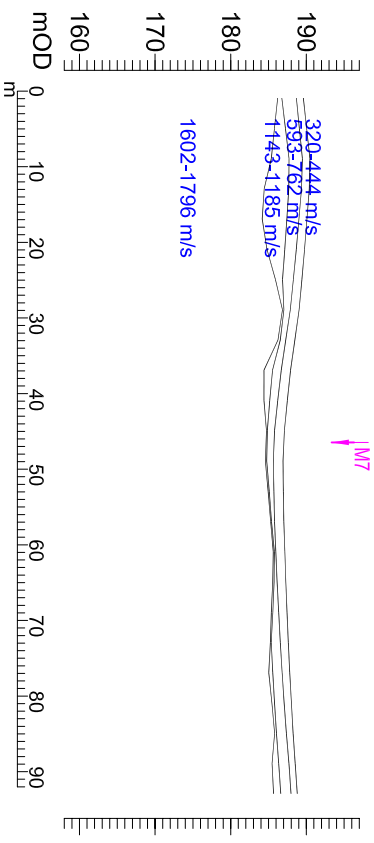
DATE: 09.11.16

CLIENT: NCI

SCALE: 1:1000 @ A4

Version	Date	Drawn By	Checked
1	09.11.16	SOR	TL

SW S8 NE



Appendix C

LABORATORY TEST RESULTS FOR BLOCK SAMPLES FROM KOA

Contents

C1	Introduction	2
C2	Index Testing & Grain Size Distribution	2
	C2.1 Sample description	3
	C2.2 Water content	3
	C2.3 Fall cone	3
	C2.4 One dimensional compression test	3
	C2.5 Liquid limit and plastic limit	3
C3	CRS Oedometer Test Results	3
	C3.1 General	3
	C3.2 Test Procedure CRS	4
	C3.3 Results	4
C4	Triaxial test results	4
	C4.1 General	4
	C4.2 Procedure	4
	C4.3 Results	5
C5	Direct Simple Shear Test Results	6
	C5.1 General	6
	C5.2 Procedure	6
	C5.3 Results	7
C6	Unconfined measurements of shear-wave velocity	8
	C6.1 General	8
	C6.2 Procedure	8
	C6.3 Results	8
C7	Triaxial tests CKoU	9
	C7.1 General	9
	C7.2 Procedure	9
	C7.3 Results	9
C8	References	10

C1 Introduction

Block sampling was performed at Koa in 2016. See location below . Three block samples of Ø160 mm were retrieved from 5,25-5,5 m, 6,75-7 m and 8,75-9 m. The samples were taken at the same location (BP10) where previously 72 mm piston samples had been taken. For information on the 72 mm piston samples and its laboratory data see report 20100685-00-3-R [1].



Location of point BP10 for block sampling in 2016.

Sample bags were taken at different depth intervals from 5 to 9 m depth in order to study the mineralogical composition of the Koa clay. This data is summarized in 20150030-12-R [2].

C2 Index Testing & Grain Size Distribution

Results from index testing are illustrated in Figures C1 to C2. Multiple analyses of grain size distribution have been carried out on the block samples. The method is referred to as "Falling drop" and is described by Moom, 1966 [3].

C2.1 Sample description

All specimens are registered and characterised after a visual examination.

C2.2 Water content

Two to three specimens from each block are tested to find the water content (weight %). Water content is determined according to NS 8013.

C2.3 Fall cone

Two specimens are tested to find the intact and remoulded shear strength using the fall cone test. Tests are carried out in accordance with NS 8015.

C2.4 One dimensional compression test

One dimensional compression test is carried out on unconsolidated specimens. Water content of this specimen is determined. The testing procedure are in accordance with NS 8016.

C2.5 Liquid limit and plastic limit

Liquid limit and plastic limit are determined on each block sample. Plasticity index (I_p), which is frequently used as characterisation parameter, is defined as: $I_p = w_L - w_P$. Determination of liquid limit and plastic limit are in accordance with NS 8002 and NS 8003 respectively.

C3 CRS Oedometer Test Results

C3.1 General

NGI laboratory has carried out one Constant Rate of Strain (CRS) oedometer test as part of this project. Cylindrical test specimens with a cross section and height of 35 cm² and 20 mm respectively were carved from cylindrical block samples with diameter and height of approximately 25 cm and 35 cm respectively.

The CRS oedometer test are carried out according to Norwegian standard NS 8018 [4]. Sandbaekken, Berre, & Lacasse (1986) [5] gives a detailed description of test procedure and equipment used at NGI.

C3.2 Test Procedure CRS

Test specimens are trimmed to a cross sectional area of 35 cm² and height of 20 mm before mounting into a stainless steel oedometer ring which prevents radial deformation. Oedometer specimens with negative excess pore pressure due to unloading from in-situ are mounted using dry filter stones to prevent swelling.

Oedometer tests are carried out to determine deformation and permeability characteristics of the soil. The one dimensional constrained modulus, M , is the relationship between stress and strain whereas the permeability characteristics can be described by the coefficient of consolidation, c_v .

This parameter is defined as: $c_v = \frac{M \cdot k}{\gamma_w}$

Here k is the coefficient of permeability and γ_w is the unit weight of water.

C3.3 Results

Results are illustrated in Figures C3 to C5. Three figures are presented for each test to provide a good basis for interpretation.

C4 Triaxial test results

C4.1 General

Three anisotropically consolidated, undrained triaxial tests have been carried out at the NGI laboratory. Two of these were subjected to compressive loading and one were subjected to tension loading. Tests have been carried out using the general NGI procedure described in Berre, 1981 [6] and Andresen & Simons, 1960 [7].

C4.2 Procedure

C4.2.1 Mounting of Specimen

Specimens are mounted using dry filter stones to prevent swelling. With the exception of very soft clays, strips of filter are mantled on the sides of the specimen to decrease consolidation time when undrained loading is to be applied. The filter strips are moisturized, but free water is removed from the surface before attachment to the sample. Strips form a spiral outside the specimen to avoid correcting the stresses invoked on the specimen.

C4.2.2 Consolidation

Isotropic stresses are first applied to the assumed negative pore pressure in the specimen. Afterwards water with the same level of salt as in situ is flushed through top and bottom filters and a zero indicator is attached immediately to the drainage tubes. The cell pressure is regulated to achieve a stable specimen volume.

Backpressure is applied to increase level of saturation in the specimen and improve pore pressure measurements. To ensure sufficient saturation a B-value of at least 0.95 is desirable for static tests.

The test is then consolidated to specific stress levels equivalent to the assumed in-situ stresses. The specimen is firstly loaded isotropically afterwards the vertical load is increased in steps to specific in situ conditions. The loading advancement speed is adapted to the speed of the consolidation. Measurements of shear wave velocity are performed at the end of consolidation.

C4.2.3 Undrained static shearing

The specimen is loaded to failure with constant deformation velocity, normally 1.4%/hour. In an anisotropically consolidated, undrained triaxial test total radial stress is kept constant while total axial stress is increased in an active stress state or decreased in a passive test.

C4.3 Results

The results are presented in Figures C6 to C11. This report presents two figures for each triaxial test, one of which illustrates the shear stress and excess pore pressure with axial strain. The second figure presents the stress path in terms of the mean average stress with shear stress. Table C1 show the results for the measurements of shear wave velocity.

Table C1 Results obtained from measurements of shear-wave velocity on Koa clay during consolidation for triaxial tests

CALCULATION OF INITIAL SHEAR MODULUS (Gmax) FROM BENDER ELEMENT MEASUREMENT

Project no.:	20150030	Pore water density:	10,0	kN/m ³	
Boring:	Koa-10	Initial specimen height:	10,9680	cm	
Tube:	1	Initial specimen volume:	256,34	cm ³	Test type: CAUe
Part:	2B	Initial specimen weight:	509,25	g	
Test:	1	Height of both elements:	0,6700	cm	Signature: MAS

Input									Calculated results		
	Date	Time	Time from increment start	Total vertical stress	Total horizontal stress	Specimen height change	Specimen volume change	Shear wave travel time	Total octahedral stress	Shear wave velocity	Initial shear modulus
	(dd.mm.yy)	(hh:mm)	(min)	(kPa)	(kPa)	(cm)	(cm ³)	(ms)	(kPa)	(m/s)	(MPa)
1	09.05.2016	23:50	-	-	-	0,0000	0,00	1,1040	#VERDI!	93	17,3
2	12.05.2016	04:40	-	110,0	66,0	0,1018	2,30	0,7600	80,7	134	35,9

C5 Direct Simple Shear Test Results

C5.1 General

The apparatus for this test is described by Bjerrum and Landva, 1966 [8] and Andresen et al. 1979 [9]. One direct simple shear tests was carried out.

C5.2 Procedure

C5.2.1 General

A cylindrical specimen with cross-sectional area of 20, 35 or 50 cm² and height of 16 mm is placed within a reinforced rubber membrane which prevents radial deformation, but allows the specimen to deform in simple shear. All samples in this project were had cross-sectional area of 50 cm².

C5.2.2 Consolidation

The axial (vertical) stress is increased in steps to the estimated effective consolidation pressure. At approximately 50 % of the estimated consolidation pressure the porous stones are saturated with water of approximately the same salt concentration as the pore water of the clay. Measurements of shear wave velocity are performed at the end of consolidation.

After saturation the specimen is either loaded to

1. $\sigma'_{max} < p'_c$, which is a low estimate of the preconsolidation stress, p'_c , and then unloaded to the final vertical consolidation stress σ'_{vc} (normally identical to the estimated in situ effective vertical stress). The specimen will have an $OCR = \sigma'_{max} / \sigma'_{vc}$.
2. $\sigma'_{max} > p'_c$, if the specimen is assumed to be normally consolidated i.e. the specimen is not unloaded before shearing and will have $OCR = 1.0$.

The samples in this project were loaded to $\sigma'_{max} < p'_c$.

After consolidation the specimen is sheared by applying a horizontal shear stress. Undrained conditions are simulated by keeping the volume constant. The volume is kept constant by adjusting the axial stress during shearing. Normally a strain rate of 5 %/hr is applied. The change in the axial stress for constant volume test is equal to the change in pore pressure for an undrained test where the total axial stress is kept constant.

The reason for performing constant volume instead of an undrained test is that drainage cannot be completely prevented and the saturation by means of backpressure cannot be performed in the simple shear device. In a drained test the axial stress is kept constant while the change in height is monitored.

C5.3 Results

Figures C12 to C15 illustrate the results obtained from DSS testing on Koa clay. Table C2 show the results for the measurements of shear wave velocity.

Table C2 Results obtained from measurements of shear-wave velocity on Koa clay during consolidation for DSS tests

CALCULATION OF INITIAL SHEAR MODULUS (Gmax) FROM BENDER ELEMENT MEASUREMENTS



Project no.:	20150030	Pore water density:	9,81 kN/m ³	
Boring:	K0a-10	Initial specimen height:	1,596 cm	
Tube:	6	Initial specimen volume:	55,86 cm ³	Test type: DSS
Part:	2C	Initial specimen weight:	117,60 g	
Test:	2	Height of both elements:	0,8470 cm	Signature: TAB

Input								Calculated results		
Increment starting time (yyyy-mm-dd hh:mm)	$\bar{\sigma}_{max}$ measuring time (yyyy-mm-dd hh:mm)	Time from increment start (min)	Total vertical stress (kPa)	FREQ. (kHz)	Specimen height change (cm)	Specimen volume change (cm ³)	Shear wave travel time (ms)	Total octahedral stress (kPa)	Shear wave velocity (m/s)	Initial shear modulus (MPa)
1		0	0,0	27,0	0,0000	0,00	0,0829		90	17,2
2	01.08.2016 10:08	02.08.2016 11:48	1540	43.3	0,0305	1,07	0,0585	99,3	123	32,1
3	02.08.2016 11:54	03.08.2016 08:54	1260	43,0	0,0277	0,97	0,0625	65,3	115	28,3

C6 Unconfined measurements of shear-wave velocity

C6.1 General

The apparatus for this test is described by Landon et al. 2007 [10]. Six measurements were performed.

C6.2 Procedure

Unconfined measurements of shear-wave velocity were collected in the laboratory using the bender element device described by Landon et al. (2007). For this, samples were carefully trimmed from block sample size to a cube about 70x70x70 mm size due to restrictions in the equipment size. Shear-wave travel time (i.e. arrival time) was calculated as the difference between two peaks of the transmitted signal minus the system calibration time.

C6.3 Results

Table C3 present the results obtained from unconfined measurements of shear-wave velocity on Koa clay.

Table C3 Results obtained from unconfined measurements of shear-wave velocity on Koa clay

Location		Setup	Soil		Sample				First crossover		Peak to Peak		Setup
Borehole	Sample	t _c ⁵⁾	γ _{soil}	ρ _{soil}	H ¹⁾	h ₁ ²⁾	h ₂ ³⁾	H _{corr} ⁴⁾	t _{cross}	V _s	t _{peak}	V _s	Frequency
-	-	ns	kN/m ³	kg/m ³	m	m	m	m	μs	m/s	μs	m/s	kHz
Koa-10	1_5.25m	5033	19,19	1956,2	62	7	8	0,047	565,1	83,92	570,2	83,16	4
		5033	19,19	1956,2	62	7	8	0,047	539,5	87,94	524,2	90,53	6
Koa-10	3_6.88m	5033	19,36	1973,5	73	7	8	0,058	544,6	107,49	560	104,51	3
		5033	19,36	1973,5	73	7	8	0,058	565,1	103,56	563,4	103,87	4
		5033	19,36	1973,5	73	7	8	0,058	568,5	102,93	558,2	104,85	6
Koa-10	6_8.95m	5033	19,56	1993,9	63	7	8	0,048	480	101,06	466,3	104,06	6,1
		1)	Height of sample/steel tube										
		2)	Height from edge of tube edge down to sample top surface after scraping of top										
		3)	Height from edge of tube edge up to sample bottom surface after scraping of bottom										
		4)	Corrected sample height(H - h1 - h2)										
		5)	Signal delay measured with bender elements tip to tip(in nano seconds)										

C7 Triaxial tests CKoU

C7.1 General

A K_0 -test (or more correct: a CK_0 -test) is a test where the cross-sectional area of the specimen is kept constant except for the initial part of the test where the initial stresses usually are isotropic.

C7.2 Procedure

Before starting the K_0 -loading, the stresses are adjusted so that the ratio between horizontal and vertical effective stresses come close to the expected value during the K_0 -loading. The change from isotropic to anisotropic effective stresses is often done so that the effective octahedral stress is kept constant. It may also be done by increasing the vertical effective stress while the effective horizontal stress is kept constant.

The CKoU is the test with K_0 -loading during consolidation as explained before followed by undrained shearing.

C7.3 Results

Figures C16 to C17 illustrate the results obtained from CKoU triaxial testing on Koa clay.

C8 References

- [1] NGI, Grunnundersøkelser Inderøy kommune. Datarapport grunnundersøkelser sone Koa, Inderøy. Rapport 20100685-00-3-R., 2011.
- [2] NGI, SP8 - Geoteknikedimensjoneringsparametere (GEODiP). Mineralogy data for Skatval, Koa and Rakkestad clay sites. Report 20150030-12-R, 2017.
- [3] J. Moum, "Falling drop used for grain size analysis of fine grained materials.," *Sedimentology*, vol. 5, no. 4, pp. 343-347, 1966.
- [4] Standard Norge, "Norsk Standard NS 8018 - Geoteknisk prøving - Laboratoriemetoder - Bestemmelse av endimensjonale konsolideringsegenskaper ved ødometerprøving - Metode med kontinuerlig belastning," Standard Norge, Oslo, 1993.
- [5] G. Sandbaekken, T. Berre and S. Lacasse, "Oedometer testing at the Norwegian Geotechnical Institute,," *Consolidation of soils: Testing and evaluation. ASTM International.*, 1986.
- [6] T. Berre, "Triaxial testing at the Norwegian Geotechnical Institute,," *Geotechnical Testing Journal, Vol. 5*, pp. 7-23, 1981.
- [7] A. Andresen and N. E. Simons, "Norwegian Triaxial Equipment and Technique,," NGI, Oslo, 1960.
- [8] L. Bjerrum and A. Landva, "Direct simple shear tests on a Norwegian quick clay,," *Geotechnique, Vol 16, No. 1*, pp. 1-20, 1966.
- [9] A. Andresen, T. Berre, A. Kleven and T. Lunne, "Procedures used to obtain soil parameters for foundation engineering in the North Sea,," *Marin Geotechnology, Vol 3, no. 3*, pp. 201-266, 1979.
- [10] D. D. a. S. T. Landon M.M., "Nondestructive sample quality assessment of a soft clay using shear-waver velocity,," *J Geotech Geoenv Eng ASCE*, vol. 133, pp. 424-432, 2007.
- [11] Statens vegvesen, "Håndbok R210. Laboratorieundersøkelser,," Statens vegvesen, Oslo, 2016.

Appendix D

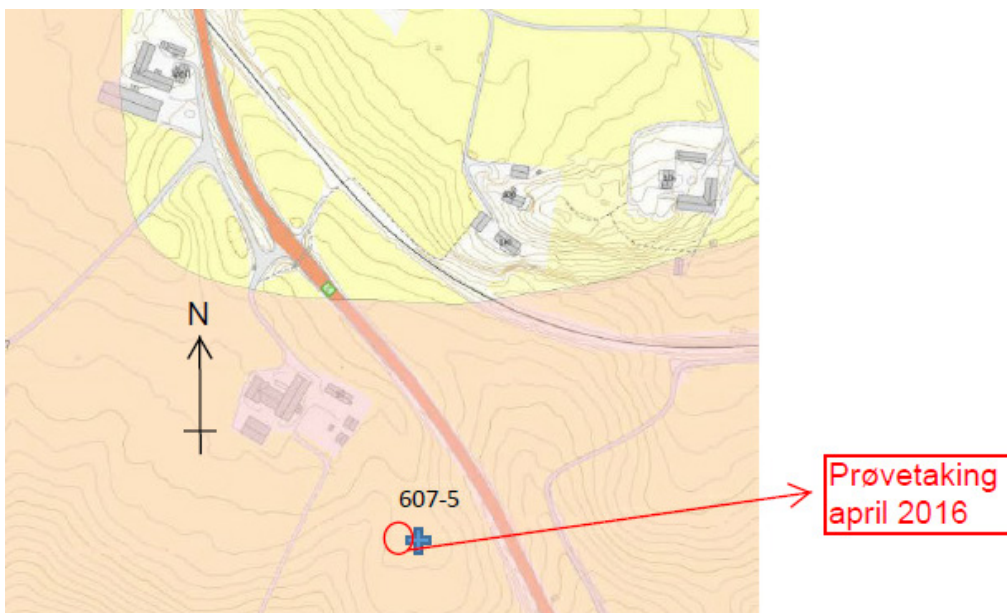
LABORATORY TEST RESULTS FOR BLOCK SAMPLES FROM SKATVAL

Contents

D1	Introduction	2
D2	Index Testing & Grain Size Distribution	2
	D2.1 Sample description	2
	D2.2 Water content	3
	D2.3 Fall cone	3
	D2.4 One dimensional compression test	3
	D2.5 Liquid limit and plastic limit	3
D3	CRS Oedometer Test Results	3
	D3.1 General	3
	D3.2 Test Procedure CRS	3
	D3.3 Results	4
D4	Triaxial test results	4
	D4.1 General	4
	D4.2 Procedure	4
	D4.3 Results	5
D5	Direct Simple Shear Test Results	7
	D5.1 General	7
	D5.2 Procedure	7
	D5.3 Results	8
D6	Unconfined measurements of shear-wave velocity	8
	D6.1 General	8
	D6.2 Procedure	8
	D6.3 Results	9
D7	Triaxial tests CKoU	12
	D7.1 General	12
	D7.2 Procedure	12
	D7.3 Results	12
D8	References	13

D1 Introduction

Block sampling was performed at Skatval in 2016. See location below. Two block samples of Ø250 mm and one block sample of Ø160 mm were retrieved from 4,40-4,67 m, 7,09-7,47 m and 7,47-7,77 m. The samples were taken at the same location (607-5) where previously 72 mm piston samples had been taken. For information on the 72 mm piston samples and its laboratory data see report 2010026-03-R [1].



Location of point 607-5 for block sampling in 2016 at Skatval.

Sample bags were taken at different depth intervals from 3 to 8 m depth in order to study the mineralogical composition of the Skatval clay. This data is summarized in 20150030-12-R [2].

D2 Index Testing & Grain Size Distribution

Results from index testing are illustrated in Figures D1 to D2. Multiple analyses of grain size distribution have been carried out on the block samples. The method is referred to as "Falling drop" and is described by Moom, 1966 [3].

D2.1 Sample description

All specimens are registered and characterised after a visual examination.

D2.2 Water content

Three specimens from each block are tested to find the water content (weight %). Water content is determined according to NS 8013.

D2.3 Fall cone

Two specimens from each block are tested to find the intact and remoulded shear strength using the fall cone test. Tests are carried out in accordance with NS 8015.

D2.4 One dimensional compression test

One dimensional compression tests are carried out on unconsolidated specimens. Water content of this specimen is determined. The testing procedure are in accordance with NS 8016.

D2.5 Liquid limit and plastic limit

Liquid limit and plastic limit are determined on each block sample. Plasticity index (I_p), which is frequently used as characterisation parameter, is defined as: $I_p = w_L - w_P$. Determination of liquid limit and plastic limit are in accordance with NS 8002 and NS 8003 respectively.

D3 CRS Oedometer Test Results

D3.1 General

NGI laboratory has carried out three Constant Rate of Strain (CRS) oedometer tests as part of this project. Cylindrical test specimens with a cross section and height of 35 cm² and 20 mm respectively were carved from cylindrical block samples with diameter and height of approximately 25 cm and 35 cm respectively.

The CRS oedometer test are carried out according to Norwegian standard NS 8018 [4]. Sandbaekken, Berre, & Lacasse (1986) [5] gives a detailed description of test procedure and equipment used at NGI.

D3.2 Test Procedure CRS

Test specimens are trimmed to a cross sectional area of 35 cm² and height of 20 mm before mounting into a stainless steel oedometer ring which prevents radial deformation. Oedometer specimens with negative excess pore pressure due to unloading from in-situ are mounted using dry filter stones to prevent swelling.

Oedometer tests are carried out to determine deformation and permeability characteristics of the soil. The one dimensional constrained modulus, M , is the relationship between stress and strain whereas the permeability characteristics can be described by the coefficient of consolidation, c_v .

This parameter is defined as: $c_v = \frac{M \cdot k}{\gamma_w}$

Here k is the coefficient of permeability and γ_w is the unit weight of water.

D3.3 Results

Results are illustrated in Figures D3 to D14. Three figures are presented for each test to provide a good basis for interpretation.

D4 Triaxial test results

D4.1 General

Four anisotropically consolidated, undrained triaxial tests have been carried out at the NGI laboratory. Three of these were subjected to compressive loading and one was subjected to tension loading. Tests have been carried out using the general NGI procedure described in Berre, 1981 [6] and Andresen & Simons, 1960 [7].

D4.2 Procedure

D4.2.1 Mounting of Specimen

Specimens are mounted using dry filter stones to prevent swelling. With the exception of very soft clays, strips of filter are mantled on the sides of the specimen to decrease consolidation time when undrained loading is to be applied. The filter strips are moisturized, but free water is removed from the surface before attachment to the sample. Strips form a spiral outside the specimen to avoid correcting the stresses invoked on the specimen.

D4.2.2 Consolidation

Isotropic stresses are first applied to the assumed negative pore pressure in the specimen. Afterwards water with the same level of salt as in situ is flushed through top and bottom filters and a zero indicator is attached immediately to the drainage tubes. The cell pressure is regulated to achieve a stable specimen volume.

Backpressure is applied to increase level of saturation in the specimen and improve pore pressure measurements. To ensure sufficient saturation a B-value of at least 0.95 is desirable for static tests.

The test is then consolidated to specific stress levels equivalent to the assumed in-situ stresses. The specimen is firstly loaded isotropically afterwards the vertical load is increased in steps to specific in situ conditions. The loading advancement speed is adapted to the speed of the consolidation. Measurements of shear wave velocity are performed at the end of consolidation.

D4.2.3 Undrained static shearing

The specimen is loaded to failure with constant deformation velocity, normally 1.4%/hour. In an anisotropically consolidated, undrained triaxial test total radial stress is kept constant while total axial stress is increased in an active stress state or decreased in a passive test.

D4.3 Results

The results are presented in Figures D15 to D22. This report presents two figures for each triaxial test, one of which illustrates the shear stress and excess pore pressure with axial strain. The second figure presents the stress path in terms of the mean average stress with shear stress. Table D1 show the results for the measurements of shear wave velocity.

Table D1 Results obtained from measurements of shear-wave velocity on Skatval clay during consolidation for triaxial tests

CALCULATION OF INITIAL SHEAR MODULUS (Gmax) FROM BENDER ELEMENT MEASUREMENTS

Project no.: 20150030	Pore water density: 10,0 kN/m ³	
Boring: 607-5	Initial specimen height: 10,9250 cm	
Tube: 7	Initial specimen volume: 255,71 cm ³	Test type: CAUa
Part: 1B	Initial specimen weight: 497,49 g	
Test: 1	Height of both elements: 0,6600 cm	Signature: MAS

Input								Calculated results			
Date	Time	Time from increment start	Total vertical stress	Total horizontal stress	Specimen height change	Specimen volume change	Shear wave travel time	Total octahedra stress	Shear wave velocity	Initial shear modulus	
(dd.mm.yy)	(hh:mm)	(min)	(kPa)	(kPa)	(cm)	(cm ³)	(ms)	(kPa)	(m/s)	(MPa)	
1	25:04:00	02:55	-	90,0	54,1	0,0710	1,70	0,7640	66,1	133	34,7

Project no.: 20150030	Pore water density: 10,0 kN/m ³	
Boring: 607-5	Initial specimen height: 10,9200 cm	
Tube: 6	Initial specimen volume: 255,56 cm ³	Test type: CAUa
Part: 2C	Initial specimen weight: 499,24 g	
Test: 2	Height of both elements: 0,6600 cm	Signature: GS

Input								Calculated results			
Date	Time	Time from increment start	Total vertical stress	Total horizontal stress	Specimen height change	Specimen volume change	Shear wave travel time	Total octahedra stress	Shear wave velocity	Initial shear modulus	
(dd.mm.yy)	(hh:mm)	(min)	(kPa)	(kPa)	(cm)	(cm ³)	(ms)	(kPa)	(m/s)	(MPa)	
1	02.05.16	01:50	-	88,1	52,9	0,0648	1,65	0,8080	64,6	126	31,2

Project no.: 20150030	Pore water density: 10,0 kN/m ³	
Boring: 607-5	Initial specimen height: 10,9000 cm	
Tube: 6	Initial specimen volume: 256,61 cm ³	Test type: CAUa
Part: 2B	Initial specimen weight: 499,87 g	
Test: 1	Height of both elements: 0,7600 cm	Signature: MAS

Input								Calculated results			
Date	Time	Time from increment start	Total vertical stress	Total horizontal stress	Specimen height change	Specimen volume change	Shear wave travel time	Total octahedra stress	Shear wave velocity	Initial shear modulus	
(dd.mm.yy)	(hh:mm)	(min)	(kPa)	(kPa)	(cm)	(cm ³)	(ms)	(kPa)	(m/s)	(MPa)	
1	28.04.2016	18:15	-	88,2	52,9	0,0668	2,30	0,7440	64,7	135	35,9

Project no.: 20150030	Pore water density: 10,0 kN/m ³	
Project no.: 20150030	Pore water density: 10,0 kN/m ³	
Boring: 607-5	Initial specimen height: 10,9500 cm	
Tube: 1	Initial specimen volume: 257,76 cm ³	Test type: CAUa
Part: 2B	Initial specimen weight: 499,60 g	
Test: 1	Height of both elements: 0,8200 cm	Signature: GS

Input								Calculated results			
Date	Time	Time from increment start	Total vertical stress	Total horizontal stress	Specimen height change	Specimen volume change	Shear wave travel time	Total octahedra stress	Shear wave velocity	Initial shear modulus	
(dd.mm.yy)	(hh:mm)	(min)	(kPa)	(kPa)	(cm)	(cm ³)	(ms)	(kPa)	(m/s)	(MPa)	
1	28.04.16	22:20	-	56,0	35,3	0,0538	1,20	0,7960	42,2	127	31,1

D5 Direct Simple Shear Test Results

D5.1 General

The apparatus for this test is described by Bjerrum and Landva, 1966 [8] and Andresen et al. 1979 [9]. One direct simple shear tests was carried out.

D5.2 Procedure

D5.2.1 General

A cylindrical specimen with cross-sectional area of 20, 35 or 50 cm² and height of 16 mm is placed within a reinforced rubber membrane which prevents radial deformation, but allows the specimen to deform in simple shear. All samples in this project were had cross-sectional area of 50 cm².

D5.2.2 Consolidation

The axial (vertical) stress is increased in steps to the estimated effective consolidation pressure. At approximately 50 % of the estimated consolidation pressure the porous stones are saturated with water of approximately the same salt concentration as the pore water of the clay. Measurements of shear wave velocity are performed at the end of consolidation.

After saturation the specimen is either loaded to

1. $\sigma'_{\max} < p'_c$, which is a low estimate of the preconsolidation stress, p'_c , and then unloaded to the final vertical consolidation stress σ'_{vc} (normally identical to the estimated in situ effective vertical stress). The specimen will have an $OCR = \sigma'_{\max} / \sigma'_{vc}$.
2. $\sigma'_{\max} > p'_c$, if the specimen is assumed to be normally consolidated i.e. the specimen is not unloaded before shearing and will have $OCR = 1.0$.

The samples in this project were loaded to $\sigma'_{\max} < p'_c$.

After consolidation the specimen is sheared by applying a horizontal shear stress. Undrained conditions are simulated by keeping the volume constant. The volume is kept constant by adjusting the axial stress during shearing. Normally a strain rate of 5 %/hr is applied. The change in the axial stress for constant volume test is equal to the change in pore pressure for an undrained test where the total axial stress is kept constant.

The reason for performing constant volume instead of an undrained test is that drainage cannot be completely prevented and the saturation by means of backpressure cannot be performed in the simples shear device. In a drained test the axial stress is kept constant while the change in height is monitored.

D5.3 Results

Figures D23 to D24 illustrate the results obtained from DSS testing on Skatval clay. Table D2 show the results for the measurements of shear wave velocity.

Table D2 Results obtained from measurements of shear-wave velocity on Skatval clay during consolidation for DSS tests

CALCULATION OF INITIAL SHEAR MODULUS (Gmax) FROM BENDER ELEMENT MEASUREMENTS

Project no.:	20150030	Pore water density:	9,18 kN/m ³	
Boring:	607_5	Initial specimen height:	1,595 cm	
Tube:	6	Initial specimen volume:	55,83 cm ³	Test type: DSS
Part:	2D	Initial specimen weight:	111,70 g	Signature: _____
Test:	1	Height of both elements:	0,7310 cm	Signature: Tab

	Input							Calculated results			
	Increment starting time (yyyy-mm-dd hh:mm)	G _{max} measuring time (yyyy-mm-dd hh:mm)	Time from increment start (min)	Total vertical stress (kPa)	FREQ. (kHz)	Specimen height change (cm)	Specimen volume change (cm ³)	Shear wave travel time (ms)	Total octahedra stress (kPa)	Shear wave velocity (m/s)	Initial shear modulus (MPa)
1	27.04.2016 11:54	28.04.2016 13:28	1534	108,0	41,4	0,0508	1,78	0,0722		113	25,8
2	28.04.2016 13:37	29.04.2016 09:21	1184	90,0	42,2	0,0503	1,76	0,0727		112	25,5

D6 Unconfined measurements of shear-wave velocity

D6.1 General

The apparatus for this test is described by Landon et al. 2007 [10]. Six measurements were performed.

D6.2 Procedure

Unconfined measurements of shear-wave velocity were collected in the laboratory using the bender element device described by Landon et al. (2007). For this, samples were carefully trimmed from block sample size to a cube about 70x70x70 mm size due to restrictions in the equipment size. Shear-wave travel time (i.e. arrival time) was calculated as the difference between two peaks of the transmitted signal minus the system calibration time.

D6.3 Results

Table D3, Table D4 and Table D5 present the results obtained from unconfined measurements of shear-wave velocity on Skatval clay on the field, lab 1 (NTNU) and lab 2 (NGI), respectively.

Table D3 Results obtained from unconfined measurements of shear-wave velocity on Skatval clay on the field

Sample	Depth m	Beam elements		Height H mm	Height H mm	Height H mm	Height corrected Hcorr mm	Width W mm	Soil		Calibration tc ns	First cross over			Peak to peak			Frequency kHz
		Bottom	Top						γ_{soil} kN/m ³	ρ_{soil} kg/m ³		t cross μ s	Vs m/s	Gmax MPa	t cross μ s	Vs m/s	Gmax MPa	
3,1-3,38 m	3,20	8P	6S	58	8	7	43	55	18,9	1927	7550	497,8	87,7	14,8	557,4	78,2	14,8	2
3,38-3,73 m	3,48	8P	6S	75	8	7	60	80	18,9	1927	7550	655,3	92,6	16,5	697,8	86,9	16,5	2
3,73-4,05 m	3,83	8P	6S	68	8	7	53	68	18,9	1927	5033	514,8	104,0	20,8	540,4	99,0	20,8	4
3,73-4,05 m	3,83	8P	6S	68	8	7	53	68	18,9	1927	7550	544,6	98,7	18,8	565,9	94,9	18,8	2
4,05-4,40 m	4,31	8P	6S	67	8	7	52	58	18,9	1927	7550	953,1	55,0	5,8	995,7	52,6	5,8	2
4,05-4,40 m	4,31	8P	6S	67	8	7	52	58	18,9	1927	5033	906,3	57,7	6,4	953,1	54,8	6,4	4
4,05-4,40 m	4,15	8P	6S	73	8	7	58	73	18,9	1927	5033	723,4	80,7	12,6	804,2	72,6	12,6	4
4,05-4,40 m	4,15	8P	6S	73	8	7	58	73	18,9	1927	7550	753,1	77,8	11,7	808,5	72,4	11,7	2
4,70-4,95 m	4,91	8P	6S	70	8	7	55	70	18,9	1927	5033	514,8	107,9	22,4	519,1	107,0	22,4	4
4,95-5,20 m	5,00	8P	6S	65	8	7	50	65	18,9	1927	2517	502,1	100,1	19,3	531,9	94,4	19,3	6
4,95-5,20 m	5,00	8P	6S	65	8	7	50	65	18,9	1927	5033	510,6	98,9	18,8	536,1	94,2	18,8	4
4,95-5,20 m	5,00	8P	6S	65	8	7	50	65	18,9	1927	7550	548,9	92,4	16,4	536,1	94,6	16,4	2
6,71-7,09 m	6,90	8P	6S	71	8	7	56	71	19,1	1947	5033	595,7	94,8	17,5	608,5	92,8	17,5	4
6,71-7,09 m	6,90	8P	6S	71	8	7	56	71	19,1	1947	7550	655,3	86,5	14,6	638,2	88,8	14,6	2
6,71-7,09 m	6,81	8P	6S	71	8	7	56	71	19,1	1947	7550	617,0	91,9	16,4	625,5	90,6	16,4	2
6,71-7,09 m	6,81	8P	6S	71	8	7	56	71	19,1	1947	5033	595,7	94,8	17,5	655,3	86,1	17,5	4
6,71-7,09 m	6,81	8P	6S	71	8	7	56	71	19,1	1947	2517	608,5	92,4	16,6	634,0	88,7	16,6	6
6,71-7,09 m	6,99	8P	6S	71	8	7	56	71	19,1	1947	2517	595,7	94,4	17,4	659,5	85,2	17,4	6
6,71-7,09 m	6,99	8P	6S	71	8	7	56	71	19,1	1947	5033	668,0	84,5	13,9	672,3	83,9	13,9	4
6,71-7,09 m	6,99	8P	6S	71	8	7	56	71	19,1	1947	7550	672,3	84,2	13,8	685,1	82,7	13,8	2

Table D4 Results obtained from unconfined measurements of shear-wave velocity on Skatval clay at lab 1 (NTNU)

Sample	Depth m	Beam elements		Height H mm	Height H mm	Height H mm	Height corrected Hcorr mm	Width W mm	Soil		Calibration tc ns	First cross over at NTNU			Peak to peak at NTNU			Frequency kHz
		Bottom	Top						γ_{soil} kN/m ³	ρ_{soil} kg/m ³		t cross μ s	Vs m/s	Gmax MPa	t cross μ s	Vs m/s	Gmax MPa	
D	6,62	8P	6S	67	8	7	52	70	18,9	1927	5033	842,5	62,1	7	897,8	58,2	7	4
D	6,62	8P	6S	67	8	7	52	70	18,9	1927	7550	855,3	61,3	7	914,8	57,3	7	2
B	6,54	8P	6S	60	8	7	45	60	18,9	1927	2517	744,6	60,6	7	825,5	54,7	7	6
B	6,54	8P	6S	60	8	7	45	60	18,9	1927	5033	778,7	58,2	7	842,5	53,7	7	4
B	6,54	8P	6S	60	8	7	45	60	18,9	1927	7550	782,9	58,0	6	838,2	54,2	6	2
A	6,50	8P	6S	70	8	7	55	70	18,9	1927	7550	893,6	62,1	7	923,4	60,1	7	2
A	6,50	8P	6S	70	8	7	55	70	18,9	1927	5033	868,0	63,7	8	923,4	59,9	8	4
A	6,50	8P	6S	70	8	7	55	70	18,9	1927	2517	855,3	64,5	8	910,6	60,6	8	6
C	6,58	8P	6S	68	8	7	53	71	18,9	1927	7550	868,0	61,6	7	910,6	58,7	7	2
C	6,58	8P	6S	68	8	7	53	71	18,9	1927	5033	829,7	64,3	8	914,8	58,3	8	4

Table D5 Results obtained from unconfined measurements of shear-wave velocity on Skatval clay at lab 2 (NGI)

Location		Setup	Soil		Sample				First crossover at NGI Oslo			Peak to Peak at NGI Oslo		
Borehole	Sample	t _c ⁵⁾	γ _{soil}	ρ _{soil}	H ¹⁾	h ₁ ²⁾	h ₂ ³⁾	H _{corr} ⁴⁾	t _{cross}	V _s	G _{max}	t _{peak}	V _s	G _{max}
-	-	ns	kN/m ³	kg/m ³	m m	m m	m m	m	μs	m/s	Mpa, MN/m ³	μs	m/s	MPa, MN/m ³
Skatval-607-5	1-2A-1-4.55m	4194	18,7125	1907,5	63	7	8	0,048	668,9	72,21	9947	737	65,50	8184
		4194	18,71	1907,2	63	7	8	0,048	653,6	73,91	10420	721,7	66,90	8536
		4194	18,71	1907,2	63	7	8	0,048	692,7	69,72	9270	733,6	65,81	8259
skatval-607-5	6-2A-1-7.15m	4194	19,2277	1960,0	68	7	8	0,053	844,2	63,09	7803	910,6	58,47	6701
		4194	19,2277	1960,0	68	7	8	0,053	805,1	66,18	8583	886,7	60,06	7069
		4194	19,2277	1960,0	68	7	8	0,053	811,9	65,62	8439	898,7	59,25	6881
skatval-607-5	7-1A-1-7.55m	4194	18,973	1934,1	67	7	8	0,052	764,2	68,42	9054	810,2	64,52	8050
		4194	18,97	1933,7	67	7	8	0,052	726,8	71,96	10014	803,4	65,06	8186
		4194	18,97	1933,7	67	7	8	0,052	714,8	73,18	10355	801,7	65,20	8221
		4194	18,97	1933,7	67	7	8	0,052	735,3	71,13	9782	832,8	62,76	7616
1)	Height of sample/steel tube													
2)	Height from edge of tube edge down to sample top surface after scraping of top													
3)	Height from edge of tube edge up to sample bottom surface after scraping of bottom													
4)	Corrected sample height(H -h1 -h2)													
5)	Signal delay measured with bender elements tip to tip(in nano seconds)													

D7 Triaxial tests CKoU

D7.1 General

A K_0 -test (or more correct: a CK_0 -test) is a test where the cross-sectional area of the specimen is kept constant except for the initial part of the test where the initial stresses usually are isotropic.

D7.2 Procedure

Before starting the K_0 -loading, the stresses are adjusted so that the ratio between horizontal and vertical effective stresses come close to the expected value during the K_0 -loading. The change from isotropic to anisotropic effective stresses is often done so that the effective octahedral stress is kept constant. It may also be done by increasing the vertical effective stress while the effective horizontal stress is kept constant.

The CKoU is the test with K_0 -loading during consolidation as explained before followed by undrained shearing.

D7.3 Results

Figures D25 to D26 illustrate the results obtained from CKoU triaxial testing on Skatval clay.

D8 References

- [1] NGI, "Datarapport – grunnundersøkelser. Detaljprosjektering Stjørdal-Steinkjer. Rapport 20160026-03-R.," 2016.
- [2] NGI, SP8 - Geoteknikedimensjoneringsparametere (GEODiP). Mineralogy data for Skatval, Koa and Rakkestad clay sites. Report 20150030-12-R, 2017.
- [3] J. Moun, "Falling drop used for grain size analysis of fine grained materials.," *Sedimentology*, vol. 5, no. 4, pp. 343-347, 1966.
- [4] Standard Norge, "Norsk Standard NS 8018 - Geoteknisk prøving - Laboratoriemetoder - Bestemmelse av endimensjonale konsolideringsegenskaper ved ødometerprøving - Metode med kontinuerlig belastning," Standard Norge, Oslo, 1993.
- [5] G. Sandbaekken, T. Berre and S. Lacasse, "Oedometer testing at the Norwegian Geotechnical Institute," *Consolidation of soils: Testing and evaluation. ASTM International.*, 1986.
- [6] T. Berre, "Triaxial testing at the Norwegian Geotechnical Institute," *Geotechnical Testing Journal*, Vol. 5, pp. 7-23, 1981.
- [7] A. Andresen and N. E. Simons, "Norwegian Triaxial Equipment and Technique," NGI, Oslo, 1960.
- [8] L. Bjerrum and A. Landva, "Direct simple shear tests on a Norwegian quick clay," *Geotechnique*, Vol 16, No. 1, pp. 1-20, 1966.
- [9] A. Andresen, T. Berre, A. Kleven and T. Lunne, "Procedures used to obtain soil parameters for foundation engineering in the North Sea," *Marin Geotechnology*, Vol 3, no. 3, pp. 201-266, 1979.
- [10] D. D. a. S. T. Landon M.M., "Nondestructive sample quality assessment of a soft clay using shear-waver velocity," *J Geotech Geoenv Eng ASCE*, vol. 133, pp. 424-432, 2007.
- [11] Statens vegvesen, "Håndbok R210. Laboratorieundersøkelser," Statens vegvesen, Oslo, 2016.
- [12] NGI, Grunnundersøkelser Inderøy kommune. Datarapport grunnundersøkelser sone Koa, Inderøy. Rapport 20100685-00-3-R., 2011.

Dokumentinformasjon/Document information		
Dokumenttittel/Document title GEODIP'S high-quality database: clay		Dokumentnr./Document no. 20150030-02-R
Dokumenttype/Type of document Rapport / Report	Distribusjon/Distribution Begrenset/Limited	Dato/Date 2015-12-18
		Rev.nr.&dato/Rev.no.&date 2 / 2018-01-17
Oppdragsgiver/Client Norwegian Research Council (NFR)		
Emneord/Keywords Clay, high-quality, correlations, index properties, undrained shear strength, compression parameters		

Stedfesting/Geographical information	
Land, fylke/Country Norway	Havområde/Offshore area
Kommune/Municipality	Felt navn/Field name
Sted/Location	Sted/Location
Kartblad/Map	Felt, blokknr./Field, Block No.
UTM-koordinater/UTM-coordinates Zone: East: North:	

Dokumentkontroll/Document control					
Kvalitetssikring i henhold til/Quality assurance according to NS-EN ISO9001					
Rev/ Rev.	Revisjonsgrunnlag/Reason for revision	Egenkontroll av/ Self review by:	Sidemanns- kontroll av/ Colleague review by:	Uavhengig kontroll av/ Independent review by:	Tverrfaglig kontroll av/ Inter- disciplinary review by:
0	Original document	2015-10-30 Priscilla Paniagua	2015-11-04 Tom Lunne Jean-Sebastien L'Heureux		
1	Changes regarding quality control of the database and addition of new data	2017-10-06 Priscilla Paniagua	2016-12-02 Jean-Sebastien L'Heureux		
2	Update of figures and final revision	2018-01-16 Priscilla Paniagua	2018-01-17 Jean-Sebastien L'Heureux		

Dokument godkjent for utsendelse/ Document approved for release	Dato/Date 17 January 2018	Prosjektleder/Project Manager Jean-Sebastien L'Heureux
--	-------------------------------------	--

NGI (Norwegian Geotechnical Institute) is a leading international centre for research and consulting within the geosciences. NGI develops optimum solutions for society and offers expertise on the behaviour of soil, rock and snow and their interaction with the natural and built environment.

NGI works within the following sectors: Offshore energy – Building, Construction and Transportation – Natural Hazards – Environmental Engineering.

NGI is a private foundation with office and laboratories in Oslo, a branch office in Trondheim and daughter companies in Houston, Texas, USA and in Perth, Western Australia

www.ngi.no

NGI (Norges Geotekniske Institutt) er et internasjonalt ledende senter for forskning og rådgivning innen ingeniørrelaterte geofag. Vi tilbyr ekspertise om jord, berg og snø og deres påvirkning på miljøet, konstruksjoner og anlegg, og hvordan jord og berg kan benyttes som byggegrunn og byggemateriale.

Vi arbeider i følgende markeder: Offshore energi – Bygg, anlegg og samferdsel – Naturfare – Miljøteknologi.

NGI er en privat næringsdrivende stiftelse med kontor og laboratorier i Oslo, avdelingskontor i Trondheim og datterselskaper i Houston, Texas, USA og i Perth, Western Australia.

www.ngi.no

